EPA-660/3-73-009
August 1973

Ecological Research Series

Dynamic Water Quality Forecasting And Management

Office of Research and Development
U.S. Environmental Protection Agency
Washington, D.C. 20460

RESEARCH REPORTING SERIES

Research reports of the Office of Research and Monitoring, Environmental Protection Agency, have been grouped into five series. These five broad categories were established to facilitate further development and application of environmental technology. Elimination of traditional grouping was consciously planned to foster technology transfer and a maximum interface in related fields. The five series are:

1. Environmental Health Effects Research
2. Environmental Protection Technology
3. Ecological Research
4. Environmental Monitoring
5. Socioeconomic Environmental Studies

This report has been assigned to the ECOLOGICAL RESEARCH series. This series describes research on the effects of pollution on humans, plant and animal species, and materials. Problems are assessed for their long- and short-term influences. Investigations include formation, transport, and pathway studies to determine the fate of pollutants and their effects. This work provides the technical basis for setting standards to minimize undesirable changes in living organisms in the aquatic, terrestrial and atmospheric environments.

EPA-660/3-73-009
August 1973

DYNAMIC WATER QUALITY

FORECASTING AND MANAGEMENT

By

Donald J. O'Connor, Robert V. Thomann, and Dominic M. Di Toro

Project No. R800369
Program Element 1BA023

Project Officer

Dr. Walter M. Sanders III
Southeast Environmental Research Laboratory
National Environmental Research Center-Corvallis
U. S. Environmental Protection Agency
Athens, Georgia 30601

Prepared for
OFFICE OF RESEARCH AND DEVELOPMENT
U. S. ENVIRONMENTAL PROTECTION AGENCY
WASHINGTON, D. C. 20460

EPA REVIEW NOTICE

This report has been reviewed by the Environmental Protection Agency and approved for publication. Approval does not signify that the contents necessarily reflect the views and policies of the Environmental Protection Agency, nor does mention of trade names or commercial products constitute endorsement or recommendation of use.

ABSTRACT

This report describes the formulation and initial verification of two modeling frameworks. The first is directed toward an analysis of the impact of the carbonaceous and nitrogenous components and wastewater on the dissolved oxygen resources of a natural water system. The second modeling framework concentrates on the interactions between the discharge of nutrient, both nitrogen and phosphorus, and the biomass of the phytoplankton and zooplankton populations which result, as well as incorporating the overall impact on dissolved oxygen. The models are formulated in terms of coupled differential equations which incorporate both the effect of transport due to tidal motion and turbulence, and the kinetics which describe the biological and chemical transformations that can occur. The modeling frameworks are applied to the Delaware and Potomac estuaries in order to estimate the ability of such models to describe the water quality effects of carbon, nitrogen, and phosphorous discharges. The agreement achieved between observation and calculation indicate that the major features of the impact of wastewater components on eutrophication phenomena can be successfully analyzed within the context of the models presented herein.

This report was submitted in fulfillment of Project Number R800369, by Manhattan College, Bronx, New York, under the sponsorship of the Environmental Protection Agency. Work was completed as of December 31, 1972.

CONTENTS

FIGURES

FIGURES

FIGURES

FIGURES

TABLES

SECTION I

CONCLUSIONS

Based on the results of the mathematical model formulations and verifications presented in this report it is concluded and the impact on water quality of the carbonaceous, nitrogenous, and phosphoric fractions of wastewaters discharged into an estuarine environment can be assessed, to guide the preliminary planning of remedial actions to improve water quality. The water quality parameters that appear susceptible to such an analysis are the dissolved oxygen levels and the phytoplankton biomass which result as a consequence of natural and man-made inputs. The analyses and verifications presented for the Delaware and Potomac estuaries are viewed as the foundation upon which a rational investigation of wastewater treatment alternatives can be based for the management and control of estuarine water quality.

SECTION II

RECOMMENDATIONS

The modeling formulations which have been developed in this study should be applied to other estuarine water bodies in an attempt to further strengthen the verification and refine the kinetic structures employed. In particular, the eutrophication analysis is an initial attempt to incorporate the varied and complex interactions which characterize the growth and decay of phytoplankton biomass in natural waters and the relationships to nutrient concentrations. This analysis should be extended to include effects of other microorganisms as well as the effect of chemical and biological parameters not included in the preliminary formulations.

In principle the models developed herein can be extended to apply to other settings such as lakes and coastal waters. The modifications and adjustments for such an attempt would be a fruitful continuation. The need for further comparisons between observed data and calculated concentrations cannot be over emphasized. Only in this way can progress be made in the understanding of the complex phenomena which control water quality in natural bodies of water.

Finally, it is recommended that the models developed in this work be applied in the planning and evaluation of water quality enhancement programs. Although the models are in no way completely satisfactory from a scientific point of view, and may in fact not incorporate certain effects which may prove to be important, they have been shown to be realistic and capable of reproducing the observed situation for the cases considered in this report. The models, therefore, are worthy of consideration in any attempt to rationally plan and execute water quality enhancement programs.

SECTION III

INTRODUCTION

As the nation moves forward in its program for water pollution control and water quality management, the need for both the short and long term operation and management of water resource systems becomes ever more important. Complex problems regarding subtle interactions between waste treatment processes and the environment must be considered. These problems can be conceptualized and formulated using the techniques of dynamic systems analyses. However the general theory must be specifically adapted to these problems. A whole expertise must be developed which enables a translation of the problems of water quality maintenance and prediction and water resources management into the abstract formulations of dynamic systems analyses.

As is well known, a sequence of profound biological changes occurs in a natural body of water receiving untreated waste water. What is not so well known, however, is the chain of events that is set into motion as a result of discharging biologically treated, nutrient-rich, effluents. When the waste is untreated, the bacterial populations predominate. These are of the form which oxidize organic carbon in their metabolic processes. When this material is removed in a biological treatment unit, the next component of the cycle, nitrification, becomes more significant. If the treatment processes are designed to allow the nitrifying bacteria to develop in the plant, then an end product of relatively stable nitrates results. If nitrification does not occur during treatment, or is only partially completed, the remaining nitrogen is discharged. Both the residual carbonaceous material and the nitrogenous material exert a separate and distinct oxygen demand on the water bodies resources.

Simultaneously, the photosynthetic and respiratory processes of the algae are operative. If nitrogen is not removed in treatment, the environment is more conducive to the growth of algae, which then proliferate. When the algal blooms exceed the capacity of the system, mass mortality may occur. Algal decay occurs and carbonaceous and nitrogenous demand is returned to the water body thereby initiating the cycle again. It is therefore necessary to proceed in a sequential manner so that these important secondary ecological effects are incorporated both in the analysis and planning phases.

Efficient dynamic regional management of these systems therefore requires a foundation of analytical tools and techniques that will buttress the solution of the very complex problems associated with short and long term water pollution control.

The basis for the methods presented herein is the principle of conservation of mass. It can be expressed in mathematical terms as a partial differential equation which related the concentration of a substance $c(r,t)$ at a position $\vec{r}$ and time t to the effects of mass transport, which are described by a velocity vector field $\vec{U}(r,t)$ and a dispersion matrix $E(r,t)$; the effects of kinetic transformations, which are described in terms of sources and sinks of the substance $S(c,r,t)$; and the effects of direct discharges to the water body $W(r,t)$. The requirement that the mass changes are accountable in these terms requires that:

$$\frac{\partial c}{\partial t} + \nabla \circ [-E(r,t)\nabla c + \vec{U}(r,t)c] = S(c,r,t) + W(r,t) \qquad (1)$$

where $\nabla = \partial/\partial x\ \vec{i} + \partial/\partial y\ \vec{j} + \partial/\partial z\ \vec{k}$. Given the mass transport and kinetic descriptions and for specified direct discharges and boundary conditions this equation is solvable, in principle, for the resulting concentration distribution $c(r,t)$ as a

function of position and time.

For complex, interacting situations, it is necessary to simultaneously characterize the concentrations $c_i(r,t)$ of a number of substances. In this case the kinetic interaction terms are usually functions of all the concentrations, $S_i(c_1, c_2, \ldots, c_n, r,t)$ so that a set of n simultaneous equations result of the form:

$$\frac{\partial c_i}{\partial t} + \nabla \cdot \vec{j}_i = S_i(c_1,\ldots,c_n,r,t) + W_i(r,t) \quad i = 1,..,n \qquad (2)$$

where $\vec{j}_i = - E(r,t)\nabla c_i + \vec{U}(r,t)c_i$, the mass flux, due to transport.

It is also common to simplify these equations by analyzing less than the three spatial dimensions. The simpliest situation occurs in a one-dimensional analysis for which the set of equations (2) becomes

$$\frac{\partial c_i}{\partial t} - \frac{1}{A}\frac{\partial}{\partial x}\left(EA\frac{\partial c_i}{\partial x}\right) + \frac{\partial}{\partial x}(Qc_i) = S_i(c_1,\ldots,c_n,x,t) + W_i(x,t) \qquad (3)$$

The procedure followed in the applications described herein has been to numerically integrate these equations in order to characterize the distribution of substances of concern.

The water quality problems investigated center on the effects of nitrogen and phosphorus discharges as well as the carbonaceous waste discharges. The analyses are directed toward the effects on the dissolved oxygen distribution on the one hand and the effects on the first two trophic levels of the food chain, the phytoplankton and zooplankton, on the other. A series of models are presented and verified in the subsequ-

ent chapters indicating the utility and power of these methods. The evolution of the modeling structure is illustrated in Figure 1 which presents the development and increasing scope of the modeling frameworks with the latter models encompassing a relatively broad range of environmental variables associated with the eutrophication phenomena.

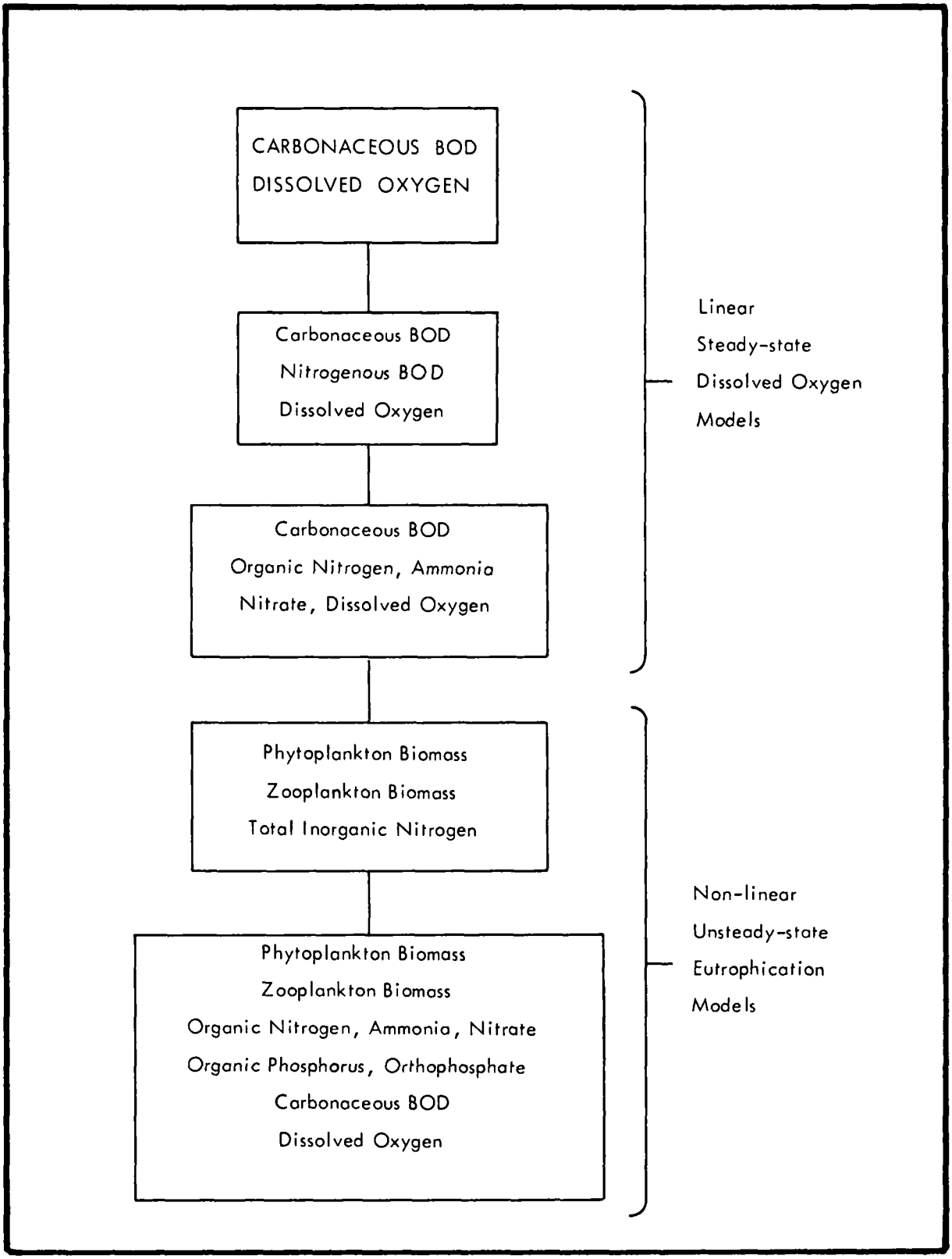

Fig. 1 Evolution of the Modeling Structures

SECTION IV

NITRIFICATION AND ITS EFFECTS ON DISSOLVED OXYGEN

The discharge of nitrogenous compounds into natural waters produces a variety of changes in water quality. Changes occur not only in the various forms of nitrogen, but also in those substances with which the nitrogen may react. The oxygen requirements for the ammonia and nitrite oxidation, the utilization of ammonia and nitrate as a nutrient by phytoplankton, and the ammonia interference with chlorination, are significant examples. The nitrogenous compounds, which may be either organic or inorganic in nature, are found in urban and agricultural runoff, domestic waste waters and industrial effluents. A "background" concentration of nitrogen is present in most water systems and is the result of a dynamic equilibrium of the natural sources of nitrogen in rainfall, from the land and within the ground. Although the man-made effects are generally of greater significance in the pollution of natural waters, background nitrogen concentrations may be present in amounts that must be considered in any modeling effort.

The purpose of this section is to present several simplified mathematical models of nitrification in rivers and estuaries which are based on first order kinetics and the assumption of temporal steady state. Specific attention is directed to the role of nitrification in the modeling of the dissolved oxygen balance. The models presented here progress from relatively simple nitrogen equivalent biochemical oxygen demand models to more complex models which incorporate feedback effects.

The broad aspects of the nitrogen cycle are reviewed and the importance of nitrogenous waste loads in the dissolved oxygen

balance of natural wastes is stressed. This review is followed by a critical review of the reaction kinetics that actually prevail in nitrification.

Figure 2 schematically outlines the major features of the nitrogen cycle that are of importance. It is appropriate to initiate the cycle at the point where organic nitrogen (amines, nitriles, proteins) and ammonia resulting from municipal and industrial waters are discharged into a water body. The organic nitrogen undergoes an hydrolytic reaction producing ammonia as one of the end products, which in addition to the ammonia present in the waste waters, provides a food source for the nitrifying bacteria. The oxidation process proceeds sequentially from ammonia through nitrite to nitrate. The conditions under which these reactions proceed are comparatively restrictive, but, if present, they provide an appropriate environment which may result in large depletions of dissolved oxygen.

The forward sequential reactions of the nitrification process often are the dominating features of the nitrogen cycle in bodies of water receiving large discharges of nitrogenous waste material. The reactions proceed in the forward direction, provided the concentration of dissolved oxygen is sufficiently high to meet the requirements of the nitrifying bacteria. However, under conditions of low concentration of dissolved oxygen, bacterial reduction of nitrate to nitrite can occur followed by the further reduction of nitrite primarily to nitrogen gas, although a few species may reduce the nitrite to ammonia. These reactions provide a source of oxygen for the microorganisms in the stabilization of organic matter without utilizing whatever dissolved oxygen is present in the water.

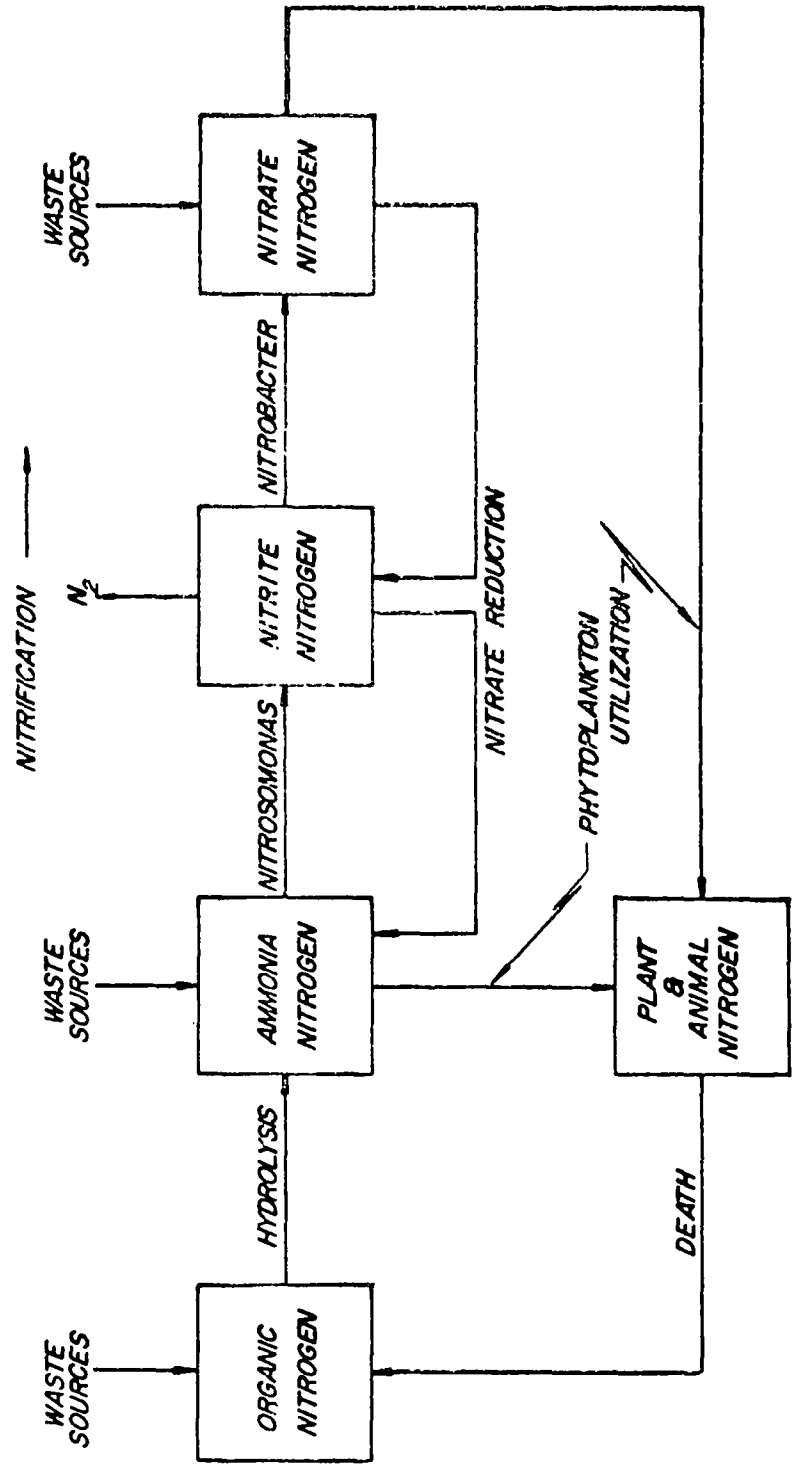

Fig. 2 Major Features of the Nitrogen Cycle

In addition to the removal of nitrate by bacterial reduction it may also be used by the phytoplankton as a nutrient source. The nitrate must be converted to ammonia by enzymatic reaction before it is assimilated. The assimilated nitrogen becomes part of the organic nitrogen in plants and subsequently in animals. Excretion and decay of this material releases organic nitrogen, thereby completing the cycle. Ammonia, or some form of nitrogen, is also required by the heterotrophic bacteria in the oxidation of carbonaceous material; however, this sink of nitrogen is relatively insignificant by contrast to the oxidation process or algal usage.

In summary there are two broad areas of concern from the water quality viewpoint with respect to the nitrogen cycle in natural waters: 1. The oxidation and possible reduction of various forms of nitrogen by bacteria and the associated utilization of oxygen. 2. The assimilation of the inorganic nitrogen and the release of organic nitrogen by phytoplankton during growth and death respectively. In some cases, either one or the other of these conditions dominate, the former in areas of large sources of waste water with little or partial treatment and the latter in water bodies receiving biologically treated effluents or agricultural drainage.

This section is concerned with the first of these broad areas. Its specific purpose is to present a mathematical model of the nitrification reactions in streams and estuaries. The basic theory of the nitrogen cycle is reviewed; several simplified kinetic mathematical models of portions of the cycle are constructed and application of the simplified models to specific situations is described.

Nitrification

Nitrogenous matter in waste waters consists of proteins, urea, ammonia and, in some cases, nitrate. The intermediate decomposition products of the proteins such as amino acids, amides and amines are also present in varying degrees. The proteins are broken down by hydrolysis in a series of steps into a variety of amino acids. Both exocellular and endocellular enzymes are involved in the process. Aeration and alkaline conditions favor the production of the exo-enzyme. The amino acids are very soluble in water and exert a strong buffering action; the carboxyl group reacting with the hydrogen ion and the amino group reacting with the hydroxyl. The decomposition of the amino acids which can occur in a number of different ways, is endocellular. Ammonia is released in this process of deamination, which may be reductive, oxidative or hydrolytic reaction, depending on the nature and structure of the amino acids. In any case, the significant end product is ammonia.

Ammonia is also released in the aerobic decomposition of proteins by heterotrophic bacteria. The ammonia, which is highly soluble, combines with the hydrogen ion to form the ammonium ion, thus tending to raise the pH. In the neutral pH zone, all of the ammonia is present in this form and at the higher pH it is evolved as a gas. The heterotrophic decomposition is the typical reaction in the first stage of the biochemical deoxygenation of natural waters. Ammonia is an end product of both this reaction and the reaction associated with the hydrolytic breakdown of proteins. The ammonia present in natural waters is thus a result of either the direct discharge of the material in waste waters or of the decomposition of organic matter in various forms.

The ammonia in turn is oxidized under aerobic conditions to nitrite by bacteria of the genus Nitrosomonas as follows: (Sawyer, 1960, Hutchinson, 1957, Stratton, 1967 and Delwiche, 1956)

$$(NH_4) + OH^- + 1.5O_2 \xrightarrow{\text{bacteria}} H^- + NO_2^- + 2H_2 + 59.4 \text{ K cal} \quad (4)$$

This reaction requires 3.43 gms of oxygen utilization for one gram of nitrogen oxidized to nitrite. The nitrite thus formed is subsequently oxidized to nitrate by bacteria of the genus Nitrobacter as follows: (Hutchinson, 1957)

$$NO_2^- + 0.5O_2 \xrightarrow{\text{bacteria}} NO_3^- + 18 \text{ K cal} \quad (5)$$

This reaction requires 1.14 gms of oxygen utilization for one gram of nitrite nitrogen oxidized to nitrate. The total oxygen utilization in the entire forward nitrification process is therefore 4.47 gms of oxygen per gm of ammonia nitrogen oxidized to nitrate. The Nitrobacter bacteria process about three times as much substrate as the Nitrosomonas bacteria to derive the same amount of energy. Nitrite is therefore converted quite rapidly to nitrate.

Essential factors for nitrification are oxygen, phosphates and an alkaline environment to neutralize the resulting acids. Nitrifying bacteria are very susceptible to action of toxic substances (e.g. manganese). These bacteria are obligate autotrophs, which derive their energy from the oxidation of simple inorganic compounds. The energy obtained from these reactions is utilized for the assimilation of carbon from either carbon dioxide or bicarbonate ion, but not from organic carbon. However, it has been indicated that Nitrobacter can be grown heterotrophically on an organic substrate, without losing its ability to oxidize nitrite. Acetate was assimilated as cell

carbon, the optimum pH range being 8.5 - 9.5. The alkaline environment is required to neutralize the acidic end-products. Below pH of 6.0, which can occur in a poorly buffered system, inhibition occurs. The presence of organic matter, particularly amino compounds in excessive concentrations, inhibits growth and respiration of the nitrifying bacteria. These excessive concentrations in the order of thousands of mg/l are seldom encountered in either waste water or natural waters. However, even concentrations of organics in the order of hundreds of mg/l which may be found in practical cases, appear to still retard the nitrification process. At these concentrations the heterotrophic bacteria probably predominate and assimilate the ammonia in their metabolic processes. After the death and lysis of these bacteria, nitrification takes place. The experimental evidence in this regard is not conclusive and, in fact, is somewhat contradictory. While the majority of reported work indicates some degree of inhibiting effects, other reports show minimal or no retardation. At lower concentrations of organic materials, as may be found in natural water bodies, both heterotrophic and autotrophic reactions may occur simultaneously.

Given the appropriate conditions, the concentration of the organisms appears to be the significant factor controlling the rate of nitrification, with the concentration of the reactant having a reduced effect. However, if there is an ample supply of organisms, the rate appears to be controlled by the concentration of the reactant (see also - Kinetic Models). The number of nitrifiers is, of course, determined by the generation time of organisms, which is in the order of one day, by contrast to an order of a few hours for many heterotrophic bacteria.

The common source of the nitrifying organisms is rich soil,

where they are usually found in high numbers. In rivers receiving waste waters, nitrifying bacteria are probably present in varying degrees depending on the nature and the treatment of waste waters. Their number in sewage is low (about 100/ml) but increases through biological treatment to an order of 1000/ml. Natural habitats are found on biological aggregates or on surfaces where the environment appears appropriate for optimum growth and acceleration metabolism. Surfaces such as these are found in trickling filters and activated sludge treatment plants as well as the rocky beds of shallow rivers.

Denitrification

Under conditions of low concentration of dissolved oxygen the bacterial reduction of nitrate can occur. This reaction is to be distinguished from the utilization of nitrate and subsequent reduction by aquatic plants. A large variety of facultative bacteria can reduce nitrate. E Coli are cited as a common bacteria capable of reducing nitrate. (Hutchinson, 1957) The reduction by bacteria of nitrate is probably all to NO_2 and then to nitrogen gas although complete reduction to ammonia may also occur. The primary reactions seem to be:

$$C_6H_{12}O_6 + 12\ NO_3^- \xrightarrow{\text{bacteria}} 12\ NO_2^- + 6\ CO_2 + 6H_2O \qquad (6)$$

which represents the reduction of nitrate to nitrite and

$$C_6H_{12}O_6 + 8\ NO_2^- \xrightarrow{\text{bacteria}} 4\ N_2 + 2\ CO_2 + 4CO_3^{=} + 6\ H_2O \qquad (7)$$

for the reduction of nitrite to nitrogen gas. It should be noted that these reactions serve in place of an oxygen source for micro-organisms in the metabolic oxidation of organic compounds in a water body, without drawing on the dissolved oxygen resources of the stream.

The dissolved oxygen conditions under which nitrate reduction becomes significant are subject to some differences of opinion resulting from the relatively small amount of work done in this area. Under completely anaerobic conditions, nitrification cannot occur since the nitrifying bacteria are strictly aerobic. There is some evidence to indicate, however, that nitrate reduction goes on constantly and is greatly accelerated under low (0-2 mg/l) dissolved oxygen conditions.

Sources of Nitrogen

Agricultural sources of nitrogen may be significant with respect to concentrations found in natural waters. The nitrogen is present in the drainage water from these lands and aside from that inherent in the soil itself, emanates from the fertilizers, legumes and barnyard and silo effluents. An attempt at a nitrogen balance for harvested crop areas of the United States is given in Table 1.

Table 1

Nitrogen Balance Sheet for the Harvested Crop Area of the United States, 1930*

	Nitrogen lb/acre/year	
Additions		
Rain and irrigation	4.7	
Seeds	1.0	
Fertilizers	1.7	
Manures	5.2	
Symbiotic nitrogen fixation	9.2	
Nonsymbiotic nitrogen fixation	6.0	
		27.8
Losses		
Harvested crops	25.1	
Erosion	24.2	
Leaching	23.0	
		72.3
Net Annual Loss		44.5

*After Allison, 1955, quoted by Feth, 1966.

The value for erosion is equivalent to an average annual value of almost 8 mg/l of nitrate as nitrogen from a drainage area of 1 square mile with a flow of 1 cubic foot per second. This value appears to be high for most natural waters but may be present in rivers draining harvested lands during certain periods of the year.

Nitrogen leached from drained soil on which alfalfa and bluegrass are grown in Kentucky can yield up to 10 pounds/acre year and corn fields in Wisconsin have yielded in the range of 20 and 40 pounds per acre year. Irrigated lands with diversified forms drained between 2 and 25 pounds of nitrogen per acre year.

Fertilizers are significant sources of nitrogen in harvested lands. The fertilizers are in forms such as ammonium sulfate and nitrate, anhydrous ammonia and in various forms of nitrates and phosphates, all of which are highly soluble. During periods of excessive runoff or when irrigation is in excess of plant requirements, nitrogen in various forms is carried off to either the ground or surface water. Barnyard and silo drainage, as well as wash waters and effluents from feedlot and dairy operations, undoubtedly add nitrogen to water courses.

A recent report described the nitrogen enrichment of surface waters by absorption of ammonia which was volatilized from cattle feedlots (Hutchinson, 1969). Laboratory studies indicate that as much as 90% of urine nitrogen may escape as ammonia from feedyards. A significant quantity of this nitrogen may be absorbed by water surfaces within a few kilometers from the feedlots (between 10 - 20 kg/ha-yr). A value of 4 kg/ha-yr was measured at a site in which there were no irrigated fields or feedlots within 3 km and no large lots or cities within 15 km. On the other hand, absorption rates of

about 35 kg/ha-yr were reported for sites 2 km from a large feedlot and 73 kg/ha-yr for sites 0.4 km from a large feedlot. Based on these measurements the investigators conclude the increase in nitrogen for a nearby lake could be as high as 0.6 mg/l.

Increases in nitrate concentration have been reported (Bormann, 1968) when forests of watershed systems are cut. Over the period of one year, during which the land was clear cut and a herbicide applied to prevent regrowth, the concentration of nitrate in the drainage increased from about 1 mg/l to approximately 40 mg/l the following year and 50 mg/l the second year. The runoff from the cleared area also increased over the period. A mass balance of the nitrogen indicated an annual loss of nitrogen from the drainage area of about 50 kg/ha. The increase is accounted for by increase flow and drainage, reduction of root surfaces and production of an environment more favorable for bacterial mineralization.

The contribution of rainfall to the nitrogen balance may be significant in larger bodies of water. Assuming a range of 0.5 to 1.0 mg/l in rainfall (Feth, 1966), the annual input would be between 5 and 10 pounds per acre year for a rainfall of about 50 inches per year.

The contribution of total nitrogen due to domestic wastes may range from 5 to 50 pounds/capita year, depending on the economic and social characteristics of the area. In urban and suburban areas population densities may vary from 5 to 25 or more people per acre. On an areal basis, therefore, nitrogen from this source may run from 25 to 250 pounds/acre year. This is obviously one of the most significant sources. The concentration of organic nitrogen in untreated municipal sewage ranges from 5 to 35 mg/l with an average of about 20 mg/l

and of ammonia ranges from 10 to 60 mg/l with an average of about 25 mg/l.

Industrial waste waters may contain appreciable quantities of nitrogen in various forms. Ammonia is one of the most commonly used industrial chemicals. Nitrogen in its various forms is used in manufacture of dye, glass, explosives, many chemicals and synthetic products, and may therefore be found in significant quantities in these waste waters. They are not usually of importance in paper, tannery, textile, metal and in some vegetable and fruit-processing wastes. On the other hand, they are present in meat-packing, brewery, dairy and coke plant wastes.

The nitrogen in plant and animal proteins is measured by the Kjeldahl method, which converts all of the organic nitrogen to ammonia, The suspended fraction includes the nitrogen present in the living and dead plankton and in the animal excreta, while the dissolved portion contains the nitrogen from excreted materials, usually associated with the degradation of cells. The inorganic forms of nitrogen, ammonia, nitrite and nitrate may be measured directly. Thus the nitrogen present in waste streams or natural waters is usually reported in terms of the specific inorganic forms or as organic nitrogen, which covers a range of compounds in various stages of degradation.

The total oxidizable nitrogen may be measured indirectly by the standard biochemical oxygen demand test. The first stage reflects primarily aerobic oxidation of the organic material, in which an end product is ammonia. Simultaneously the organic nitrogen is hydrolyzed to release ammonia. The ammonia thus formed from these two sources, in combination with the ammonia present in waste waters undergoes oxidation through nitrite to

nitrate. This process of nitrification is often referred to as the second stage of biochemical oxygen demand. In untreated and heavily polluted water, the two stages do not usually occur together, the first being substantially completed before the second is significantly underway. In treated effluents and less polluted waters, the lag between the two is reduced. As the first stage is reduced and with nitrifying organisms present, the two stages may occur simultaneously. An example of this reaction in BOD samples is shown in Figure 3. (O'Connor, 1968).

Kinetic Models

The nitrification process, in which ammonia is converted through nitrite to nitrate is an autotrophic biochemical reaction. The energy for the growth of the microorganisms is obtained from the oxidation of ammonia or nitrite (see Eqs. (4) and (5). In reactions of this type the rate is generally assumed to be proportional to the concentration of the substrate and also of the microorganisms. The substrate concentration dependency, however, may be modified by stipulating that the rate of the reaction is independent of the concentration of substrate at high substrate concentration and becomes increasingly concentration dependent as the concentration decreases. Substrate limiting kinetics have been used in the analysis of biological waste treatment phenomena (Lawrence and McCarty, 1970; Pearson, 1968). A general review of the literature is given in Lawrence and McCarty (1970). The growth equation for the microorganisms may be written as:

$$\frac{dM}{dt} = KM \qquad (8)$$

where M = the microbial concentration
K = microbial growth coefficient.

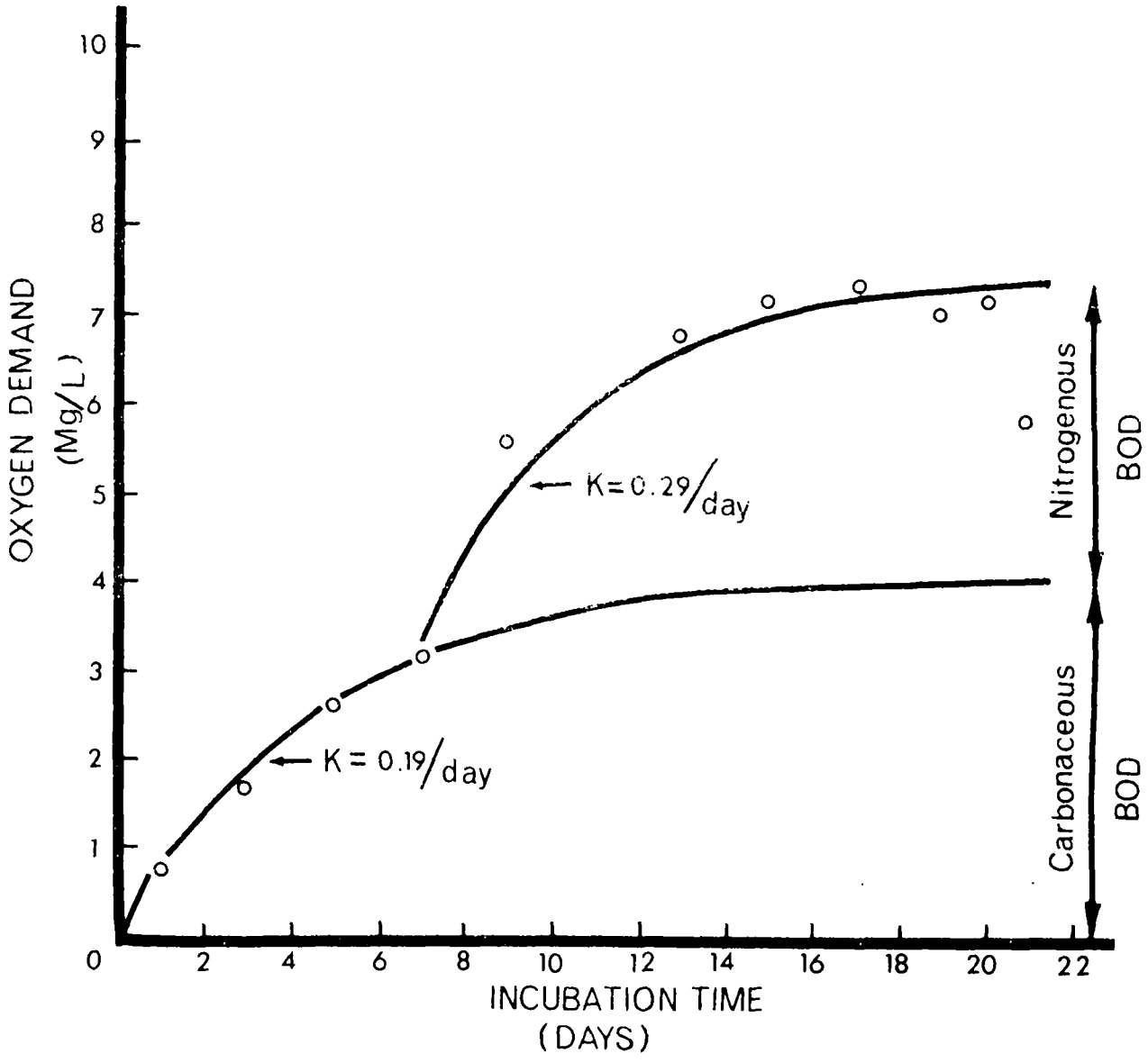

Fig. 3 Two-state BOD Curve - Mohawk River at St. Johnsville, N.Y.

In unlimited growth, the solution of Eq. (8) indicates that the microbial population would grow at an exponential rate. If however, a single substrate (say nitrogen) plays an important role in limiting the growth, one must also consider the utilization of the substrate and consider that the growth coefficient, K, in Eq. (8) is not a constant but depends on a substrate concentration. Thus, let

$$K = \frac{K_m c}{K_s + c} \tag{9}$$

where K_m is the maximum growth rate (1/day), c is the concentration of substrate (mg/l) and K_s (the so-called Michaelis or half-saturation constant) is the concentration (mg/l) at which the growth rate is one-half of the saturated rate. Fig.4 is a sketch of this functional form.

Substitution of Eq. (9) into (8) gives:

$$\frac{dM}{dt} = \frac{K_m M c}{K_s + c} \tag{10}$$

This form of kinetic equation was first developed by Michaelis and Menton to explain enzymatic reactions. It was later applied by Monod (1942) to systems involving growth of biological organisms. This equation can be written in terms of microorganisms only by substituting for the substrate concentration its equivalence in terms of microorganism i.e a unit increase of organisms is equal to a unit decrease in substrate multiplied by the appropriate stochiometric or yield coefficient. This is simply an expression of the conservation law, in which the total mass, M, is equal to the sum of the initial organisms present plus the substrate utilized to produce microbes, i.e:

$$M = M_o + a(c_o - c) \tag{11}$$

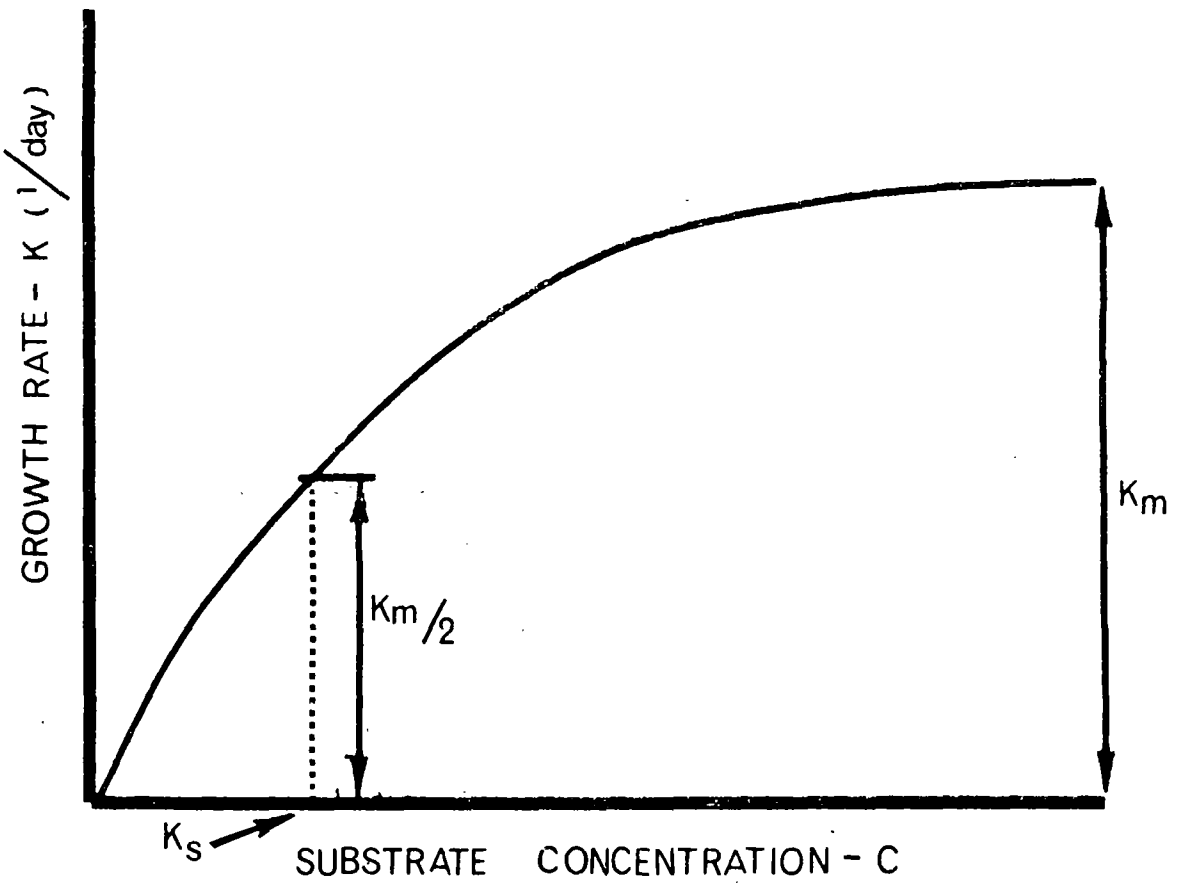

Fig. 4 Variation of Growth Rate with Substrate Concentrations

in which a = stochiometric or yield constant (mg bacterial mass per mg substrate)

M_o = initial bacterial mass

c_o = initial substrate concentration

Substitution of Eq. (11) into Eq. (10) gives upon integration

$$K_m t = \frac{K_s}{M_o + ac_o} \ln \left(\frac{c_o}{c_o - 1/a(M-M_o)}\right) + \frac{aK_s + M_o + ac_o}{M_o + ac_o} \ln \frac{M}{M_o} \qquad (12)$$

A detailed dimensionless analysis of the behavior of this type of equation is given below in terms of the utilization of the substrate.

Equation (10) indicates that at high concentrations of substrate ($c >> K_s$), the rate is independent of c and the rate expression reduces to a first-order reaction in which the growth rate is proportional to the concentration of microorganisms:

$$\frac{dM}{dt} = K_m M \qquad (13)$$

This equation indicates an unlimited exponential growth of organisms. At low concentration of substrate ($K_s >> c$), the expression reduces to a second-order reaction in which the rate is proportional to the product of the concentration as in

$$\frac{dM}{dt} = \frac{K_m Mc}{K_s} \qquad (14)$$

This equation can also be written entirely in terms of microbial mass by considering the bacterial equivalent of the initial substrate concentration and letting M_T be the sum of

the initial organisms and the substrate. Thus:

$$\frac{dM}{dt} = K_2 M (M_T - M) \tag{15}$$

where $M_T = M_o + ac_o$ and

$$K_2 = \frac{K_m}{aK_s}$$

Equation (15) is referred to as an autocatalytic reaction in which the rate is increased by the concentration of the end products of the reaction. It is autocatalyzed by the microorganisms which increase as substrate is oxidized.

The interacting differential equations for the substrate c and the microbial mass are given by

$$\frac{dc}{dt} = \frac{-K_m M' c}{K_s + c} \tag{16}$$

and

$$\frac{dM'}{dt} = \frac{K_m M' c}{K_s + c} \tag{17}$$

where all quantities are now expressed in terms of their equivalent substrate concentrations. Thus, M' = M/a, the microbial mass in substrate equivalents. Eq. (17) is the same as Eq. (14) except in terms of the substrate concentration. In the interests of mathematical simplicity, the microbial loss due to endogenous respiration has been neglected in these equations. The solution to Eqs. (16) and (17) is:

$$K_m t = \frac{d_s}{1 + d_M} \log \left[\frac{1+d_M - c/c_o}{d_M\ c/c_o}\right] + \log \left[\frac{1+d_M - c/c_o}{d_M}\right] \tag{18}$$

where $d_s = K_s/c_o$, a dimensionless "Michaelis Number" and

$dM = M'_o/c_o$, a dimensionless microbial-substrate concentration ratio.

Equation (18) is simply a dimensionless reexpression of Eq. (12) One can examine several special cases of Eqs. (16) and (17) which will provide some understanding of the behavior of these equations.

Case I - Small Michaelis constant, small initial microbial mass

The limiting value for this case is $K_s = 0$ which results in the exponential growth of microbes as given from the solution to Eq. (13) The substrate utilization is then

$$c/c_o = 1 - d_M \exp(K_M t) \tag{19}$$

In Eq. (18) the second term dominates for this case.

Case II - Large Michaelis constant, small initial microbial mass

For this case, d_s is considered large and one obtains the logistic growth equations (Eq. (15). In terms of substrate utilization, the solution is

$$c/c_o = \frac{(1+d_M)\exp(-(K_M t)(1+d_M)/d_s)}{d_M + \exp(-K_M t(1+d_M)/d_s)} \tag{20}$$

for small d_M (initial microbial mass relative to initial substrate concentration)

$$c/c_o = \frac{\exp(-K_M t/d_s)}{d_M + \exp(-K_M t/d_s)} = \frac{1}{1+d_M \exp(1-K_M t/d_s)} \tag{21}$$

Case III - Large initial microbial mass, large Michaelis constant

In this case, d_M is considered large, i.e. there is a large microbial mass relative to c_o at t = O. Under this condition, M' is relatively constant since the additional microbes produced by metabolism of c_o is small and $M' \simeq M'_o$. The appropriate dimensionless differential equation is then

$$\frac{d(c/c_o)}{d(K_M t)} = \frac{-d_M(c/c_o)}{d_s + c/c_o} \qquad (21)$$

whose solution is

$$d_s \log c/c_o + (c/c_o - 1) = K_M d_M t \qquad (23)$$

therefore, for large d_s, i.e small concentration of substrate relative to the Michaelis constant, the substrate decays exponentially as

$$c = c_o \exp\left(-K_M \frac{d_M}{d_s} t\right) \qquad (24)$$

Case IV - Large initial microbial mass, small Michaelis constant

On the other hand, for small d_s, i.e $K_s << c_o << M'_o$, the solution (Eq.20) is linear:

$$c = c_o (1 - K_M d_M t) \qquad (25)$$

until $\log (c/c_o) ds \tilde{} (c/c_o - 1)$ where the total solution (Eq. 20) indicates an exponential "tail".

Intermediate solutions can be thought of as a "linear combination" of two separate models: (a) Case I, an exponential

growth of microorganisms, as given by Eq. (13) where nutrients are not limiting, (K_s = 0 in Eq. (10)) and (b) Case II, logistic growth of microorganisms, as given by Eq. (14) where K_s >> c. In terms of the substrate utilization and utilizing the dimensionless notation, these two limits can be summarized as shown in Fig. 5. As indicated, therein, for various $d_M = M'_o/c_o$, the substrate utilization varies from a linear decrease to exponential to an autocatalytic form. Under certain conditions, therefore, an appropriate exponential decrease (first order kinetics) may be assumed in mathematical modeling under full recognition that other forms may prevail depending on the "mix" of microbial population, nutrient concentration and Michaelis constant. In the logistic growth region, for $0.1 < d_M < 1.0$ Fig. 5 shows that for complex river or estuarine systems it would be very difficult to detect departures from exponential substrate decay. Some data are available on laboratory studies to evaluate the range of M'_o. However, actual field estimates of microbial mass, and substrate concentrations are not available. As a consequence, laboratory studies generally use "large" initial substrate concentrations (d_s and d_M small) leading to specific non-exponential substrate utilization. Stratton and McCarty (1967) for ammonia oxidation obtained values of M_o @ 20°C of 0.0033 mg bacterial mass/l. At a yield coefficient, a, of 0.28 mg cells/mg substrate, this is equivalent to M'_o of about 0.01 mg/l NH_3-N. For this case however, K_s = 2.6 mg/l and c_o = 5.5 mg/l or d_s - 0.47. Stratton thus obtained ammonia curves similar to those shown in Fig. 5 for low values of d_M intermediate between exponential and logistic microbial growth. This then represents an initial low nitrifying population and "high" initial substrate concentration. At 20°C, for K_s ≈ 1-3.0 mg/l Knowles et al (1965) for normally low initial ammonia concentrations in natural waters, (0.5 mg/l), d_s for ammonia could be "large". If the ratio of initial cell mass, M'_o to initial concentrations is from 0.1 - 1.0 one should expect to see appropriate exponenti-

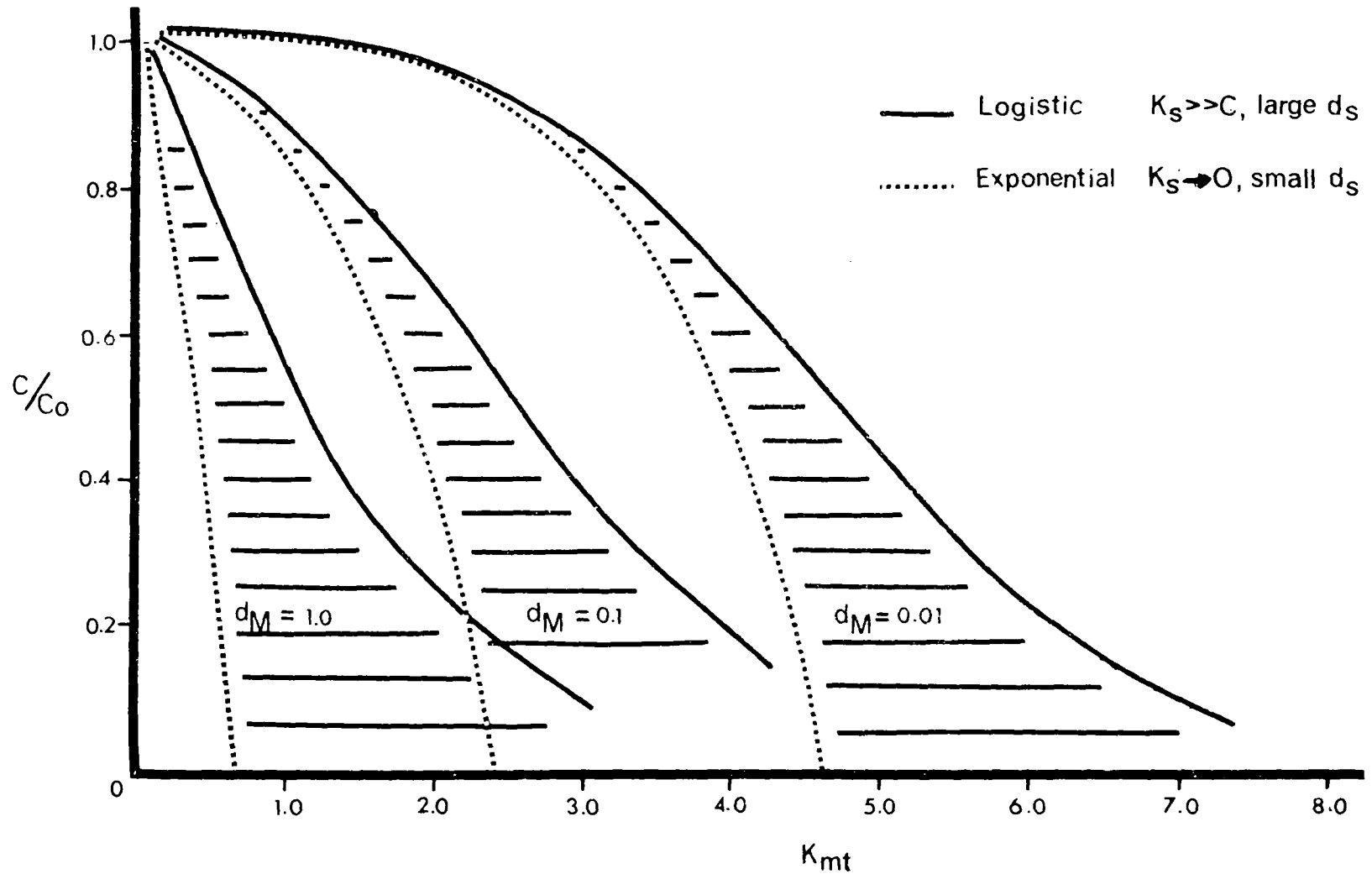

Fig. 5 Logistic and Exponential Growth of Microorganisms and Accompanying Nutrient Utilization

al behavior in the substrate. Therefore, for "dilute" systems where substrate concentrations are "low" and for "well seeded" systems where initial nitrifying populations are high relative to initial substrate concentrations, first order decay of substrate may be approximately justified. The actual application of these conditions must of course be made with care but as a first approximation, first order kinetics reactions for the nitrification phenomenon is a meaningful step and can aid in understanding the behavior of observed nitrogen forms in natural water systems.

First Order Steady State Mathematical Model of Streams and Estuaries

With an assumption of first order kinetic reactions and steady state conditions, several levels of mathematical models can be constructed each of which are useful in predictions of long-term effects of nitrification on water quality. The three levels of modeling are:

a) BOD equivalent models
b) Sequential reaction models
c) General feedback models

Each of the levels increases somewhat in the complexity of the equations and provides greater detail in understanding the phenomenon. The major reason for even considering several problem levels of first order kinetic models is that all problem contexts do not necessarily require complex models for their solution. Much can be learned from the first order models although it is important to stress again that the actual kinetic mechanisms are more complex than those which are considered herein. If it is obvious that non-linear kinetics apply then one should use the models presented below only as a gross approximation, if at all. For some problem contexts,

the first order kinetics assumption may be justified on the basis of the previous analysis. In any case, first order kinetics simplifies the structure of the models (linearity is presumed) and provides for rapid numerical solutions.

BOD equivalent models are particularly appropriate when the major portion of the nitrogenous demand is present as ammonia. Either a direct measurement of the ammonia and its oxygen equivalence or the second stage BOD measurement may be used. Either is then inputted as a sink of dissolved oxygen in a DO model. This approach becomes more approximate as the concentration of organic nitrogen becomes more significant. The organic nitrogen breaks down by hydrolysis to yield, among other products, ammonia. The oxidation of ammonia and the associate use of dissolved oxygen may therefore be delayed in accordance with the hydrolytic rate of reaction. This effect, if appreciable, is taken into account in the oxygen model by a reduction in the reaction coefficient of the nitrogenous BOD or by empirically introducing a lag in the initiation of nitrification. In spite of its simplicity, this model is quite adequate in a number of practical cases.

As indicated above, the nitrogenous oxygen demand, NBOD is given approximately by:

$$NBOD = 4.57\ (Org\text{-}N + NH_3\text{-}N)$$

This demand can be considered as an oxygen sink in the pair of equations describing the distribution of NBOD and DO deficit. For one dimensional steady state systems with constant coefficients, these equations are:

$$O = E \frac{d^2L_N}{dx^2} - u \frac{dL_N}{dx} - K_N L_N + W_N(x) \qquad (26)$$

$$0 = E \frac{d^2 D_N}{dx^2} - u \frac{dD_N}{dx} - K_a D_N + K_N L \qquad (27)$$

where E = dispersion coefficient (usually included only for estuaries), u = river velocity or net downstream velocity for estuaries, x = distance, L_N = nitrogenous BOD, D_N = DO deficit (due to nitrogenous BOD), K_N = rate of oxidation of NBOD, K_a = reaeration coefficient, W_N = waste discharges of NBOD.

Eqs. (26) and (27) can be recognized as the same set of equations that are used to describe the DO deficit due to the discharge of carbonaceous BOD (CBOD). For the constant coefficient case, the solutions to Eqs. (26) and (27) are:

$$L_N = L_{No} \exp(j_N X) \qquad (28a)$$

$$D_N = \frac{K_N L_{No}}{K_a - K_N} [\exp(j_N X) - \exp(j_a X)] \qquad (28b)$$

where for rivers where dispersive effects are small

$$j_N = \frac{K_N}{u}$$

$$j_a = \frac{K_a}{u} \qquad (29)$$

$$L_{No} = \frac{W_N}{Q}$$

and for estuaries where the tidal dispersion effect is im-

portant

$$j_N = \frac{u}{2E}\left(1 \pm \sqrt{1 + \frac{4K_N E}{u^2}}\right)$$

$$j_a = \frac{u}{2E}\left(1 \pm \sqrt{1 + \frac{4K_a E}{u^2}}\right) \qquad (30)$$

$$L_{No} = \frac{W_N}{Q\sqrt{1 + \frac{4KE}{u^2}}}$$

where for j_N and j_a the positive sign of the radical is associated with the negative x direction and the negative sign is associated with the positive x direction. The DO deficit profile due to the nitrogenous waste discharge is thus given by Eq. (28) The DO deficit due to the carbonaceous BOD must be added to this profile to determine the total DO deficit due to waste discharges.

The disadvantage of this simple model is that usually some judgment must be exercised in determining the spatial distribution of the reaction rate, K_N. In some instances, the field data may indicate that for various reasons (organic nitrogen hydrolysis, insufficient nitrifiers) an apparent lag exists in the exertion of the NBOD. The judgment incorporation of this effect becomes particularly significant when projections are made of expected water quality under different treatment schemes.

However, it is still somewhat surprising that even this simple model is often not considered in DO balance studies. This appears to be especially true in the numerous analyses conducted to estimate the effects of different levels of waste treatment

where the nitrogen discharges are largely unaffected by standard high rate biological treatment.

Sequential reaction models answer some of the disadvantages described above and especially apply when organic as well as ammonia nitrogen are present as inputs. Furthermore, when it is desirable to trace the individual components of the downstream nitrification process; organic, ammonia, nitrite and nitrate, this approach is useful. The lag effect is incorporated into the kinetic expression by the first step of a sequence of the coupled reactions. By contrast to the previous simplified approach, modeling with consecutive reactions is slightly more complicated analytically, requires more data, time and experience, but provides greater understanding and increased confidence in prediction.

The sequential reaction models follow each of the nitrogen components individually. The ammonia and nitrite outputs are then converted to oxygen demands and used as inputs into the DO deficit equation. The general constant coefficient equations are:

$$O = E\frac{d^2N_1}{dx^2} - u\frac{dN_1}{dx} - K_{11}N_1 + W_1(x) \quad (31)$$

$$O = E\frac{d^2N_2}{dx^2} - u\frac{dN_2}{dx} - K_{22}N_2 + K_{12}N_1 + W_2(x) \quad (32)$$

$$O = E\frac{d^2N_3}{dx^2} - u\frac{dN_3}{dx} - K_{33}N_3 + K_{23}N_2 + W_3(x) \quad (33)$$

$$O = E\frac{d^2N_4}{dx^2} - u\frac{dN_4}{dx} - K_{44}N_4 + K_{34}N_3 + W_4(x) \quad (34)$$

where N_1, N_2, N_3, and N_4 are organic, ammonia, nitrite and nitrate nitrogen respectively, K_{ii} represents the first order decay of substance i, K_{ij} is the forward reaction coefficient and W_i is the discharge of substance $_i$.

Equations (31) through (34) permit the determination of the individual nitrogen components and therefore represent a more realistic description of the nitrification process than Eqs.(26) and (27). The forcing functions for the DO deficit are 3.43 $K_{23}N_2$ and 1.14 $K_{34}N_3$; the first representing ammonia oxidation and the second nitrite oxidation. The entire scheme is sketched in a block diagram form in Figure 6. The equation for DO deficit due to the oxidation of nitrogen forms is:

$$0 = E\frac{d^2D_N}{dx^2} - u\frac{dD_N}{dx} - K_aD_N + 3.43K_{23}N_2(x) + 1.14K_{34}N_3(x) \quad (35)$$

where $N_2(x)$ and $N_3(x)$ are given from solutions of Eqs. (31) through (34).

Particular utilization of Eqs. (31) - (34) again depends on the water system either a river system where E = 0 or an estuarine system where tidal dispersion effects embodied in the dispersion coefficient may be significant.

The nature of the solutions to Eqs. (31) - (34) can be determined by considering the river case where advective forces dominate and dispersion can be considered zero. Further, one can assume that $K_{ii} = K_{i,i+1} \equiv k_i$ i.e that all material is conserved in each system and none of the forms of nitrogen are lost, for example, to the bottom sediments, ($K_{ii} > K_{i,i+1}$). The rate equations for the advective stream are then:

$$\frac{dN_1}{dt^*} = -K_1N_1 + W_1(x) \quad (36a)$$

$$\frac{dN_2}{dt^*} = K_1N_1 - K_2N_2 + W_2(x) \quad (36b)$$

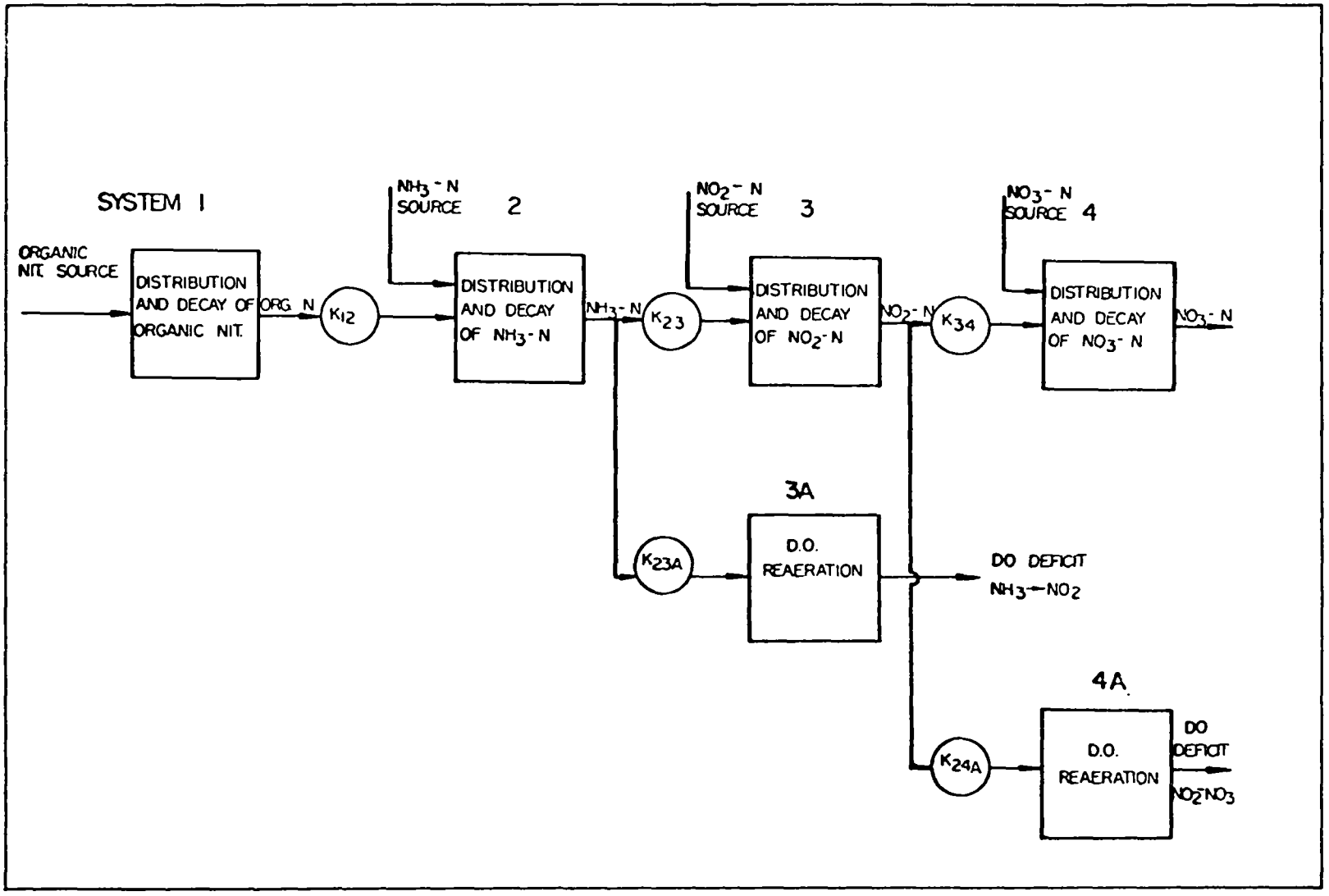

FIGURE 6

BLOCK DIAGRAM OF NITRIFICATION & DISSOLVED OXYGEN UTILIZATION

$$\frac{dN_3}{dt^*} = K_2N_2 - K_3N_3 + W_3(x) \qquad (36c)$$

$$\frac{dN_4}{dt^*} = K_3N_3 - K_4N_4 + W_4(x) \qquad (36d)$$

where $t^* = x/u$, the time of travel.

Eqs. (36) represent a series of first order coupled equations. The solution of Eq. (36a) is:

$$N_1 = N_{01} \exp(-K_1 t^*)$$

where N_{01} is the initial value of N_1 @ $x = 0$ given by mass balance incorporating $W_1(x)$.

Substitution of this solution into Eq. (36b) and integration gives the solution for ammonia, N_2 as:

$$N_2 = \frac{K_1 N_{01}}{K_2 - K_1} (\exp(K_1 t^*) - \exp(-K_2 t^*)) + N_{02}\exp(-K_2 t^*) \qquad (37)$$

Sequential substitution and integration gives the concentrations of nitrite and nitrate. For example, for nitrite,

$$N_3 = \frac{K_1 K_2}{K_2 - K_1} \left[\frac{\exp(-K_1 t^*) - \exp(-K_3 t^*)}{K_3 - K_1} - \frac{\exp(-K_2 t^*) - \exp(-K_3 t^*)}{K_3 - K_2}\right] N_{01}$$

$$+ \frac{K_2}{K_3 - K_2} [\exp(-K_2 t^*) - \exp(-K_3 t^*)] N_{02} \qquad (38)$$

$$+ K_3 N_{03} \exp(-K_3 t^*)$$

Each of the preceding inputs is reflected in this equation. In general, the total amount of end product formed by virtue

of the initial sources, $C_{01} \longrightarrow C_{0n}$ (for n reaction steps) is:

$$C_{n0} = \sum_{t=1}^{n} C_{0i} \exp(-K_i t^*)$$

and due to the intermediate steps is

$$C_{ni} = \sum_{i=1}^{n} \frac{K_{i-1} C_{0,i-1}}{K_i - K_{i-1}} [\exp(K_{i-1} t^*) - \exp -K_i t^*)$$

the sequential nature of these solutions is shown in Figure 7 where the last nitrogen form, the nitrate nitrogen is assumed conservative, i.e $K_4 = 0$.

For estuarine situations, the solutions essentially follow the same form except that a series of unknown coefficients are introduced by virtue of mass balances that are required. The number of coefficients is equal to the number of equations that can be written down so that explicit numerical determination of the coefficients is possible. For example, the solution to Eq. (31) for point source loads is

$$N_1 = B_1 \exp(S_1 x) + C_1 \exp(V_1 x) + YBN \qquad (39)$$

where $S_1 = \frac{u}{2E} (1 + \sqrt{1 + 4 K_1 E/u^2})$

$$V_1 = \frac{u}{2E} (1 - \sqrt{1 + 4 K_{11} E/u^2})$$

B_1 and C_1 = constants to be evaluated from consideration of boundary conditions

and YBN = particular integral of sources and sinks of N_1.

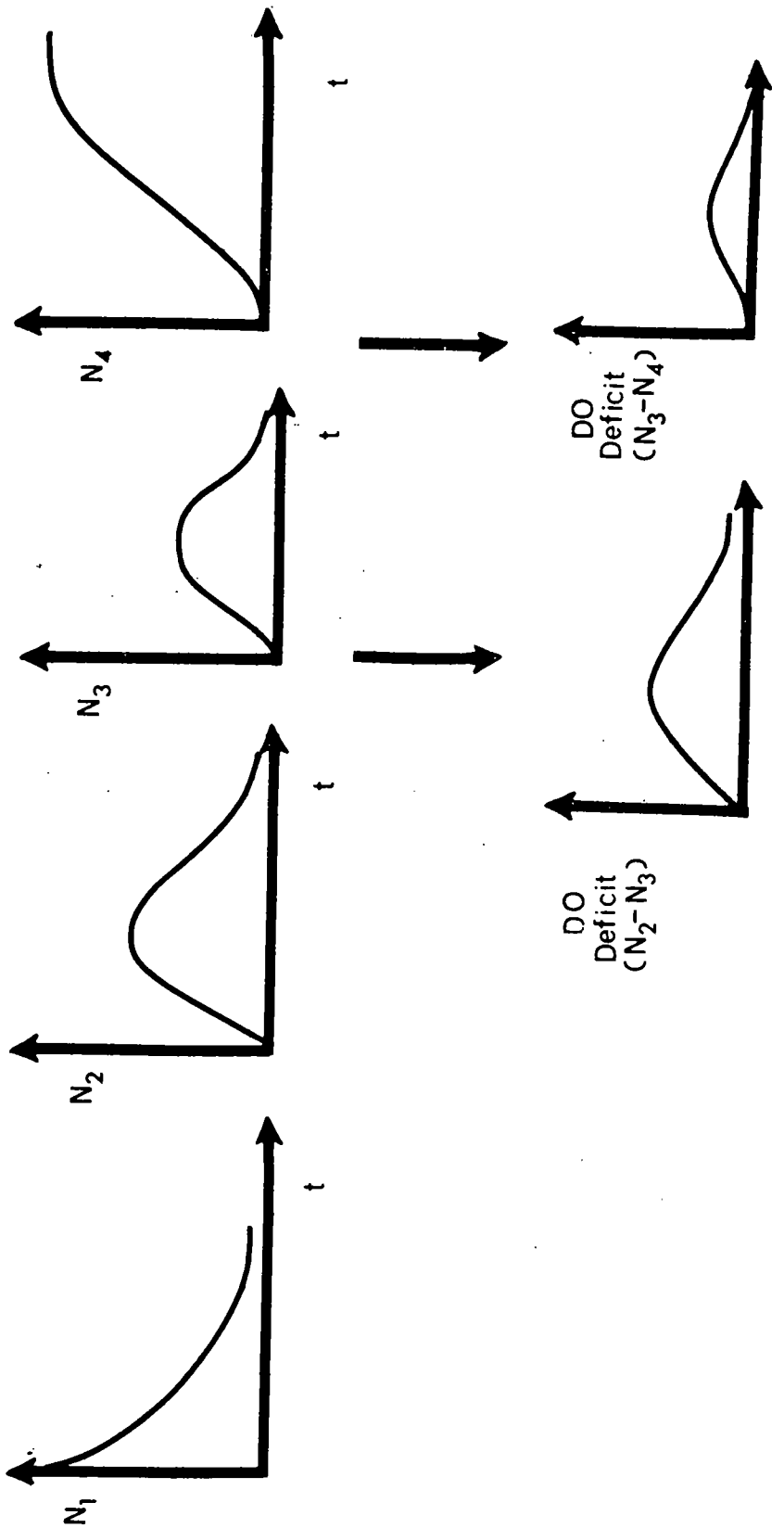

Fig.7 Sequential Reactions in Nitrification - First Order Kinetics - Stream System

An equation similar to (39)can also be written down for N_2 with the input from N_1 appearing in the particular integral. Thus,

$$N_2 = B_2\exp(S_2x) + C_2\exp(V_2x) + \frac{K_{12}}{K_{22}-K_{11}}[B_1\exp(S_1x) + C_1\exp(V_1x)] \quad (40)$$

Eq. (40) can be compared to Eq. (37). This procedure is repeated for each nitrogen form resulting in four solution equations (see also Eq. (38)) in eight coefficients. Application of boundary conditions, mass balance and concentration equality at each section provides the necessary equations to evaluate these coefficients. Details are given in Anon., 1969 and the application of this model to the Delaware Estuary is discussed below.

Another approach that can be used to model sequential reactions is to replace the spatial derivatives with finite approximations. This results in a series of algebraic equations which can be solved simultaneously to obtain the spatial distribution of each nitrogen form. A generalization of this approach is explored in detail in the next section.

In summary, models of sequential reactions are readily structured utilizing the steady state and first order kinetic assumptions. For the nitrification effect, these models "track" the spatial distribution of each of a series of forms allowing direct computation of the DO deficit due to nitrogen oxidation. For streams, the solutions can be obtained directly while for estuaries some type of computer solution is often required.

Feedback models incorporate feedback loops between any of the respective systems. In principle, this third model can include

many of the features of the complete nitrogen cycle if one accepts the assumptions of linearity and first order kinetics. Typical examples of feedback systems include denitrification and algal utilization. The denitrification phenomenon may involve two feedback loops; NO_3 to NO_2 (with attendant evolution of N_2 gas) and NO_2 to NH_3. Both of these feedback reactions occur under conditions of "low" dissolved oxygen. Actually, a more complete model of the system would include a non-linear interaction between DO and the feedback reaction rates.

The utilization of ammonia and nitrate by phytoplankton also introduces feedback loops. Organic nitrogen is formed as a part of the complex living matter in algae cells which upon death release the organic nitrogen in dissolved form thereby completing the cycle. This is an obvious over-simplification of the actual mechanism which is dynamic and includes non-linear growth limiting terms. However, the problem addressed here is to introduce the feedback aspect into the steady state sequential models discussed in the previous section.

The general feedback model makes use of a finite difference approximation to Eqs. (31) - (34) and incorporates the first order feedback reaction coefficients. The differential equations which incorporate feedback are:

$$
\begin{aligned}
0 &= E\frac{d^2N_1}{dx^2} - u\frac{dN_1}{dx} - K_{11}N_1 + K_{21}N_2 + \ldots K_{41}N_4 + W_1(x) \\
0 &= E\frac{d^2N_2}{dx^2} - u\frac{dN_2}{dx} + K_{12}N_1 - K_{22}N_2 + K_{32}N_3 + K_{42}N_4 + W_2(x) \qquad (41) \\
0 &= E\frac{d^2N_4}{dx^2} - u\frac{dN_4}{dx} - K_{44}N_4 + K_{14}N_1 + \ldots + K_{34}N_4 + W_4(x)
\end{aligned}
$$

Equations (41) indicate all possible feedforward reactions K_{ij} (j>i) and all possible feedback reactions (i>j). The separate inclusion of K_{ii} allows for possible loss of material from the system due for example to bottom deposition. In general, to prevent creation of nitrogen it is true that

$$K_{ii} \geq \sum_{j} K_{ij} \quad (i \neq j)$$

If a finite difference approximation is made to these equations (or equivalently a mass balance is constructed around a finite section) a series of n algebraic equations results where n is the number of finite sections (Thomann, 1972). It should be noted that this approach is not restricted to one-dimensional systems.

A finite difference approximation to the first equation of Eq. 41 is given for spatial segment k as:

$$\begin{aligned} 0 = &\sum_{j} \{-Q_{kj} (\alpha_{kj} N_{1,k} + \beta_{kj} N_{1,j}) + E'_{kj} (N_{1,j} - N_{1,k})\} \\ &- V_k K_{11,k} N_{1,k} + V_k K_{21,k} N_{2,k} + \cdots V_k K_{41,k} N_{4,k} \\ &+ W_{1,k} \qquad (k = 1,2 \ldots n) \end{aligned} \tag{42}$$

where Q_{kj} is the net flow from section k to j (positive outward); V_k is the volume of the k^{th} segment; α_{kj} is a finite difference weight = max (1/2, 1-E'/Q) chosen for solution stability; $\beta_{kj} = 1 - \alpha_{kj}$; E_{kj} is a bulk tidal dispersion coefficient given by

$$E'_{kj} = \frac{E_{kj} A_{kj}}{L_k + L_j}$$

where A_{kj} is the interfacial cross sectional area and L_k and L_j are segment lengths of segments k and j; and $W_{1,k}$ is the direct discharge of waste material, N_1. The notation $N_{1,k}$ indicates the spatial distribution in all k segments of the water body of the first nitrogen form. If in Eq. (37) all terms involving the dependent variables N_1 are grouped on the left hand side and the input forcing function, $W_{1,k}$ and other nitrogen forms, N_i on the right hand side, one obtains:

$$a_{kk}N_{1,k} + \sum_j a_{kj}N_{1,j} = W_{1,k} + V_kK_{21,k}N_{2,k} + \cdots V_kK_{41,k}N_{4,k} \quad (43)$$

where

$$a_{kk} = \sum_j (Q_{kj}\alpha_{kj} + E'_{kj}) + V_kK_{11,k} \quad (43a)$$

$$a_{kj} = Q_{kj}\beta_{kj} - E'_{kj} \quad (43b)$$

A total of n equations similar to Eq. (43) can be written down for each of the spatial segments. The system of equations is then

$$a_{11}N_{1,1}+a_{12}N_{1,2}+\cdots a_{1n}N_{1,n} = W_{1,1}+V_1K_{21,1}N_{2,1}+\cdots V_1K_{41,1}N_{4,1}$$

$$a_{21}N_{1,1}+a_{22}N_{1,2}+\cdots a_{2n}N_{1,n} = W_{1,2}+V_2K_{21,2}N_{2,2}+\cdots V_2K_{41}N_{4,2}$$

$$\vdots$$

$$a_{n1}N_1+a_{n2}N_{1,2}+\cdots a_{nn}N_{1,n} = W_{1,n}+V_nK_{21,n}N_{2,n}+\cdots V_nK_{41,n}N_{4,n}$$

In matrix form, Eqs.(44) are

$$[A_1]\ (N_1) = (W_1) + [VK_{21}](N_2) + [VK_{31}](N_3) + [VK_{41}](N_4) \quad (44)$$

where the subscripts refer to the nitrogen forms and $[VK_{ij}]$ is a diagonal matrix of the product of volumes and reaction

rates. The dimensionality of the matrices and vectors represents the spatial distribution of the nitrogen species. Thus, [A] is a n X n matrix and (N_k) are n x 1 vectors.

The entire procedure used to obtain Eq. (44) for the first nitrogen form is now repeated for the second through fourth forms. The four matrix equations are then given by

$$\begin{aligned}
[A_1](N_1) &= (W_1) + [VK_{21}](N_2) + [VK_{31}](N_3) + [VK_{41}](N_4) \\
[A_2](N_2) &= (W_2) + [VK_{12}](N_1) + [VK_{32}](N_3) + [VK_{42}](N_4) \\
[A_3](N_3) &= (W_3) + [VK_{13}](N_1) + [VK_{23}](N_2) + [VK_{43}](N_4) \\
[A_4](N_4) &= (W_4) + [VK_{14}](N_1) + [VK_{24}](N_2) + [VK_{34}](N_3)
\end{aligned} \tag{45}$$

It should be recalled that in Eqs. (45), the $[A_i]$ matrices differ only in the reaction coefficient K_{ii} on the main diagonal (see Eq. 43a). There are 4 n algebraic equations in Eqs. (45) which can be solved by a variety of block decomposition and relaxation techniques. Some additional insight can be obtained by continuing the matrix analysis. The set of matrix equations (45) can be written as

$$\begin{bmatrix}
[A_1] - [VK_{21}] - [VK_{31}] - [VK_{41}] \\
-[VK_{12}] \quad [A_2] - [VK_{32}] - [VK_{42}] \\
-[VK_{13}] - [VK_{23}] \quad [A_3] - [VK_{43}] \\
-[VK_{14}] - [VK_{24}] - [VK_{34}] \quad [A_4]
\end{bmatrix}
\begin{pmatrix} (N_1) \\ (N_2) \\ (N_3) \\ (N_4) \end{pmatrix}
\begin{pmatrix} (W_1) \\ (W_2) \\ (W_3) \\ (W_4) \end{pmatrix} \tag{46}$$

or

$$[\bar{A}]\ (\bar{N}) = (\bar{W}) \tag{47}$$

where $[\bar{A}]$ is a 4n X 4n matrix and $(\bar{N})$ and $(\bar{W})$ are 4n X 1 vectors. Of course, in Eqs.(46) not all feedback or feedforward loops need be included. For a given sequence of

loops, the solution for the four variables in all spatial segments is formally given by

$$(\bar{N}) = [\bar{A}]^{-1} (\bar{W}) \tag{48}$$

The DO deficit due to these reactions is now readily computed. If (N_2) represents ammonia and (N_3) nitrite then a similar differencing procedure yields for the DO deficit

$$[B](D)_N = 3.43\ [VK_{23}](N_2) + 1.14\ [VK_{34}](N_3) \tag{49}$$

where [B] is an n X n matrix identical to the form of the $[A_i]$ matrices except that the reaeration rate, K_a, appears on the main diagonal instead of K_{ii} and $(D)_N$ represents the spatial distribution vector of DO deficit due to the nitrification effect. Note that once Eqs (45) have been programmed Eq. (49) is a special case of that set of equations and does not require a separate computer program.

A general multi-dimensional first order kinetic steady state water quality problem with any number of variables and system configuration can thus be structured by solving an MN system of equations (Eqs. (45)) where M is the number of variabled forms (for nitrogen, M = 4).

For one-dimensional estuaries, the form of the matrices $[A_i]$ is tridiagonal which simplifies the computations. If no feedback loops are incorporated, Eqs. (45) reduce to the sequential reaction models discussed in the previous section and $[\bar{A}]$ becomes upper triangular. In any case, multidimensional systems with interacting (first order) reactions can be readily and quickly analyzed by simply solving a set of linear algebraic equations. This of course by-passes the entire issue of how one determines the K_{ij} coefficients. This is discussed in the succeeding sections on applications.

Application of First-Order Models to the Delaware Estuary

This estuary extends for about 86 miles from Trenton, N.J. to Delaware Bay. The river flows past the metropolitan Philadelphia area and enters Delaware Bay about 50 miles from the Atlantic Ocean. The estuary receives large amounts of carbonaceous and nitrogenous wastes from municipalities and industries and is characteristic of a system where bacterial nitrification leading to oxygen depletion appears to be predominant (Anon., 1969; O'Connor et al, 1969). The municipal and industrial nitrogenous components are indicated in Table 2.

Table 2

Estimated Municipal and Industrial Nitrogen Discharges to Delaware Estuary *
(pounds/day)

	Organic Nitrogen	Ammonia Nitrogen	Nitrate Nitrogen
Municipal	28,500	48,500	2,000
Industrial	-	32,500	30,500
	28,500	81,000	32,500
Delaware River @ Trenton (3,000 cfs)	9,000	1,000	16,000
Total	37,500	82,000	48,500

*Anon (1969)

A total direct load of 109,500 lbs of oxidizable nitrogen per day is discharged from the municipal and industrial waste sources.

In order to incorporate the effect of local drainage along the length of the estuary, a runoff load equivalent to about

110 pounds of organic nitrogen/day/mile was inputted together with an equal amount of ammonia nitrogen.

A continuous solution model was used to represent the organic, ammonia, nitrite and nitrate forms. Only sequential bacterial nitrification was included specifically in the model. Algal and denitrification effects were included qualitatively. The continuous solution model (see Eqs. 39-40) was applied to seven reaches of the estuary each of which included its representative geometry (area, depth) and sequential reaction coefficient (Anon, 1969). This type of model in contrast to the finite difference approximation models results in continuous solutions. Thus, although the first segment in the Delaware Estuary nitrogen model under discussion here is thirty miles long, a continuous solution (for constant spatial parameters) is obtained throughout this length. The cross-sectional area changes in the estuary were therefore approximated by the seven segments. Major point discharges were grouped according to this segment breakdown. This is a simplification introduced to avoid numerous segment junctions at each discharge location.

The verification procedure consisted of comparing calculated profiles from the four system model to a set of observed data representative of steady-state summer conditions. The reaction rates obtained for each of the nitrogen components were then used in the examination and verification of other profiles under different flow and temperature conditions. A consistent set of first-order reaction coefficients was therefore obtained which provides a reasonable representation of the observed phenomena.

Figure 8 shows the results of the first verification analysis of data collected by the Delaware Water Pollution Commission during July - August, 1964. The reaction coefficients shown

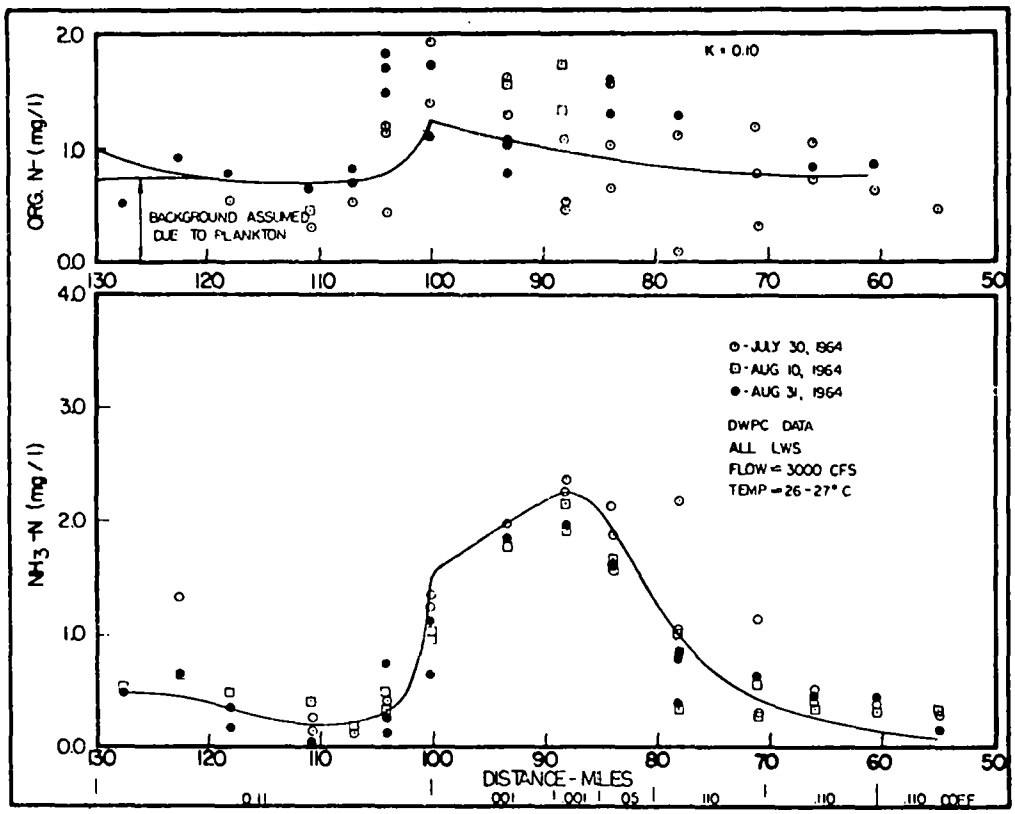

Fig. 8 Observed vs. Computed (solid line) Nitrogen Profile August 1964 (after Anon.1969)

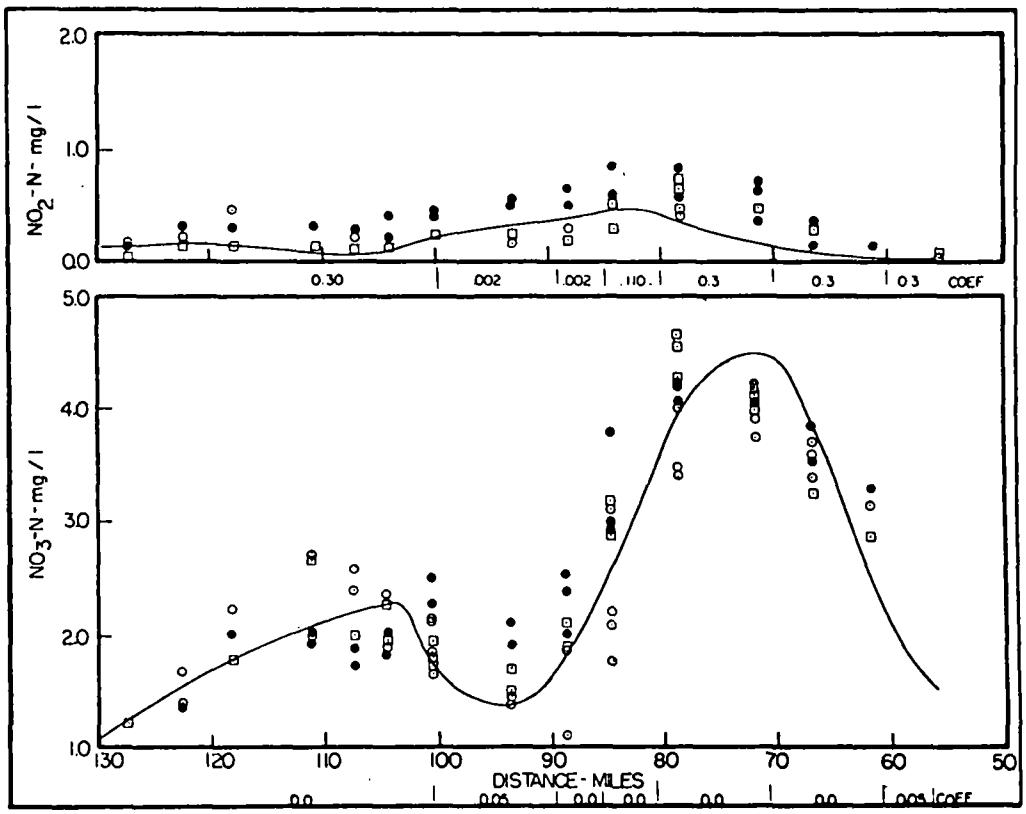

for each of the species do not constitute a unique set of rate coefficients but represent a trial and error fit of the observed data. The coefficients are consistent however with other verification analyses. This is explored further below.

Several other points should be noted in this verification analysis. The direct discharge of organic nitrogen waste loads does not alone account for the total of about 1/mg/l that was observed. It was therefore hypothesized that 0.75 mg/l of organic nitrogen was due to the presence of plankton and does not enter into subsequent nitrification reactions. This is equivalent to about 75 µg/l to 150 µg/l which is within the range of observed chlorophyll measurements for the Delaware.

It can also be noted that the ammonia profile was verified by employing a reduced reaction rate from mile 100 to mile 85. This was justified because of the low dissolved oxygen (< 2 mg/l and minimums of about 0.7 mg/l) in this reach.

The nitrate analysis indicates two areas of nitrate decay. The first reach from mile 100-90 is attributed to denitrification. Because feedback loops were not used in this investigation, it was not possible to recycle this nitrate reduction into the system. Nitrate decay at the lower end of the estuary was assumed to be due to increased phytoplankton utilization of nitrate.

Experimental information on the influence of temperature on nitrification is meager. Work on the Thames estuary (Anon, 1964) indicated for the temperature dependence of the oxidation of ammonia:

$$K_T = K_{20}\theta^{T-20}$$

with θ = 1.017. Laboratory work however indicated θ = 1.10. Others (Stratton and McCarty, 1967; Buswell et al, 1959) have estimated θ at about 1.08 while for nitrite oxidation a value of 1.06 has been determined (Stratton and McCarty, 1967). After review of available results, the temperature dependence of the reaction rates was hypothesized as shown in Figure 9.

Data were available for the period November 1967 when water temperatures were 7° - 10°C and river flows at Trenton were about 8900 cfs. 1964 loads were used. Figure 10 summarizes the results of the application of the model to these lower temperature data. A reaction rate of 0.025 (@ temperature = 7.5°C) was used for the conversion of organic nitrogen, .01 for ammonia, .05 for nitrite and 0.0 for nitrate. At these low rates, almost all forms behave as conservative variables. It was not necessary in this case to make the assumption that plankton had synthesized nitrogen into living tissue. At the low estuary temperatures, most plankton activity would be minimal. The ammonia plot in Figure 10 distinctly shows the effect of reduced nitrification. This can be especially seen by comparing the Nov. 1967 data (Fig. 10) to the August 1964 data (Fig. 8). The reduced nitrification effect at low temperatures is also evident in the nitrite and nitrate profiles. This effect will also be reflected in reduced oxygen utilization and has a significant impact on treatment programs that may use nitrification.

The final step in the verification analyses was to use the preceding reaction coefficients temperature dependence and supporting assumption to "independently" verify other profiles. Figure 11 is an example. As indicated, agreement is good supporting the assumption of a consistent set of coefficients. The only change in the coefficients was to distribute the area

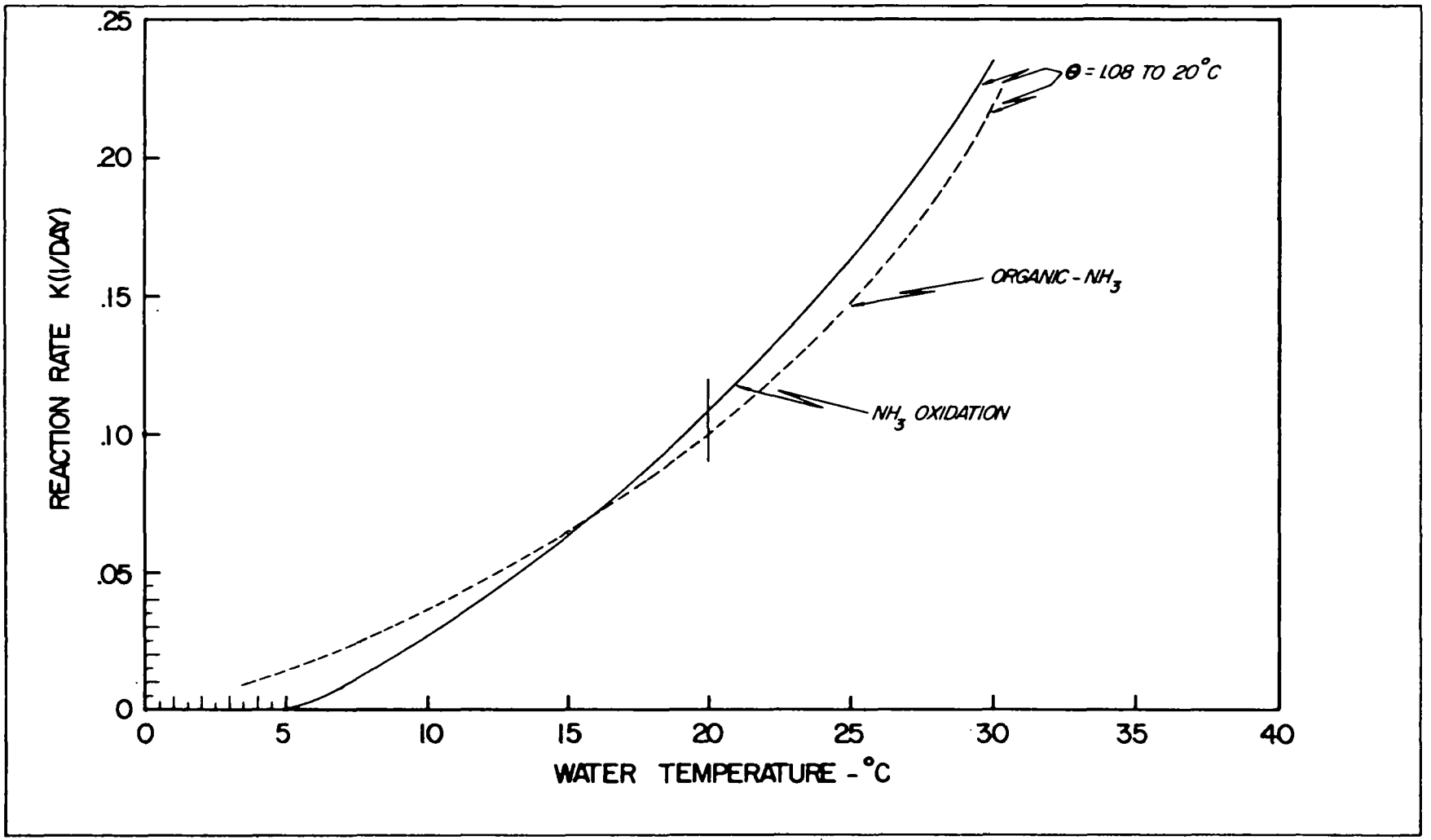

Figure 9

Estimated Temperature Dependence of Nitrification Reaction Rates (after Anon.1969)

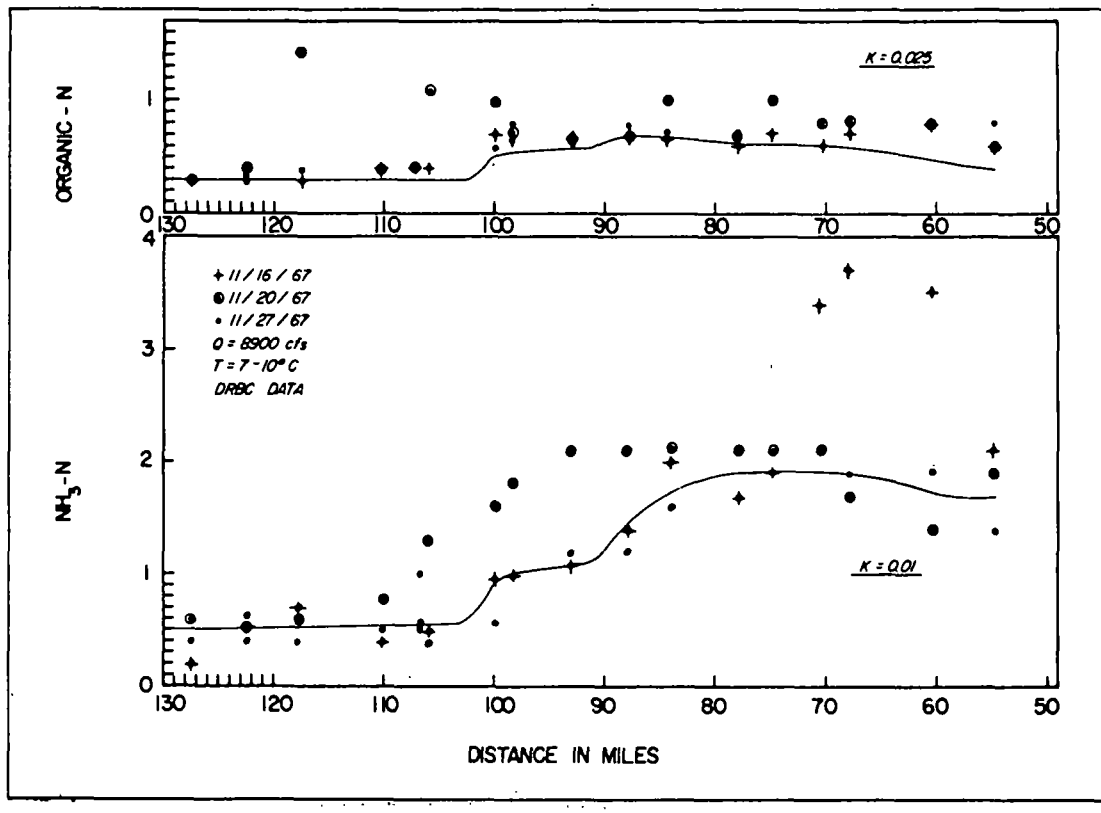

Figure 10
Observed vs. Computed (solid line) - Nitrogen Profiles
November 1967 (after Anon, 1969)

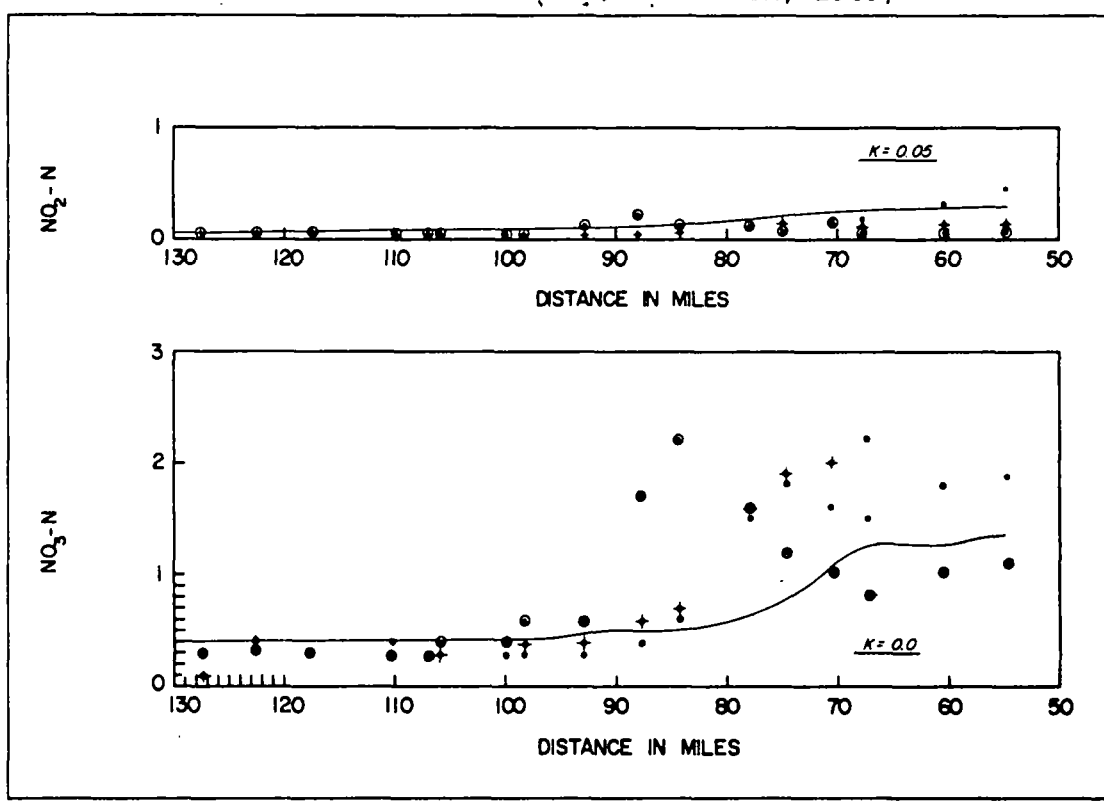

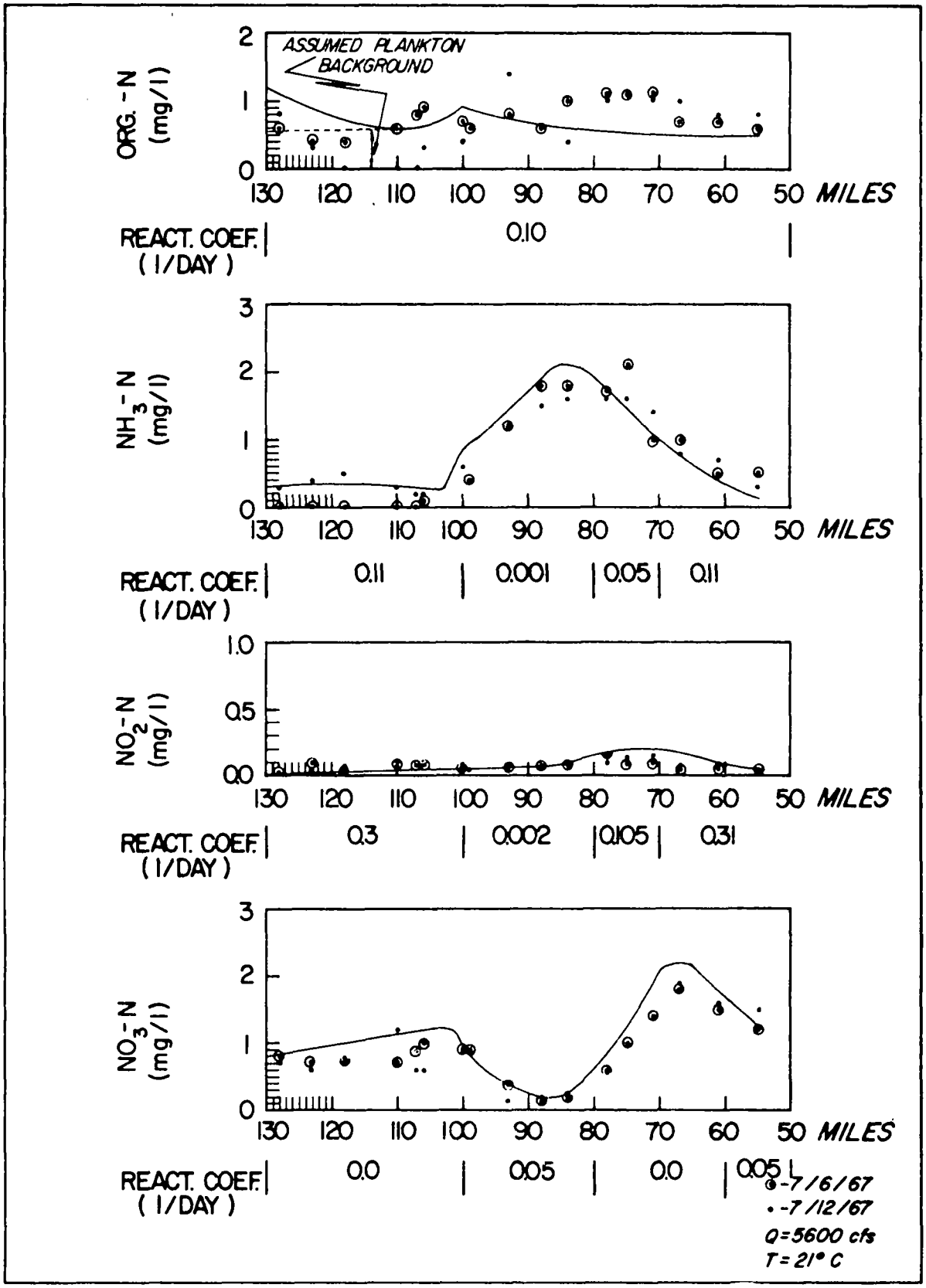

Figure 11
Observed vs. Computed (solid line) - Nitrogen Profiles
July 1967 (after Anon.,1969)

of nitrification inhibition in accordance with low DO reaches. The additional verifications were obtained with ease, once the order of the coefficients had been established from the August 1964 and November 1967 analyses. The consistency of the reaction coefficients is illustrated in Table 3. While the set of coefficients is certainly not unique, Table 3 shows that the general order of magnitude of the coefficients is consistent providing allowance is made for variable spatial distributions of the coefficients due to low dissolved oxygen values.

The four system model can be used to estimate the effects of the nitrification reaction on the dissolved oxygen deficit, as indicated in Figure 6.

The organic and ammonia waste sources are inputted into the initial two systems. The output from the ammonia system is then multiplied by the reaction rate K_{23A}, which is given by 3.43 K_{23}. This then represents the sink of dissolved oxygen due to ammonia oxidation and is inputted into the third system which now represents the dissolved oxygen system with its accompanying reaeration rate. The total of three systems are therefore used and the output from the third system represents the dissolved oxygen deficit due to NH_3 - NO_2 oxidation. A similar procedure is followed for the NO_2 - NO_3 oxidation, where $K_{34A} = 1.14K_{34}$.

Figure 11 shows a typical result for the July - August 1964 condition. The reaction rates for nitrification shown in Figure 8 were used in the computation together with a constant spatial reaeration rate of 0.18/day at 20°C. The two components of the nitrification are shown. A slight shift downstream of the NO_2 - NO_3 component relative to the NH_3 - NO_2 component can be noted. Also, the peak in the total deficit occurs some

Table 3

SUMMARY OF REACTION COEFFICIENTS
DETERMINED IN VERIFICATION ANALYSIS OF NITROGEN
IN DELAWARE ESTUARY

Survey	Reach No.	Org. to NH_3 (K_{12})	NH_3 to NO_2 (K_{23})	NO_2-NO_3 (K_{34})	NO_3 (K_{44})
		First Order Reaction Coefficient @ 20°C			
July-Aug. 1964	1	0.1	0.11	0.3	0.0
Q = 3000 cfs	2	↓	0.001	0.002	0.05
T = 26°C	3	↓	0.001	0.002	0.0
	4	↓	0.05	0.110	0.0
	5-6	↓	0.11	0.3	0.0
	7	0.1	0.11	0.3	0.5
June-July 1965	1	0.1	0.11	0.3	0.0
Q = 2000 cfs	2	↓	0.001	0.002	0.05
T = 20°C	3	↓	0.001	0.002	0.0
	4	↓	0.5	0.110	↓
	5	↓	0.110	0.3	↓
	6	↓	↓	↓	↓
	7	↓	↓	↓	0.05
	8	0.1	0.110	0.3	0.05
July 1967	1	0.1	0.11	0.3	0.0
Q = 5600 cfs	2	↓	0.001	0.002	0.05
T = 21°C	3	↓	0.001	0.002	0.05
	4	↓	0.001	0.002	0.05
	5	↓	0.05	0.105	0.0
	6	↓	0.11	0.3	0.0
	7	0.1	0.11	0.3	0.05
		First Order Reaction Coefficient @ 7-10°C			
Nov. 1967	1	0.025	0.01	0.05	0.0
Q = 8900 cfs	2	↓	↓	↓	↓
T = 7-10°C	3	↓	↓	↓	↓
	4	↓	↓	↓	↓
	5	↓	↓	↓	↓
	6	↓	↓	↓	↓
	7	0.025	0.01	0.05	0.0

10 - 15 miles downstream of the major waste sources reflecting the inhibited nitrification upstream due to low dissolved oxygen. It is also quite interesting to note a general background of 0.7 - 1.0 mg/l dissolved oxygen deficit due to the nitrogenous discharges from tributaries and run-off as well as municipal and industrial sources. The peak value of 2.5 mg/l dissolved oxygen deficit is somewhat lower than previous estimates which placed the peak at about 3.0 mg/l dissolved oxygen deficit, but at approximately the same location. Part of this difference is attributable to the use of the four system model rather than an approximation through "nitrogenous BOD" with associated reduction in nitrogenous BOD decay rate or simple translation of the input of nitrogenous BOD. In general, then, Figure 12 confirms previous work which recognized a downstream shift of the satisfaction of the nitrogenous oxygen demand. The results indicate that this phenomenon is due to low upstream dissolved oxygen values which together with the discharge of potentially toxic materials have an inhibitory effect on the nitrifying bacteria. As the dissolved oxygen recovers, the nitrifying flora begins to develop and bacterial nitrification proceeds at a relatively rapid pace. This is then accompanied by an increasing utilization of oxygen.

Projected effects of a nitrogen removal program can be estimated using this model. Nitrogen removal from waste effluents can be accomplished in several ways including biological nitrification, air stripping and ion exchange. Each of the methods accomplishes varying degrees of removal of nitrogenous components and at widely varying costs.

Figure 12 showed the estimated dissolved oxygen deficit due to nitrification for 1964 summer conditions. It should be recalled that the peak dissolved oxygen deficit occurred at about mile 75 because of assumed nitrification inhibition

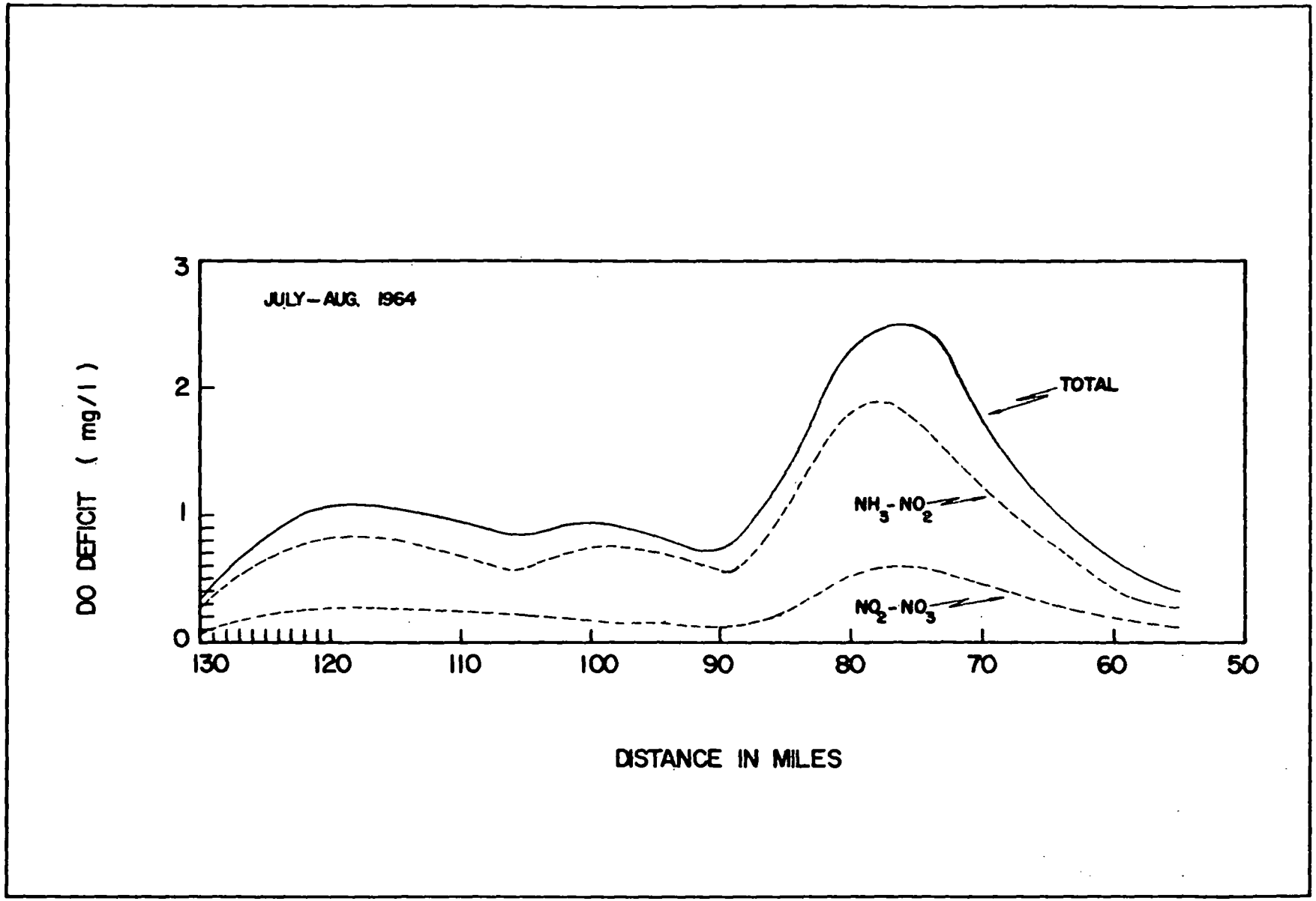

FIGURE 12
ESTIMATED DO DEFICIT DUE TO NITRIFICATION (After Anon.,1969)

from mile 100 - 85. This inhibition was ascribed to low dissolved oxygen conditions in that reach. If, following implementation of the waste control program, dissolved oxygen conditions were at a higher level (say greater than 2 mg/l everywhere), it is informative to explore the resulting effect of nitrification on dissolved oxygen. Two possibilities exist under improved dissolved oxygen:

a) ammonia oxidation will take place throughout the entire length of the estuary at approximately a rate of 0.1/day. This will result in a shift of the maximum dissolved oxygen deficit upstream.
b) because of generally improved water quality, algal utilization of ammonia may now increase throughout the length of the estuary. Since many algal species utilize ammonia preferentially, the ammonia would be tied up in organic form, and not contribute to the deficit until some time later in the year. The rate of this phenomenon is unknown.

Both effects will probably proceed simultaneously. However, in order to provide a somewhat conservative estimate, it can be assumed that all the ammonia will be oxidized and will contribute to the dissolved oxygen deficit. Under this assumption, model runs were made using ammonia oxidation rates of 0.11/day everywhere, and the dissolved oxygen deficit was computed. The results are shown in Figure 13.

As shown, under favorable nitrification conditions, with ammonia oxidation proceeding uniformly, the maximum dissolved oxygen deficit shifts upstream to about mile 90. There is a decrease of about 0.2 mg/l in the maximum, and a general spreading over a larger area. At mile 90, the deficit increases from about 0.5 mg/l to about 2.2 mg/l under favorable nitrification conditions. On the other hand, at mile 75, the

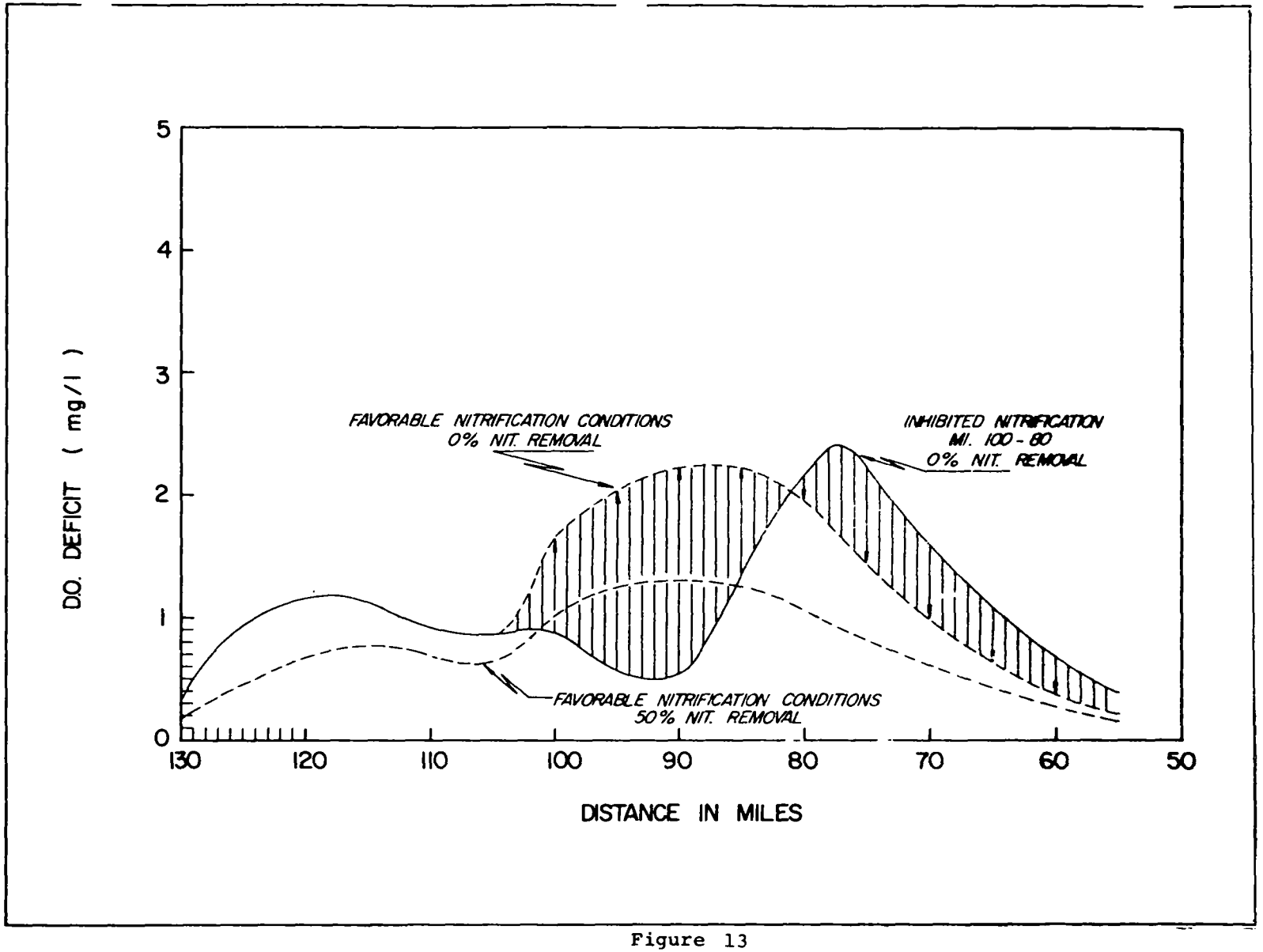

Figure 13

DO Deficits Under Different Nitrification Conditions (after Anon.,1969)

dissolved oxygen deficit decreases from about 2.2 mg/l to about 1.4 mg/l. The difference between the downstream dissolved oxygen deficit and upstream increase is due to the increasing cross-sectional area of the estuary as one proceeds in the downstream direction. If a 50% removal of oxidizable nitrogen were accomplished, the estimated disxolved oxygen deficit profile is as shown in Figure 13. A general decrease is noted with a maximum dissolved oxygen deficit of about 1.3 mg/l in the area of mile 90. In order to provide an overall estimate of the effect of this shift in the dissolved oxygen deficit profile and projected water quality goals, a preliminary analysis was made of the estimated dissolved oxygen profile under existing waste removal requirements.

The estuary proper has been divided by the Delaware River Basin Commission into four (4) zones with ultimate carbonaceous BOD removal requirements ranging from 86% to 89%, based on raw 1964 waste loads. These requirements will generally be met by various types of secondary treatment, including for municipalities, biological waste reduction. It is difficult at this stage to estimate the extent of nitrogen reduction to be expected from this program. The particular design practices will govern this factor. However, for estimating purposes, a value of about 20% oxidizable nitrogen reduction appears reasonable.

A dissolved oxygen analysis was therefore made, using the same sectional breakdown as used in the nitrification model. The analysis indicated that under a 20% nitrogen removal of 1964 loads the dissolved oxygen goal of the DRBC will probably be met. The critical region is in the vicinity of mile 100-90. Under 50% nitrogen removal of 1964 loads, the DRBC dissolved oxygen goals will be met with a greater degree of

assurance; the steady-state DO profile is estimated to be everywhere above 4.0 mg/l.

The 20% removal program is equivalent to a discharge load about 95,000 lbs/day of oxidizable nitrogen which would be allowable while a 50% removal program is equivalent to a discharge load of about 60,000 lbs/day of oxidizable nitrogen. Ultimately therefore waste removal programs must assign both carbonaceous BOD loads and nitrogen loads both on a pounds/day basis. General unquantifiable factors that will tend to further enhance the attainment of dissolved oxygen goals include algal utilization of ammonia with subsequent reductions in the dissolved oxygen deficit due to nitrification, ammonia oxidation at a slower rate than that assumed and specific encouragement of nitrogen removal. Factors that will tend to mitigate against achievement of the objective include a faster rate of ammonia oxidation which will intensify and shorten the area of minimum dissolved oxygen or carbonaceous removal designs that result in oxidizable nitrogen removal of less than 20%.

Application of First-Order Model to the Potomac Estuary

The Potomac River discharges into Chesapeake Bay and extends over 100 miles upstream to the head of the estuary at Little Falls. The major waste source is the effluent of the Washington, D.C. secondary waste treatment plant. Water quality problems include low dissolved oxygen in the vicinity of the District of Columbia discharge and generally high algal concentrations.

Hetling and O'Connell (1968) and Jaworski, et al (March, 1969; May, 1969) summarized data pertaining to dissolved oxygen, nutrients and chlorophyll. These results were obtained from

a series of sampling stations in the Potomac where data were collected over a period of months during 1967, 1968 and again during 1969. Waste load information from the point waste discharge locations as well as from land run-off has also been obtained.

A steady state feedback model which considers organic ammonia and nitrate nitrogen form was constructed. The assumption of first order kinetics prevailed throughout. A feedback loop is incorporated which represents ammonia and nitrate nitrogen utilization by algae with the subsequent nitrogen release upon death recycled to the organic nitrogen form. The nitrification phenomenon was also inputted to the dissolved oxygen deficit system. A total of five systems was therefore modeled.

The equations are:

$$
\begin{aligned}
0 &= \frac{1}{A}\frac{d}{dx}\left(EA \frac{dN_1}{dx} \right) - \frac{1}{A} d(QN_1)/dx - K_{11}N_1 + K_{41}N_4 \\
0 &= \frac{1}{A}\frac{d}{dx}\left(EA \frac{dN_2}{dx} \right) - \frac{1}{A} d(QN_2)/dx - K_{22}N_2 + K_{12}N_2 \\
0 &= \frac{1}{A}\frac{d}{dx}\left(EA \frac{dN_3}{dx} \right) - \frac{1}{A} d(QN_3)/dx - K_{33}N_3 + K_{23}N_2 \qquad (50) \\
0 &= \frac{1}{A}\frac{d}{dx}\left(EA \frac{dN_4}{dx} \right) - \frac{1}{A} d(QN_4)/dx - K_{44}N_4 + K_{24}N_2 + N_{34}N_3 \\
0 &= \frac{1}{A}\frac{d}{dx}\left(EA \frac{dD}{dx} \right) - \frac{1}{A} d(QD)/dx - K_aD + K_{25}N_2
\end{aligned}
$$

where N_1 is organic nitrogen, N_2 is ammonia nitrogen, N_3 is nitrite plus nitrate nitrogen, N_4 is algal nitrogen, D is the dissolved oxygen deficit and $K_{25} = 4.57\ K_{32}$. As indicated previously, $K_{ii} \geq K_{ij}$ for all i. The feedback loop appears as $K_{41}N_4$, a source term in the first equation which

utilizes the solution of the fourth equation.

A finite difference approximation was employed to solve Eq. (50). The spatial segmentation and system parameters of other work (Hetling and O'Connell, 1968; Jaworski et al, March 1969 and May 1969) was used. A total of 23 spatial segments was applied to the reach of the Potomac from Little Falls downstream, a distance of about 100 miles to the approximate entrance to Chesapeake Bay. In matrix form, the equations to be solved are (see also Eq. (46).

$$\begin{bmatrix} [A_1] & 0 & 0 & -[VK_{41}] & 0 \\ -[VK_{12}] & [A_2] & 0 & 0 & 0 \\ 0 & [VK_{23}] & [A_3] & 0 & 0 \\ 0 & -[VK_{24}] & -[VK_{34}] & [A_4] & 0 \\ 0 & -[VK_{25}] & 0 & 0 & [A_5] \end{bmatrix} \begin{matrix} (N_1) \\ (N_2) \\ (N_3) \\ (N_4) \\ (D) \end{matrix} = \begin{matrix} (W_1) \\ (W_2) \\ 0 \\ 0 \\ 0 \end{matrix} \qquad (51)$$

where the $[A_i]$ are 23 x 23 triadiagonal matrices incorporating net advective flow and dispersion with the K_{ii} appearing on the main diagonal. Note that $[A_5]$ has the reaeration rate K_a on the main diagonal, $[VK_{ij}]$ are 23 x 23 diagonal matrices (N_i) and (D) and (W) are 23 x 1 vectors of the nitrogen forms, DO deficit and input nitrogen loads, respectively. The matrix Equation (48) is therefore composed of a system of 115 algebraic equations, the simultaneous solution of which provides the steady state distribution of the four nitrogen forms and the DO deficit in all 23 segments.

Data were available for the period July-August 1968 for verification purposes. These data included Kjeldahl nitrogen (representing the sum of organic nitrogen from waste discharges, ammonia nitrogen and algal nitrogen), nitrite and nitrate nitrogen and chlorophyll a measurement. Major input nitrogen

loads are summarized in Table 4 below.

Table 4

Estimated Significant Input Nitrogen Loads

Potomac Estuary

July-August, 1968

	Ult.Carb.BOD lbs/day	Org. N. lbs/day	NH_3-N lbs/day
Arlington, Va.	5,900	1,300	2,100
Washington D.C.	132,000	20,000	20,000
Alexandria	11,700	1,300	2,300
Ft. Westgate	20,800	1,400	1,100

Figures 14 and 15 show the results of a verification analysis of data collected during July-August, 1968. The first order reaction coefficients for the verification analyses shown in these figures are given in Table 5.

Table 5

First Order Reaction Coefficients

Potomac Estuary

July-August, 1968

Temp. = 28°C

Reaction Step	Symbol	Reaction Coef. (1/day)
Decay of Organic - NH	K_{11}	0.2
Organic Nit. → NH -Nit.	K_{12}	0.1
Decay of NH_3 - Nit.	K_{22}	0.30
NH_3 Nit. → NO_3 - Nit.	K_{23}	0.28
NH_3 Nit. → Algal Nit.	K_{24}	0.02
Decay of NO_3 - Nit.	K_{33}	0.10
NO_3 Nit. → Algal Nit.	K_{34}	0.10
Decay of Algal Nit.	K_{44}	0.12
Algal Nit. → Organic Nit.	K_{41}	0.12

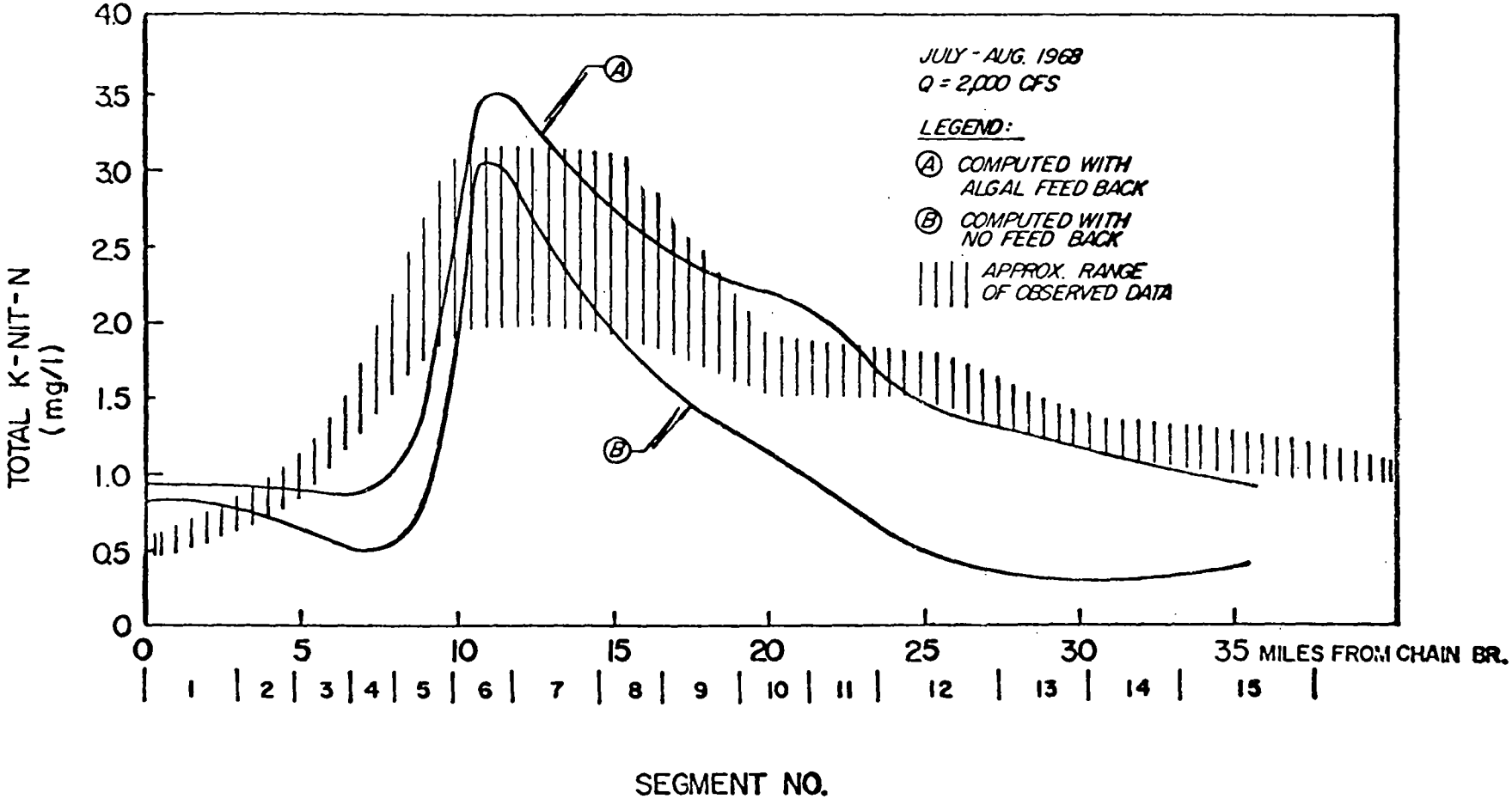

Figure 14

Verification of Kjeldahl Nitrogen for Potomac Estuary

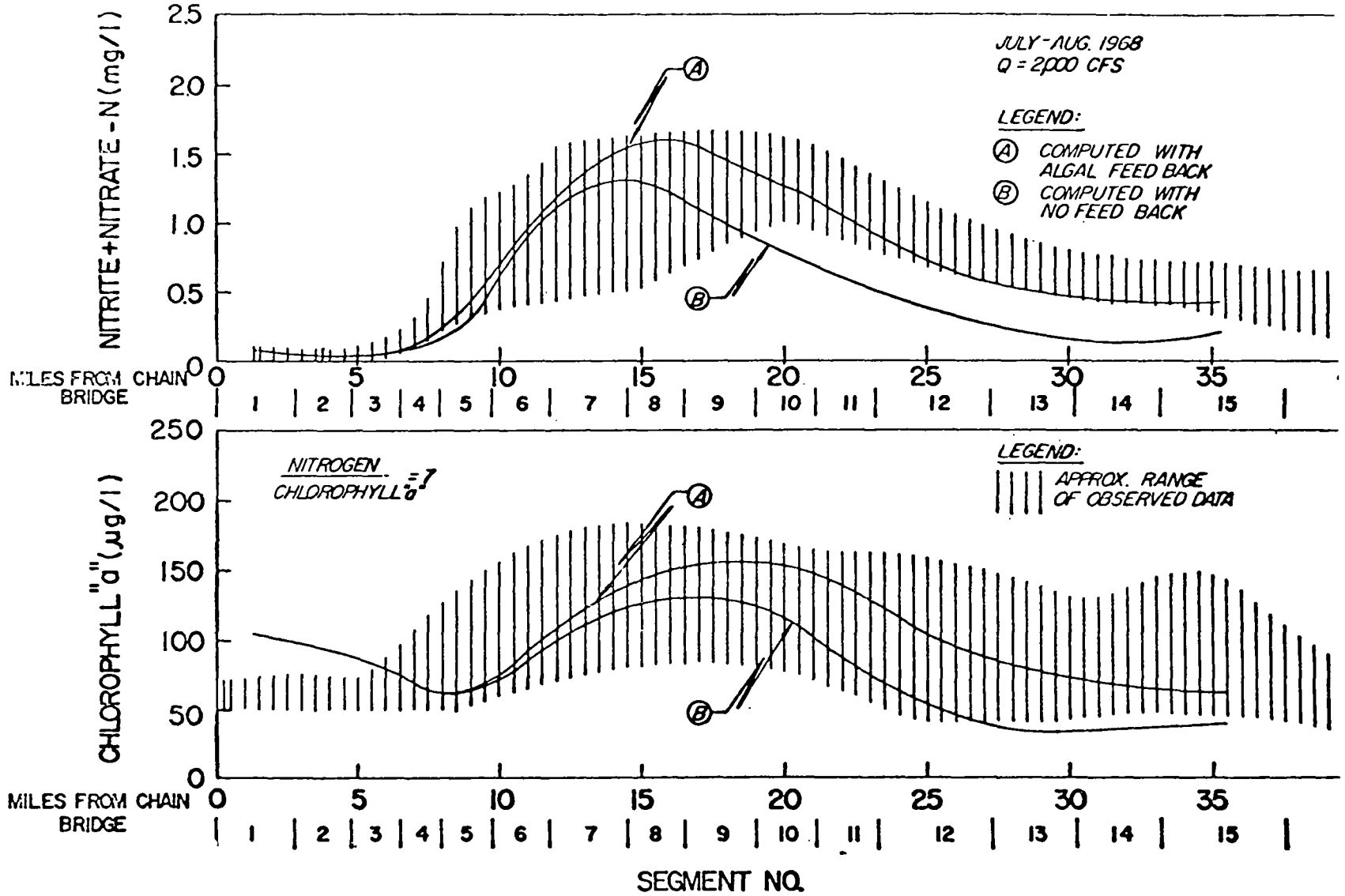

Figure 15

Verification of Nitrite and Nitrate Nitrogen (upper plot) and Chlorophyll "a" (lower plot) for Potomac Estuary

These coefficients represent the end result of many solutions of Eq. (51) which tested the effects of various interactions and levels of coefficients. It can be noted that organic nitrogen is "settled out" of the system because of the difference between the decay coefficient of organic nitrogen and the conversion of organic nitrogen to ammonia nitrogen. This was justified on the basis of bottom sampling which indicated significant deposits in the vicinity of the Washington D.C. outfall. Ammonia nitrogen followed two paths: a) utilization in the algal nitrogen loop (K = 0.02 per day) and b) oxidation to nitrate (K = 0.28 per day). This split allowed a proper spatial profile to be maintained. Nitrate was recycled to algal nitrogen all of which was allowed to decay to organic nitrogen.

Figures 14 and 15 compare the observed data of the various nitrogen forms to computed values generated by the model with and without the feedback of ammonia and nitrate nitrogen to organic nitrogen. For Figure 14 only Kjeldahl nitrogen observed data were available. The effects of the feedback loop are to increase all profiles in a non-linear spatial manner. The relative downstream shift of the various nitrogen forms is interesting and reflects the sequential nature of these types of reactions. Steady state analyses such as shown in Figures 14 and 15 can provide a basis for estimating the effects of environmental changes on nitrogen distribution in addition to the effects of nitrification on the oxygen regimes.

This latter effect is shown in Figure 16 where the dissolved oxygen deficit due to nitrification is given with and without algal feedback of nitrogen. Therefore, if the nitrogen is completely stored in the algae, the dissolved oxygen deficit is lower at greater distances downstream than if the algal nitrogen is released and available for further nitrification.

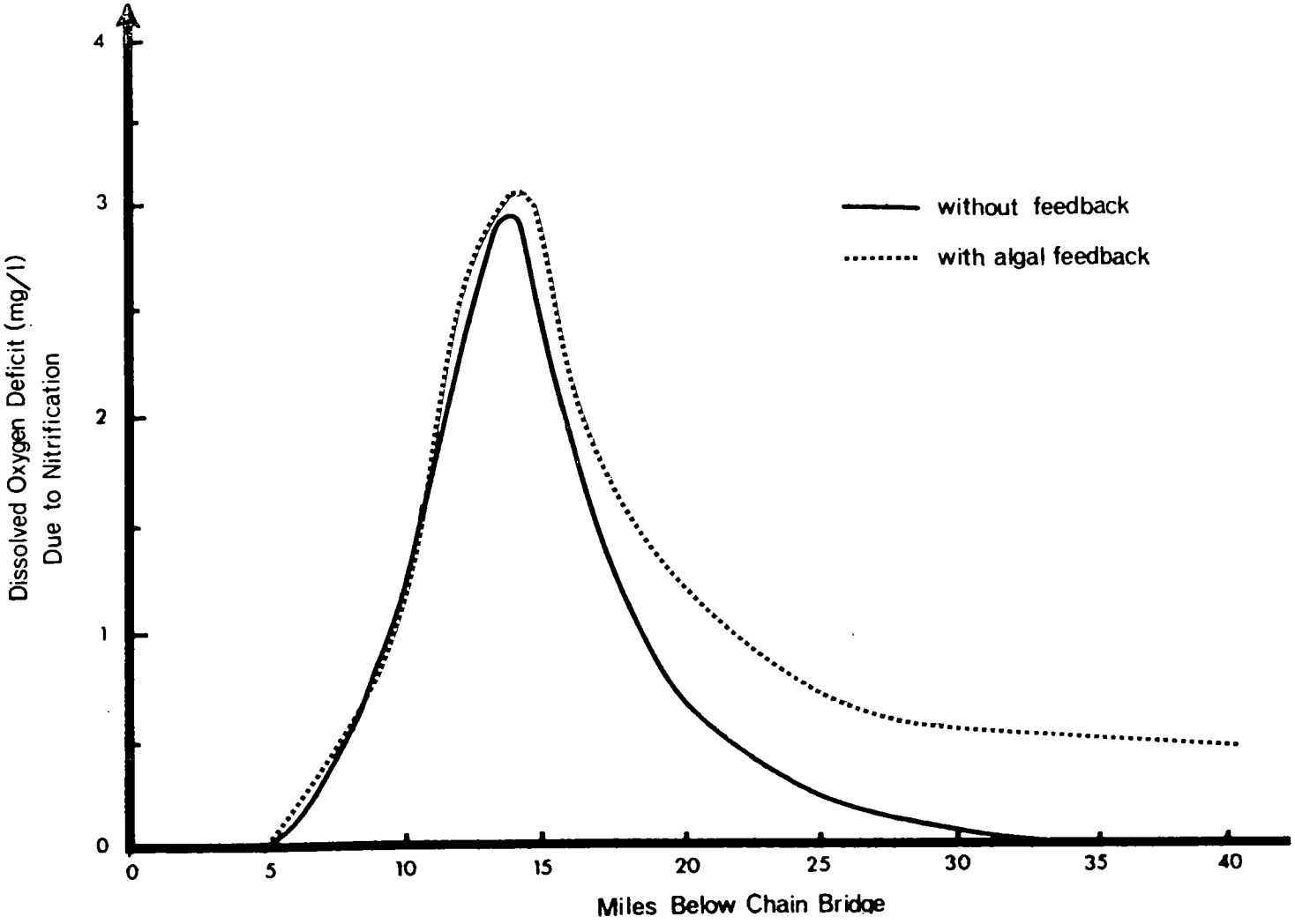

Figure 16

Computed Dissolved Oxygen Deficit Due to Nitrification
in Potomac Estuary, July - August, 1968

The peak value of 3 mg/l DO deficit is significant from a water quality management viewpoint and indicates the need for nitrification of the principal waste discharges.

The nitrogen algal cycle in the Potomac estuary is obviously more complex than given by this model. Non-linear kinetics, algal growth dynamics and environmental influences of temperature and light all affect the observed data. As a planning tool however the simplified model using first order kinetics provides a rapid means for estimating order of magnitude responses and points the direction for more complex modeling efforts.

SECTION V

A DYNAMIC MODEL OF PHYTOPLANKTON POPULATIONS IN NATURAL WATERS

The quality of natural waters can be markedly influenced by the growth and distribution of phytoplankton. Utilizing radiant energy, these microscopic plants assimilate inorganic chemicals and convert them to cell material which, in turn, is comsumed by the various animal species in the next tropic level. The phytoplankton, therefore, are the base of the food chain in natural waters, and their existence is essential to all aquatic life.

The quality of a body of water can be adversely affected if the population of phytoplankton becomes so large as to interfere with either water use or the higher forms of aquatic life. In particular, high concentrations of algal biomass cause large diurnal variations in dissolved oxygen which can be fatal to fish life. Also, the growths can be nuisances in themselves, especially when they decay and either settle to the bottom or accumulate in windrows on the shoreline. Phytoplankton can cause taste and odor problems in water supplies and, in addition, contribute to filter clogging in the water treatment plant.

The development of large populations of phytoplankton and, in some cases, larger aquatic plants can be accelerated by the addition of nutrients which result from man's activities or natural processes. The resulting fertilization provides more than ample inorganic nutrients, with the resulting development of excessive phytoplankton. This sequence of events is commonly referred to as eutrophication.

Generally, the management of water systems subjected to accelerated eutrophication because of waste discharges has been

largely subjective. Extensive programs of nutrient removal have been called for, with little or no quantitative prediction of the effects of such treatment programs. A quantitative methodology is required to estimate the effect of proposed treatment programs that are planned to restore water quality or to predict the effects of expected future nutrient discharges. This methodology should include a model of the phytoplankton population which approximates the behavior of the phytoplankton in the water body of interest and, therefore, can be used to test the effects of the various control procedures available. In this way, rational planning and water quality management can be instituted with at least some degree of confidence that the planned results actually will be achieved.

This chapter presents a phytoplankton population model in natural waters, constructed on the basis of the principle of conservation of mass. This is an elementary physical law which is satisfied by macroscopic natural systems. The use of this principle is dictated primarily by the lack of any more specific physical laws which can be applied to these biological systems. An alternate conservation law, that of conservation of energy, can also be used. However, the details of how mass is transferred from species to species are better understood than the corresponding energy transformations. The mass interactions are related, among other factors, to the kinetics of the populations and it is this that the bulk of this chapter is devoted to exploring.

Review of Previous Models

The initial attempts to model the dynamics of a phytoplankton population were based on a version of the law of conservation

of mass in which the hydrodynamic transport of mass is assumed to be insignificant. Let P(t) be the concentration of phytoplankton mass at time t in a suitably chosen region of water. The principle of conservation of mass can be expressed as a differential equation

$$\frac{dP}{dt} = S$$

where S is the net source or sink of phytoplankton mass within the region. If hydrodynamic transport is not included, then the rate at which P increased or decreases depends only on the internal sources and sinks of phytoplankton in the region of interest.

The form of the internal sources and sinks of phytoplankton is dictated by the mechanisms which are assumed to govern the growth and death of phytoplankton. Fleming (1939), as described by Riley (1963), postulated that spring diatom flowering in the English Channel is described by the equation,

$$\frac{dP}{dt} = [a - (b + ct)]P$$

where P is the phytoplankton concentration, a is a constant growth rate, and (b + ct) is a death rate resulting from the grazing of zooplankton. The zooplankton population, which is increasing owing to its grazing, results in an increasing death rate which is approximated by the linear increase of the death rate as a function of time.

The less empirical model has been proposed by Riley (1963) based on the equation

$$\frac{dP}{dt} = [P_h - R - G]P$$

where P_h is the photosynthetic growth rate, R is the endogenous respiration rate of the phytoplankton, and G is the death rate owing to zooplankton grazing. A major improvement in Riley's equation is the attempt to relate the growth rate, the respiration rate, and the grazing to more fundamental environmental variables such as incident solar radiation, temperature, extinction coefficient, and observed nutrient and zooplankton concentration. As a consequence, the coefficients of the equations are time-variable since the environmental parameters vary throughout the year. This precludes an analytical solution to the equation, and numerical integration methods must be used. Three separate applications (Riley, 1946, 1947, 1949) of these equations to the near-shore ocean environment have been made, and the resulting agreement with observed data is quite encouraging.

A complex set of equations, proposed by Riley, Stommel and Bumpus (1949) first introduced the spatial variation of the phytoplankton with respect to depth into the conservation of mass equation. In addition, a conservation of mass equation for a nutrient (phosphate) was also introduced, as well as simplified equations for the herbivorous and carnivorous zooplankton concentrations. The phytoplankton and nutrient equations were applied to 20 volume elements which extended from the surface to well below the euphotic zone. In order to simplify the calculations, a temporal steady-state was assumed to exist in each volume element. Thus, the equations apply to those periods of the year during which the dependent variables are not changing significantly in time. Such conditions usually prevail during the summer months. The results of these calculations were compared with observed data, and again the results were encouraging.

Steele (1956) found that the steady-state assumption did not

apply to the seasonal variation of the phytoplankton population. Instead, he used two volume segments to represent the upper and lower water levels and kept the time derivatives in the equations. Thus, both temporal and spatial variations were considered. In addition, the differential equations for phytoplankton and zooplankton concentration were coupled so that the interactions of the populations could be studied, as well as the nutrient-phytoplankton dependence. The coefficients of the equations were not functions of time, however, so that the effects of time-varying solar radiation intensity and temperature were not included. The equations were numerically integrated and the results compared with the observed distribution. Steele (1964) applied similar equations to the vertical distribution of chlorophyll in the Gulf of Mexico.

The models proposed by Riley et al and Steele are basically similar. Each consider the primary dependent variables to be the phytoplankton, zooplankton, and nutrient concentration. A conservation of mass equation is written for each species, and the spatial variation is incorporated by considering finite volume elements which interact because of vertical eddy diffusion and downward advective transport of the phytoplankton. Their equations differ in some details (for example, the growth coefficients that were used and the assumptions of steady state) but the principle is the same. In addition, these equations were applied by the authors to actual marine situations and their solutions compared with observed data. This is a crucial part of any investigation discussion wherein the assumptions that are made and the approximations that are used are difficult to justify a priori.

The models of both Riley and Steele have been reviewed in greater detail by Riley (1963) in a discussion of their applicability and possible future development. The difficulties

encountered in formulating simple theoretical models of phytoplankton-zooplankton population models were discussed by Steele (1965).

Other models have been proposed which follow the outlines of the equations already discussed. Equations with parameters that vary as a function of temperature, sunlight, and nutrient concentration have been presented by Davidson and Clymer (1966) and simulated by Cole (1967). A set of equations which model the population of phytoplankton, zooplankton, and a species of fish in a large lake have been presented by Parker (1968). The application of the techniques of phytoplankton modeling to the problem of eutrophication in rivers and estuaries has been proposed by Chen (1970). The interrelations between the nitrogen cycle and the phytoplankton population in the Potomac Estuary has been investigated using a feed-forward-feed-back model of the dependent variables, which interact linearly following first order kinetics (Thomann, 1970).

The formulations and equations presented in the subsequent sections are modifications and extensions of previously presented equations which incorporate some additional physiological information on the behavior of phytoplankton and zooplankton populations. In contrast to the majority of the applications of phytoplankton models which have been made previously, the equations presented in the subsequent sections are applied to a relatively shallow reach of the San Joaquin River and the estuary further downstream. The motivation for this application is an investigation of the possibility of excessive phytoplankton growths as environmental conditions and nutrient loadings are changed in this area. Thus, the primary thrust of this investigation is to produce an engineering tool which can be used in the solution of engineering problems to protect the water quality of the region of interest.

Phytoplankton System Interactions

The major obstacle to a rigorous quantitative theory of phytoplankton population dynamics is the enormous complexity of the biological and physical phenomena which influence the population. It is necessary, therefore, to idealize and simplify the conceptual model so that the result is a manageable set of dependent systems or variables and their interrelations. The model considered in the following sections is formulated on the basis of three primary dependent systems: the phytoplankton population, whose behavior is the object of concern; the herbivorous zooplankton population, which are the predators of the phytoplankton, utilizing the available phytoplankton as a food supply; and the nutrient system, which represents the nutrients, primarily inorganic substances, that are required by the phytoplankton during growth. These three systems are affected not only by their interactions, but also by external environmental variables. The three principal variables considered in this analysis are temperature, which influences all biological and chemical reactions, dispersion and advective flow, which are the primary mass transport mechanisms in a natural body of water, and solar radiation, the energy source for the photosynthetic growth of the phytoplankton.

In addition to these external variables, the effect of man's activities on the system is felt predominately in the nutrient system. Sources of the necessary nutrients may be the result of, for example, inputs of wastewater from municipal and industrial discharges or agricultural runoff. The man-made waste loads are in most cases the primary control variables which are available to affect changes in the phytoplankton and zooplankton systems. A schematic representation of these systems and their interrelations is presented in Figure 17.

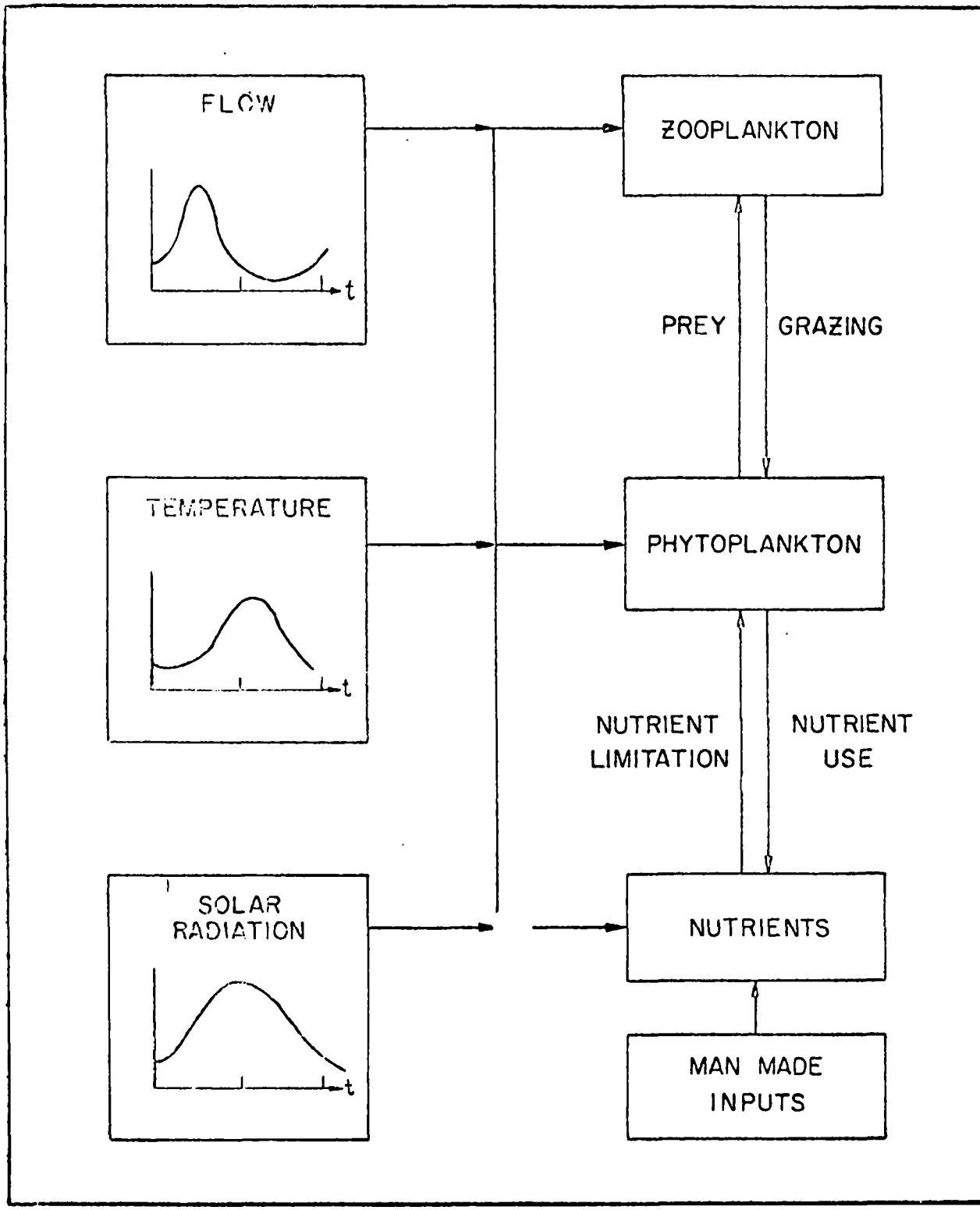

Fig. 17 Interactions of Environmental Variables and the Phytoplankton, Zooplankton and Nutrient Systems

In addition to the conceptual model which isolates the major interacting systems, a further idealization is required which sets the lower and upper limits of the temporal and spatial scales being considered. Within the context of the problem of eutrophication and its control, the seasonal distribution of the phytoplankton is of major importance, so that the lower limit of the temporal scale is on the order of days. The spatial scale is set by the hydrodynamics of the water body being considered. For example, in a tidal estuary, the spatial scale is on the order of miles whereas in a small lake it is likely a good deal smaller. The upper limits for the temporal and spatial extent of the model are dictated primarily by practical considerations such as the length of time for which adequate information is available and the size of the computer being used for the calculations.

These simplifying assumptions are made primarily on the basis of an intuitive assessment of the important features of the systems being oonsidered and the experience gained by previous attempts to address these and related problems in natural bodies of water. The basic principle to be applied to this conceptual model, which can then be translated into mathematical terms, is that of conservation of mass.

Conservation of Mass

The principle of conservation of mass is the basis upon which the mathematical development is structured. Alternate formulations, such as those based on the conservation of energy, have been proposed. However, conservation of mass has proved a useful starting point for many models of the natural environment.

The principle of conservation of mass simply states that the

mass of the substances being considered within an arbitrarily selected volume must be accounted for by either mass transport into and out of the volume or as mass produced or removed within the volume. The transport of mass in a natural water system arises primarily from two phenomena: dispersion, which is caused by tidal action, density differences, turbulent diffusion, wind action, etc.; and advection owing to a unidirectional flow - for example, the fresh water flow in a river or estuary or the prevailing currents in a bay or a near-shore environment. The distinction between the two phenomena is that, over the time scale of interest, dispersive mass transport mixes adjacent volumes of water so that a portion of the water in adjacent volume elements is interchanged, and the mass transport is proportional to the difference in concentrations of mass in adjacent volumes. Advective transport, however, is transport in the direction of the advective flow only. In addition to the mass transport phenomena, mass in the volume can increase resulting from sources within the volume. These sources represent the rate of addition or removal of mass per unit time per unit volume by chemical and biological processes.

A mathematical expression of conservation of mass which includes the terms to describe the mass transport phenomena and the source term is a partial differential equation of the following form

$$\frac{\partial P}{\partial t} = \nabla \cdot E\nabla P - \nabla \cdot \underline{Q}P + S_p \qquad (52)$$

where $P(x,y,z,t)$ is the concentration of the substance of interest - e.g., phytoplankton biomass - as a function of position and time; E is the diagonal matrix of dispersion coefficients; $\underline{Q}$ is the advective flow rate vector; S_p is the vector whose terms are the rate of mass addition by the sources and sinks; and ∇ is the gradient operator. This partial differential

equation is too general to be solved analytically, and the numerical techniques are used in its solution.

An effective approximation to Equation (52) is obtained by segmenting the water body of interest into n volume elements of volume V_j and representing the derivatives in Equation (52) by differences. Let V be the n x n diagonal matrix of volumes V_j; A, the n x n matrix of dispersive and advective transport terms; S_p, the n vector of source terms S_{pj}, averaged over the volume V_j; and P, the n vector of concentrations P_j, which are the concentrations in the volumes. Then the finite difference equations can be expressed as a vector differential equation

$$\overset{o}{VP} = AP + VS_p \tag{53}$$

where the dot denotes a time derivative. The details of the application of this version of the dispersion advection equation to natural bodies of water has been presented by Thomann (1963) and reviewed by O'Connor et al (1966).

The main interest in this report is centered on the source terms S_{pj} for the particular application of these equations to the phytoplankton population in natural water bodies. It is convenient to express the source term of phytoplankton, S_{pj}, as a difference between the growth rate, G_{pj}, of phytoplankton and their death rate, D_{pj}, in the volume V_j. That is

$$S_{pj} = (G_{pj} - D_{pj})P_j \tag{54}$$

where G_{pj} and D_{pj} have units [day^{-1}]. The subscript p identifies the quantities as referring to phytoplankton; the subscript j refers to the volume element being considered. The balance between the magnitude of the growth rate and death rate determines the rate at which phytoplankton mass is created or destroyed in the volume element V_j. Thus, the form of the growth

and death rates as functions of environmental parameters and dependent variables is an important element in a successful phytoplankton population model.

Phytoplankton Growth Rate

The growth rate of a population of phytoplankton in a natural environment is a complicated function of the species of phytoplankton present and their differing reactions to solar radiation, temperature, and the balance between nutrient availability and phytoplankton requirements. The complex and often conflicting data pertinent to this problem have been reviewed recently by Hutchinson (1967), Strickland (1965), Lund (1965) and Raymont (1963). The available information is not sufficiently detailed to specify the growth kinetics for individual phytoplankton species in natural environments. Hence, in order to accomplish the task of constructing a growth rate function, a simplified approach is followed. The problem of different species and their associated nutrient and environmental requirements is not addressed. Instead, the population is characterized as a whole by a measurement of the biomass of phytoplankton present. Typical quantities used are the chlorophyll concentration of the population, the number of organisms per unit volume, or the dry weight of the phytoplankton per unit volume (Vollenweider, 1969). With a choice of biomass units established, the growth rate expresses the rate of production of biomass as a function of the important environmental variables. The environmental variables to be considered below are light, temperature, and the various nutrients which are necessary for phytoplankton growth.

Consider a population of phytoplankton, either a natural association or a single species culture, and assume that the optimum or saturating light intensity for maximum growth rate

of biomass is present and illuminates all the cells, and further that all the necessary nutrients are present in sufficient quantity so that no nutrient is in short supply. For this condition, the growth rate that is observed is called the maximum or saturated growth rate, K'. Measurements of K' (base e) as a function of temperature are shown in Figure 18 and listed in Table 6. The experimental conditions under which these data were collected appear to meet the requirements of optimum light intensity and sufficient nutrient supply. The data presented are selected from larger groups of reported values, and they represent the maximum of these reported growth rates. The presumption is that these large values reflect the maximum growth rates achievable. From an ecological point of view, it is necessary to consider the species most able to compete, and, in terms of growth rate, it is the species with the largest growth rate which will predominate. A straight-line fit to this data appears to be a crude but reasonable approximation of the data relating saturated growth rate K' to temperature, T

$$K' = K_1 T \tag{55}$$

where K_1 has values in the range 0.10 ± 0.025 day^{-1} $°C^{-1}$. This coefficient indicates an approximate doubling of the saturated growth rate for a temperature change from 10° to 20°C, in accordance with the generally reported temperature-dependence of biological growth rates. The optimum temperature for algal growth appears to be in the range between 20° and 25°C, although thermophilic strains are known to exist (Fogg, 1965). At higher temperatures, there is usually a suppression of the saturated growth rate, and the straight-line approximation is no longer valid. It should also be noted that the scatter in the data in Figure 18 is sufficiently large so that the linear

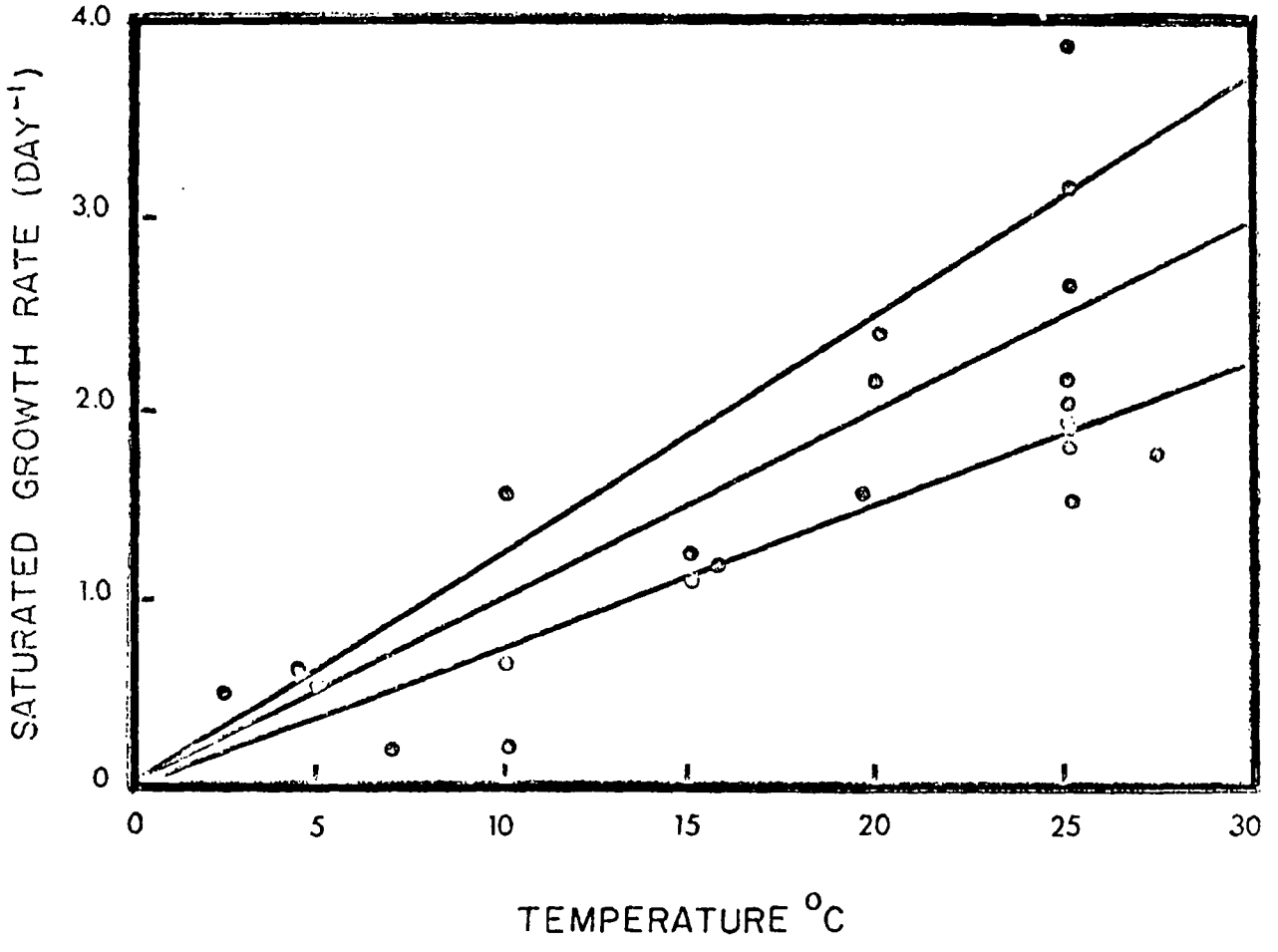

Fig. 18 Phytoplankton Saturated Growth Rate (Base e) as a Function of Temperature

Table 6

Maximum Growth Rates
As a Function of Temperature

Reference	Organism	Temperature	Saturated Growth Rate, K' ($Base_e$, Da^{-1})
Tamiya et al, 1964	Chlorella ellipsoidea (green alga)	25 15	3.14 1.2
Yentsch 1966	Nannochloris atomus (marine flagellate)	20 10	2.16 1.54
Spencer 1954	Nitzschia closterium (marine diatom)	27 19 15.5 10	1.75 1.55 1.19 0.67
Riley 1949b	Natural association	4 2.6	0.63 0.51
Myers 1964	Chlorella pyrenoidosa	25	1.96
"	Scenedesmus quadricauda	25	2.02
Sorokin 1958	Chlorella pyrenoidosa	25	2.15
"	Chlorella vulgaris	25	1.8
"	Scenedesmus obliquus	25	1.52
"	Chlamydomonas reinhardti	25	2.64
Sorokin 1962	Chlorella pyrenoidosa (synchronized culture) (high-temperature strain)	10 15 20 25	0.2 1.1 2.4 3.9

dependence on temperature and also the magnitude of K' can vary considerably in particular situations.

In the natural environment, the light intensity to which the phytoplankton are exposed is not uniformly at the optimum value but it varies as a function of depth because of the natural turbidity present and as a function of time over the day. Thus, the phytoplankton in the lower layers are exposed to intensities below the optimum and those at the surface may be exposed to intensities above the optimum so that their growth rate would be inhibited. Figure 19b,c,d from Ryther (1956) are plots of the photosynthesis rate normalized by the photosynthesis rate at the optimum or saturating light intensity vs the light intensity, I, incident on the populations. Figure 19a is a plot of function

$$F(I) = \frac{I}{I_s} \exp\left[-\frac{I}{I_s} + 1\right] \qquad (56)$$

for I_s = 2000 ft-candles, proposed by Steele (1965) to describe the light-dependence of the growth rate of phytoplankton.

The similarity between this function and data from Ryther is sufficient to warrant the use of this expression to express the influence of nonoptimum light intensity on the growth rate of phytoplankton. Other workers have suggested different forms for this relationship (Shelef et al, 1970; Vollenweider, 1965).

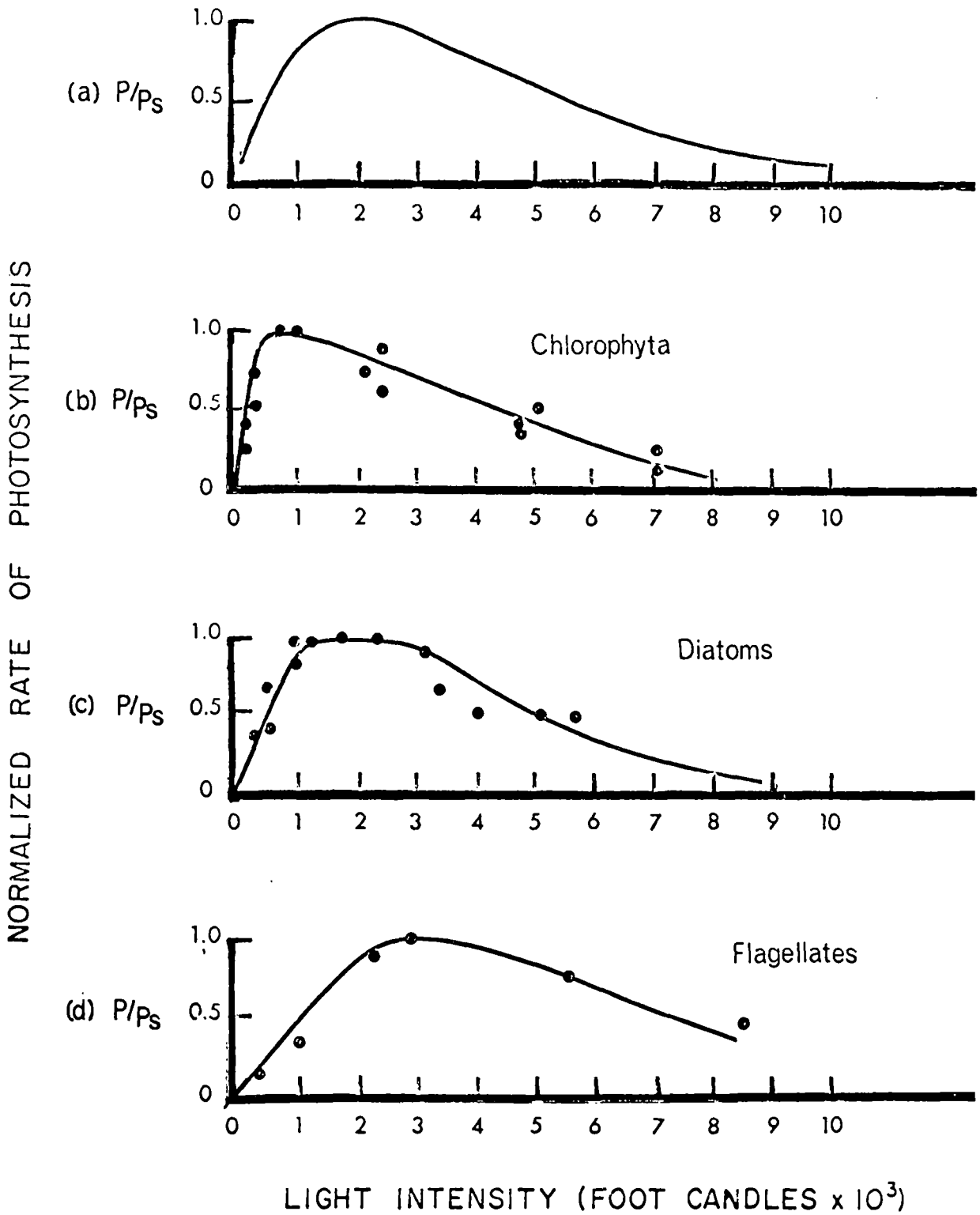

Fig. 19 Normalized Rate of Photosynthesis vs. Incident Light Intensity: (a) Theoretical Curve after Steele (1965) (b,c,d) Data after Ryther (1956)

These variations approximately follow the shape of Equation (56) for low light intensities but differ for the region of high light intensities, usually by not decreasing after some optimum intensity is reached. In particular, Tamiya et al (1964) have investigated the growth rate of Chlorella ellipsoidea to various light and temperature regimes. The saturated growth rates as a function of temperature are included in Figure 18. The influence of varying light intensity fits the function

$$F(I) = \frac{I}{I + K'/\alpha} \tag{57}$$

where K' is the saturated growth rate and ($\alpha = 0.45$ day^{-1} kilolux^{-1}). However, since K' is a function of temperature, the saturating light intensity for Equation (57) is also a function of temperature. Similar data obtained by Sorokin et al (1962) using a high-temperature strain of Chlorella pyrenoidosa support the temperature-dependence of the saturating light intensity for chlorella. Therefore, in using Equation (56), a temperature-dependent light saturation intensity may be warranted.

At this point in the analysis, the effect of the natural environment on the light available to the phytoplankton must be included. Equation (56) expresses the reduction in the growth rate caused by nonoptimum light intensity. This expression can therefore be used to calculate the reduction in growth rate to be expected at any intensity. However, this is too detailed a description for conservation of mass equations which deal with homogeneous volume elements, V_j, and the growth rate within these elements. What is required is averages of the growth rate over the volume elements.

In order to calculate the light intensity which is present in the volume, V_j, the light penetration at the depth of

water where V_j is located must be evaluated. The rate at which light is attenuated with respect to depth is given by the extinction coefficient, k_e. That is, at a depth z, the intensity at that depth, I(z), is related to the surface intensity, I_o, by the formula

$$I(z) = I_o \exp(-k_e z) \tag{58}$$

where z = 0 is the water surface and z is positive downward. Thus, the reduction of the saturated growth rate at any depth z resulting from the nonoptimum light intensity present is given by Equation (58), substituted into Equation (56).

$$F[I(z)] = \frac{I_o e^{-k_e z}}{I_s} \exp\left[\frac{-I_o e^{-k_e z}}{I_s} + 1\right] \tag{59}$$

To apply this equation to the finite volume elements, within which it is assumed that the phytoplankton concentration is uniform, it is necessary to average this reduction factor throughout the depth of the volume element V_j. Let H_{oj} and H_{1j} be the depths of the surface and bottom, respectively, of the volume element V_j. For example, if the volume element V_j extends from the water surface to the bottom of the water body, then $H_{oj} = 0$ and H_{1j} is the water depth at the location of V_j. For the sake of simplicity, it is assumed that this is the case. If $H_{oj} \neq 0$, a straight-forward generalization of the following average is required.

In addition to an average over depth, it is also expedient to average the phytoplankton growth rate over a time interval. Since the time scale within which this analysis is addressed is the week-to-week change in the population over a year, a daily average is appropriate. For simplicity, it is assumed that the incident solar radiation as a function of time over a day is given by the function

$$I_o(t) = I_a \qquad 0 < t < f$$
$$I_o(t) = 0 \qquad f < t < 1 \tag{60}$$

where f is the daylight fraction of the day (i.e. the photo period) and I_a is the average incident solar radiation intensity during the photo period.

Let r_j be the reduction in growth rate attributed to nonoptimum light conditions in volume V_j, averaged over depth and time. Then r_j is given by

$$r_j = \frac{1}{H_j} \int_o^{H_j} \frac{1}{T} \int_o^f \frac{I_a e^{-k_{ej}z}}{I_s} \exp\left[\frac{-I_a e^{-k_{ej}z}}{I_s} + 1\right] dt\, dz \tag{61}$$

where T = 1 day, the time-averaging interval, $H_{1j} = H_j$ = the depth of segment V_j, and k_{ej} is the extinction coefficient in V_j. The result is

$$r_j = \frac{1}{k_{ej}H_j} e^{-\alpha_{1j}} - e^{-\alpha_{oj}} \tag{62}$$

where

$$\alpha_{1j} = \frac{I_a}{I_s} e^{-k_{ej}H_j} \tag{63}$$

$$\alpha_{oj} = \frac{I_a}{I_s}$$

The integral given by Equation (61) is a form of an integral used by Steeman Nielson (1952, Talling (1957), and Ryther (1952) and Yentsch (1957), as described by Vollenweider (1958), and, in particular, Steele (1965), for the purpose of relating an instantaneous rate (e.g., growth, photosynthesis, etc) to an average day rate and an average depth rate.

The reduction factor r_j is a function of the extinction coefficient K_{ej} of the volume V. However, the extinction coefficient is a function of the phytoplankton concentration present if their concentration is large. Thus, an important feedback mechanism exists which can have a marked effect on the growth rate of phytoplankton. As the concentration of phytoplankton in a volume element increases, the extinction coefficient, particularly at the green wavelengths, starts to increase. This mechanism is called self-shading. The most straightforward approach to including this effect into the growth rate expression is to specify the extinction coefficient as a function of the phytoplankton concentration

$$k_{ej} = k'_{ej} + h(P_j) \tag{64}$$

where k'_{ej} is the extinction coefficient attributable to other causes and k_{ej} includes the phytoplankton's contribution. The function $h(P_j)$ has been investigated by Riley (1956), who found that it can be approximated by

$$h(P_j) = 0.0088\ P_j + 0.054\ P_j^{2/3} \tag{65}$$

where P_j has the units $\mu g/liter$ $chlorophyll_a$ concentration and h has units m^{-1}. A more recent investigation (Small,1968) shows that this relationship applies to coastal waters of Oregon for a range in $chlorophyll_a$ concentration of from 0 to 5.0 mg Chl_a/m^3.

A theoretical basis for this relationship is the Beer-Lambert law, which expresses the extinction coefficient in terms of the concentration of light-absorbing material. For dense algal cultures, this law has been experimentally verified (Oswald, et al, 1953). A similar relationship based on this law has been proposed by Chen (1970) from the data of Azad and

Borchardt (1969)

$$h(P_j) = 0.17\ P_j \qquad (66)$$

for h in m^{-1} and P_j, the phytoplankton concentration is mg/liter of dry weight. This expression gives values comparable with Equation (65) for a reasonable conversion factor for the units involved.

To summarize the analysis to this point, the saturated growth rate K' has been estimated from available data and its temperature dependence established. The reduction to be expected from nonoptimum light intensities has been quantified and used to calculate the reduction in growth rate, r_j, to be expected in each volume element V_j as a function of the extinction coefficient and the depth of the segment. The mechanism of self-shading has been included by specifying the chlorophyll dependence of the extinction coefficient. It remains to evaluate the effect of nutrients on the growth rate.

The effects of various nutrient concentrations on the growth of phytoplankton has been investigated and the results are quite complex. As a first approximation to the effect of nutrient concentration on the growth rate, it is assumed that the phytoplankton population in question follow Monod growth kinetics with respect to the important nutrients. That is, at an adequate level of substrate concentration, the growth rate proceeds at the saturated rate for the temperature and light conditions present. However, at low substrate concentration, the growth rate becomes linearly proportional to substrate concentration. Thus, for a nutrient with concentration N_j in the j^{th} segment, the factor

by which the saturated growth rate is in the j^{th} segment reduced is: $N_j/(K_m + N_j)$. The constant, K_m, which is called the Michaelis or half saturation constant, is the nutrient concentration at which the growth rate is half the saturated growth rate. There exists an increasing body of experimental evidence to support the use of this functional form for the dependence of the growth rate on the concentration of either phosphate (Dugdale, 1967), nitrate, or ammonia (Eppley, 1969) if only one of these nutrients is in short supply. An example of this behavior, using the data from Ketchum (1939) is shown in Figure 20a for the nitrate uptake rate as a function of nitrate concentration and in Figure 20b for the phosphate uptake as a function of phosphate concentration. These results are from batch experiments. Similar results from chemostat experiments, which seem to be more suitable but more lengthy for this type of analysis, have also been obtained. Table 7 is a listing of measured and estimated Michaelis constants for ammonia, nitrate, and phosphate. The estimates are obtained by taking one-third the reported saturation concentration of the nutrients. These measurements and estimates indicate that the Michaelis constant for phosphorus is approximately 10 µg P/liter and for inorganic nitrogen forms in the range from 1.0 to 100 µg N/liter, depending on the species and its previous history.

The data on the effects of the concentration of other inorganic nutrients on the growth rate is less complete. Since algae use carbon dioxide as their carbon source during photosynthesis, this is clearly a nutrient which can reduce the growth rate at low concentrations (Kuentzel, 1969). Reported saturation concentration for Chlorella is < 0.1% atm (Myers, 1964).

The silicate concentration is a factor in the growth rate of diatoms for which it is an essential requirement. The satu-

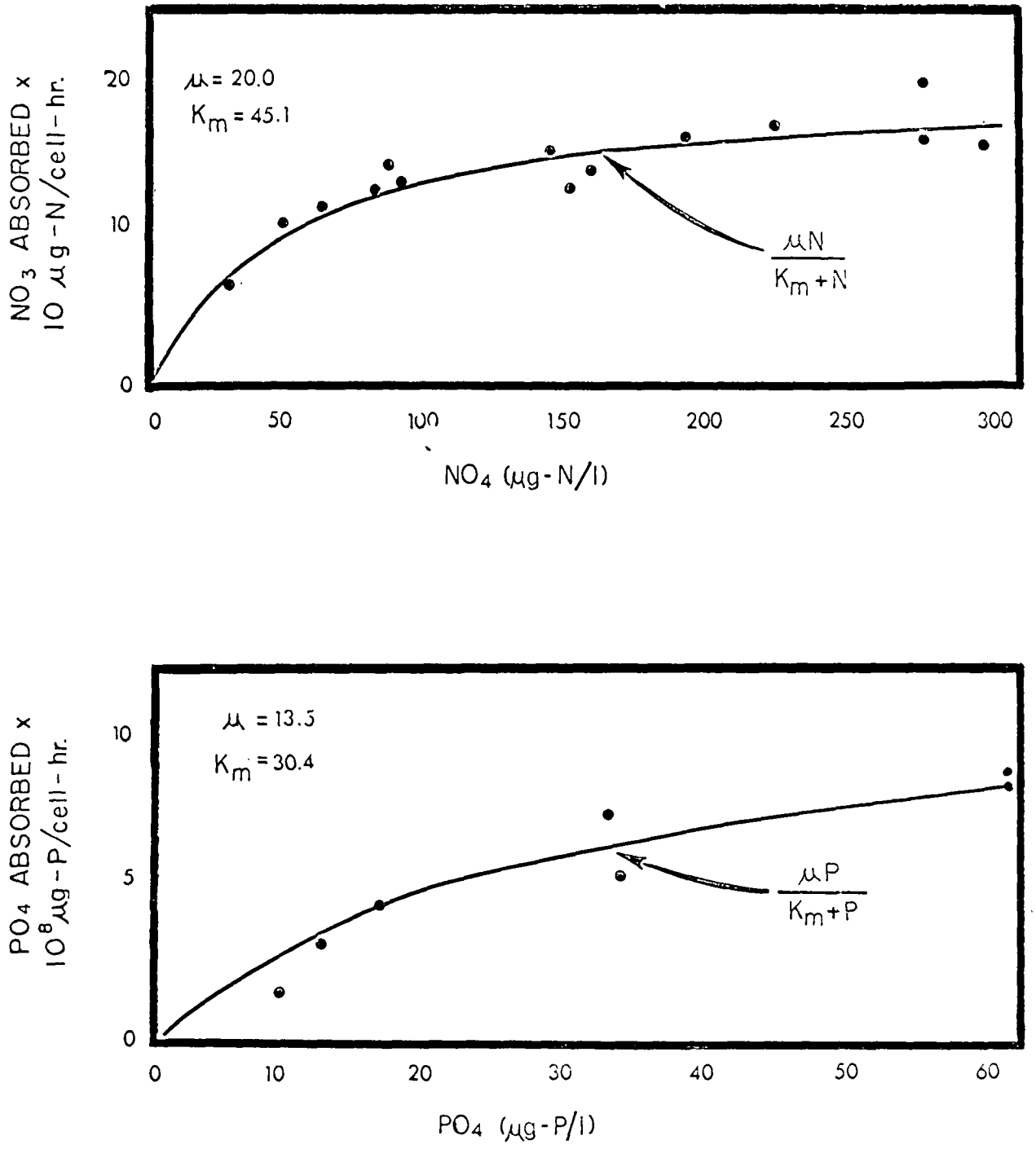

Fig. 20 Nutrient Absorption Rate as a Function of Nutrient Concentration: Comparison of Michaelis Menten Theoretical Curve with Data from Ketchum (1939)

Table 7

Michaelis Constants
for Nitrogen and Phosphorus

Reference			
Thomas 1968	Chaetoceros gracilis (marine diatom)	PO_4	25
L.Tahoe A.C.1969	Scenedesmus gracile	total N total P	150 10
Riley 1965	Natural association	PO_4	6[a]
	Microcystis aeruginosa (blue-green)	PO_4	10[a]
Gerloff 1957	Phaeodactylum tricornutum	PO_4	10
Eppley et al 1969	Oceanic species	NO_3	1.4-7.0
	Oceanic species	NH_3	1.4-5.6
"	Neritic diatoms	NO_3	6.3-28
	Neritic diatoms	NH_3	7.0-120
"	Neritic or littoral Flagellates	NO_3	8.4-130
		NH_3	7.0-77
MacIsaac et al 1969	Natural association Oligotropic	NO_3	2.8
		NH_3	1.4-8.4
"	Natural association Eutrophic	NO_3	14
		NH_3	18

[a]Estimated.

rated growth rate concentration is in the range of 50-100 µg Si/liter (Stickland 1965).

There are a large number of trace inorganic elements which have been implicated in the growth processes of algae, among which are iron [for which a Michaelis constant of 5 µg/liter for reactive iron has been reported by Lake Tahoe Area Council (Anon, May 1969)], manganese, calcium, magnesium, and potassium (Lund, 1965). However, the significance of these elements in the growth of phytoplankton in natural waters is still unclear. Trace organic nutrients have also been shown to be necessary for most species of algae: 80% of the strains studied require vitamin B_{12}, 53% require thiamine, and 10% require biotin (Droop, 1962). Presumably, these nutrients are available in sufficient quantities in natural waters so that their concentration does not appreciably affect the growth rate.

In the preceding discussion of nutrient influences on the growth rate, it is tacitly assumed that only one nutrient is in short supply and all the other nutrients are plentiful. This is sometimes the case in a natural body of water. However, it is also possible that more than one nutrient is in short supply. The most straightforward approach to formulating the growth rate reduction caused by a shortage of more than one nutrient is to multiply the saturated growth rate by the reduction factor for each nutrient. This approach has also been suggested by Chen (1970). As an example, the data from Ketchum (1939) for the rate of phosphate absorption as a function of both phosphate and nitrate concentration can be satisfactorily fit with a product of two Michaelis-Menton expressions. The resulting fit, obtained by a multiple nonlinear regression analysis, is shown in Figure 21. The Michaelis constants that result are 28.4 µg NO_3-N/liter and

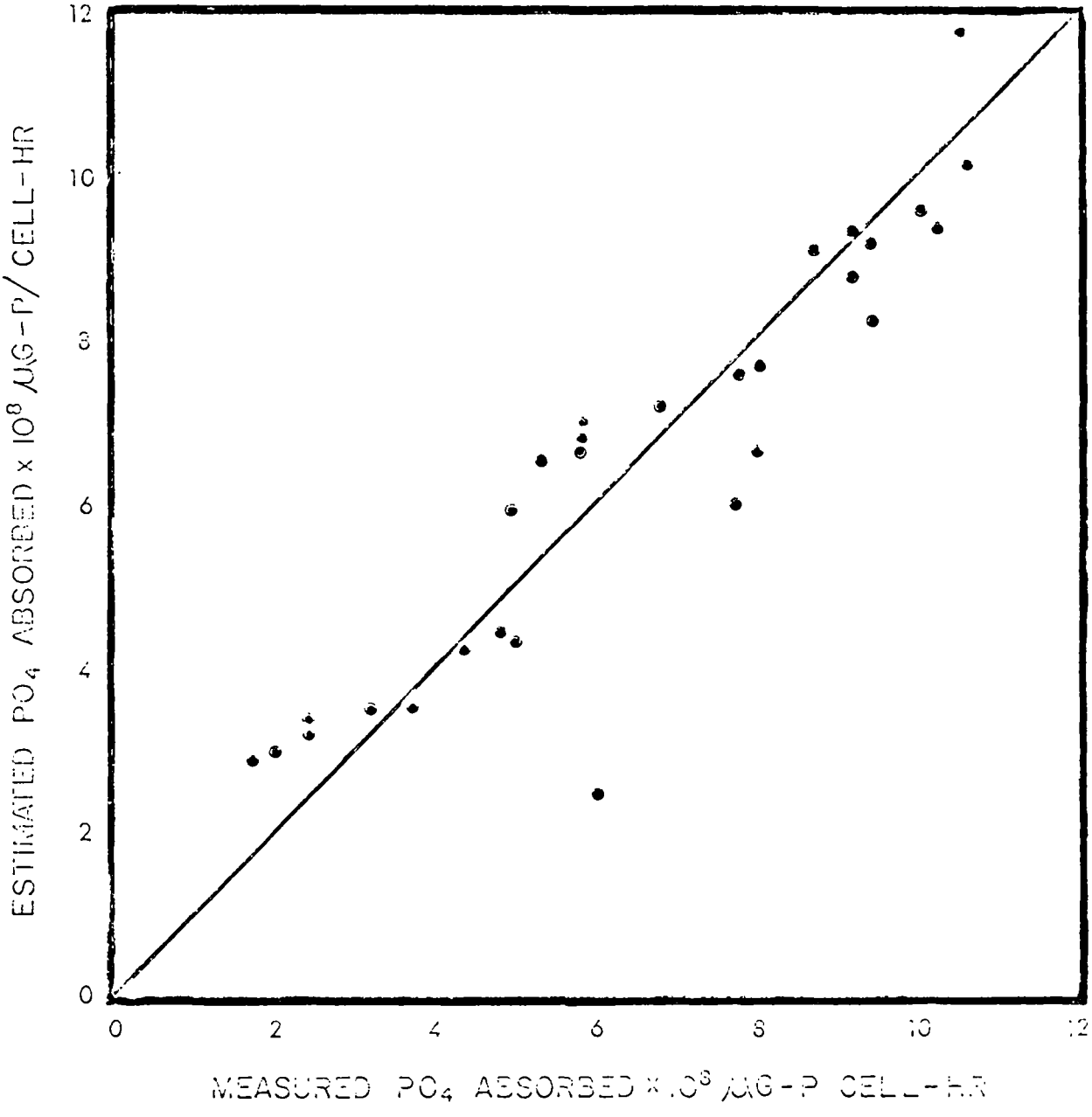

Fig. 21 Measured Phosphate Absorption Rate, after Ketchum (1939), vs. Phosphate Absorption Rate Estimated Using $\mu N_1 N_2/(K_{m1}+N_1)(K_{m2}+N_2)$ where N_1 and N_2 are the Nitrate and Phosphate Concentrations, Respectively

30.3 μg PO_4-P/liter, with a saturated absorption rate of 15.1×10^{-8} μg PO_4-P/cell-hr. This approximation to the growth rate behavior as a function of more than one nutrient must be regarded as only a first approximation, however, since the complex interaction reported between the nutrients is neglected.

The result of the above investigation is the following growth rate expression. For the case of one limiting nutrient, N, with Michaelis constant K_m, the growth expression for the rate in the j^{th} segment is

$$G_{pj} = K_1 T_j \left(\frac{2.718f}{k_{ej} H_j} \left(e^{-\alpha_{1j}} - e^{-\alpha_{oj}} \right) \right) \left(\frac{N_j}{K_m + N_j} \right) \qquad (67)$$

in which Equations (55) and (62) have been combined. This is the functional form that is used subsequently in the applications of these equations to natural phytoplankton populations.

Comparison with Other Growth Rate Expressions

The most extensive investigation of the relationship between the growth rate of natural phytoplankton populations and the significant environment variables, within the context of phytoplankton models, is that of Riley et al (1949). The expression which results from their work is

$$\log \left[\frac{G_p}{K' I_o - G_p} \right] = 22.884 + \log \nu_p - \log I_o - \frac{6573.8}{T'} \qquad (68)$$

where G_p is the growth rate (day^{-1}), K' = 7.6, I_o = average daily incident solar radiation (ly/min), T' - temperature in °K, and ν_p is the nutrient reduction factor for phosphate concentration, N_p, defined as

$$\begin{aligned} \nu_p &= 1.0 && N_p > 0.55 \text{ mg-at/m}^3 \\ \nu_p &= (0.55)^{-1} N_p && N_p < 0.55 \text{ mg-at/m}^3 \end{aligned} \tag{69}$$

where G_p is the growth rate (day^{-1}), K' = 7.6, I_o = average daily incident solar radiation (ly/min), T' = temperature in °K, and ν_p is the nutrient reduction factor for phosphate concentration, N_p, defined as

$$\begin{aligned} \nu_p &= 1.0 && N_p > 0.55 \text{ mg-at/m}^3 \\ \nu_p &= (0.55)^{-1} N_p && N_p < 0.55 \text{ mg-at/m}^3 \end{aligned}$$

In order to compare this expression with that in the previous section, let the nutrient reduction factor be replaced by a Michaelis-Menton expression

$$\nu_p = \frac{N_p}{K_{mp} + N_p} \tag{70}$$

where K_{mp} is the Michaelis constant for phosphate. To be comparable with Equation (67), K_{mp} should equal approximately 0.20 mg-at/m^3 (6.2 mg P/m^3). Using Equation (70) for ν_p, the growth rate expression becomes

$$G_p = K' I_o \left[\frac{\gamma'(T)}{\gamma'(T)+I_o}\right] \left[\frac{N_p}{K_m\left[\frac{I_o}{\gamma'(T)+I_o}\right] + N_p}\right] \tag{71}$$

where

$$\log_{10}\gamma_1(T) = \frac{22.9(T) - 336.4}{T + 273} \qquad (72)$$

and T is temperature in degrees centigrade. To compare this expression with that proposed in the previous section, consider first the nutrient saturated growth rate as a function of solar radiation intensity and temperature. The equations are compared in Figure 22a as a function of total daily solar radiation for three temperatures. The dotted line is Equation (71), and the solid line is the product of Equations (55) and (56). The rate expressions are comparable, although two differences are apparent. In Riley's expression the effect of temperature is less pronounced in the 15° to 25°C range, and the effect of higher daily average solar radiation intensities is opposite (i.e., tends to increase the rate) to that of Equation (56) based on Steele's expression. The growth rate equations averaged over depth are compared in Figure 22. The depth average rate resulting from Riley's expression is

$$G_p = \frac{K'r_1(T)}{k_e H} \ln\left[1 + I_o/r_1(T)\right] \qquad (73)$$

which is compared with Equation (67). The differences are now more pronounced. In particular, the higher growth rates at lower light intensities given by Equation (67) are reflected in the increased depth average growth rate. This is not unexpected since the majority of the population is exposed to lower light levels at the lower depths. Also, the dependence on temperature is quite different, being linear in the case of Equation (67) but practically suppressed in Equation (73).

An interesting feature of Riley's Equation (71) is the multiplication of the Michaelis constant by an expression which

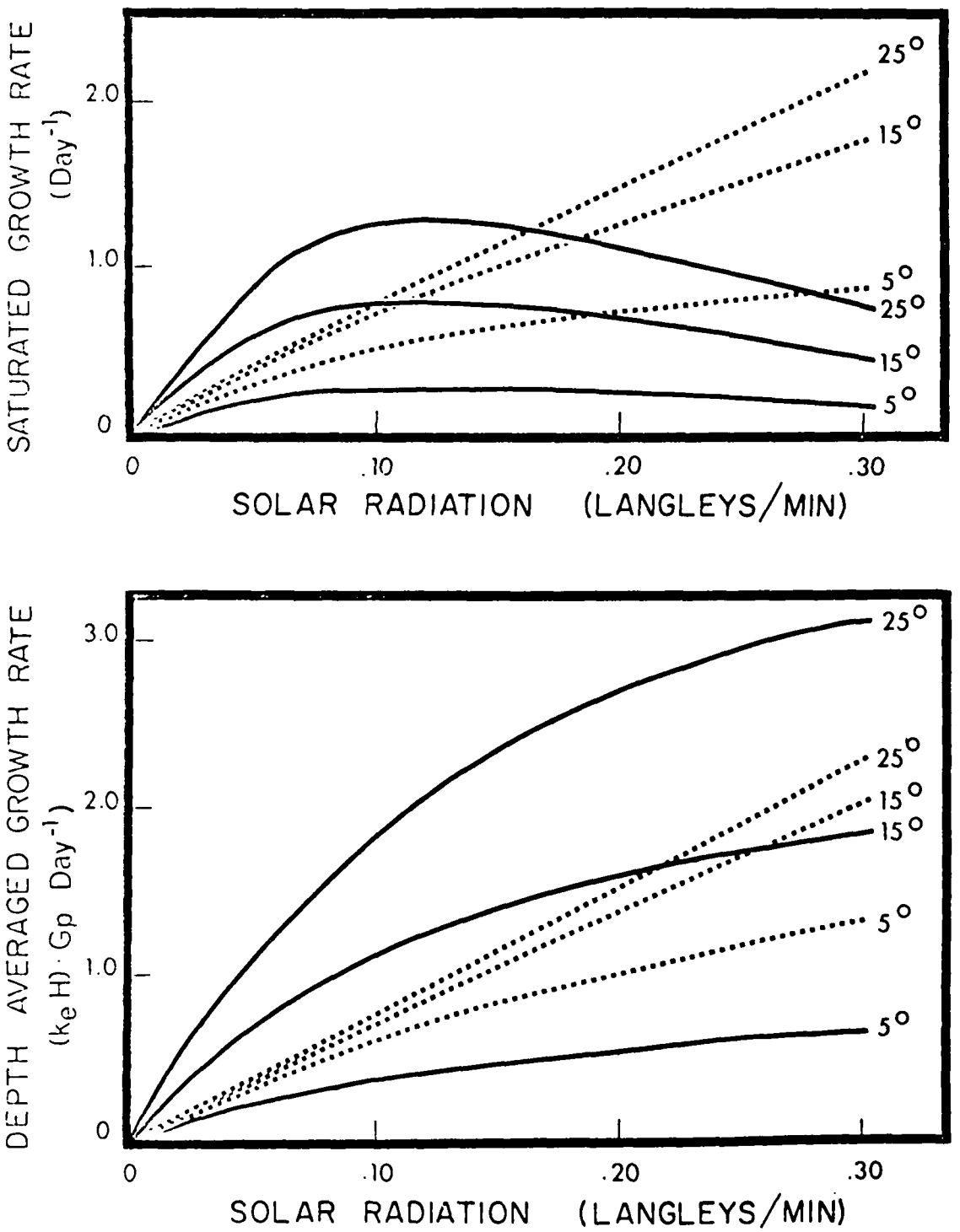

Fig. 22 Comparison of Phytoplankton Growth Rates as a Function of Incident Solar Radiation Intensity and Temperature

depends on temperature and light intensity. The effect is to lower the Michaelis constant at high temperatures and at high light intensity levels, which seems to be a reasonable behavior for a phytoplankton population.

More elementary growth rate formulations have been proposed which do not span the range of conditions attempted in Equations (67) and (71). In particular, a common proposal is to make the growth rate linearly proportional to the various environmental variables. For example, Davidson and Clymer (1966) assumed that the growth rate is proportional to phosphate concentration and photoperiod and a temperature factor given by exp $[-(T - 18)^2/18]$. This temperature factor is quite different from all others proposed and greatly magnifies the effect of temperature on the growth rate. For example, at T = 18°C, the factor equals 1.0, whereas at T = 9°C, the factor drops to 0.01, a 100-fold decrease, compared with approximately a 2-fold decrease predicted by Equations (67) and (71). This exaggerated effect seems to be unrealistic.

A complete investigation of the environmental influences on the growth rate is still to be made. In particular, it has been emphasized that there is an interaction between nitrogen and phosphorus limitations as well as other effects which influence the phytoplankton growth rate. Also, these effects are different for differing species. The species-dependent effects are important in the problem of the seasonal succession of phytoplankton species.

For any particular application, it is advisable to investigate the growth rate of the already-existing population, as the resulting expression may differ significantly from the general over-all behavior as described by Equations (67) and (71). Also, in dealing with natural associations of species of phyto-

plankton, the various constants which result from such an investigation can be considered to be averages over the population, and so they represent in some average way the population behavior as a whole.

Phytoplankton Death Rate

Numerous mechanisms have been proposed which contribute to the death rate of phytoplankton: endogenous respiration rate, grazing by herbivorous zooplankton, a sinking rate, and parasitization (Fogg, 1965). The first three mechanisms have been included in previous models for phytoplankton dynamics, and they have been shown to be of general importance.

The endogenous respiration rate of phytoplankton is the rate at which the phytoplankton oxidize their organic carbon to carbon dioxide per unit weight of phytoplankton organic carbon. Respiration is the reverse of the photosynthesis process and as such contributes to the death rate of the phytoplankton population. If the respiration rate of the population as a whole is greater than the photosynthesis or growth rate, there is a net loss phytoplankton carbon, and the population biomass is reduced in size. The respiration rate as a function of temperature has been investigated, and some measurements are presented in Figure 23 and Table 8. A straight line seems to give an adequate fit of the data; that is, Respiration Rate = K_2T. For the respiration rate in $days^{-1}$ and T in °C, the value of K_2 is in the range 0.005 ± 0.001. The lack of any more precise data precludes exploring the respiration rate's dependence on other environmental variables. However, an important interaction has been suggested by Lune (1965). During nutrient-depleted conditions, "many algae pass into morphological or physiological resting stages under such unfavorable conditions. Resting stages are absent in Asterionella formosa,

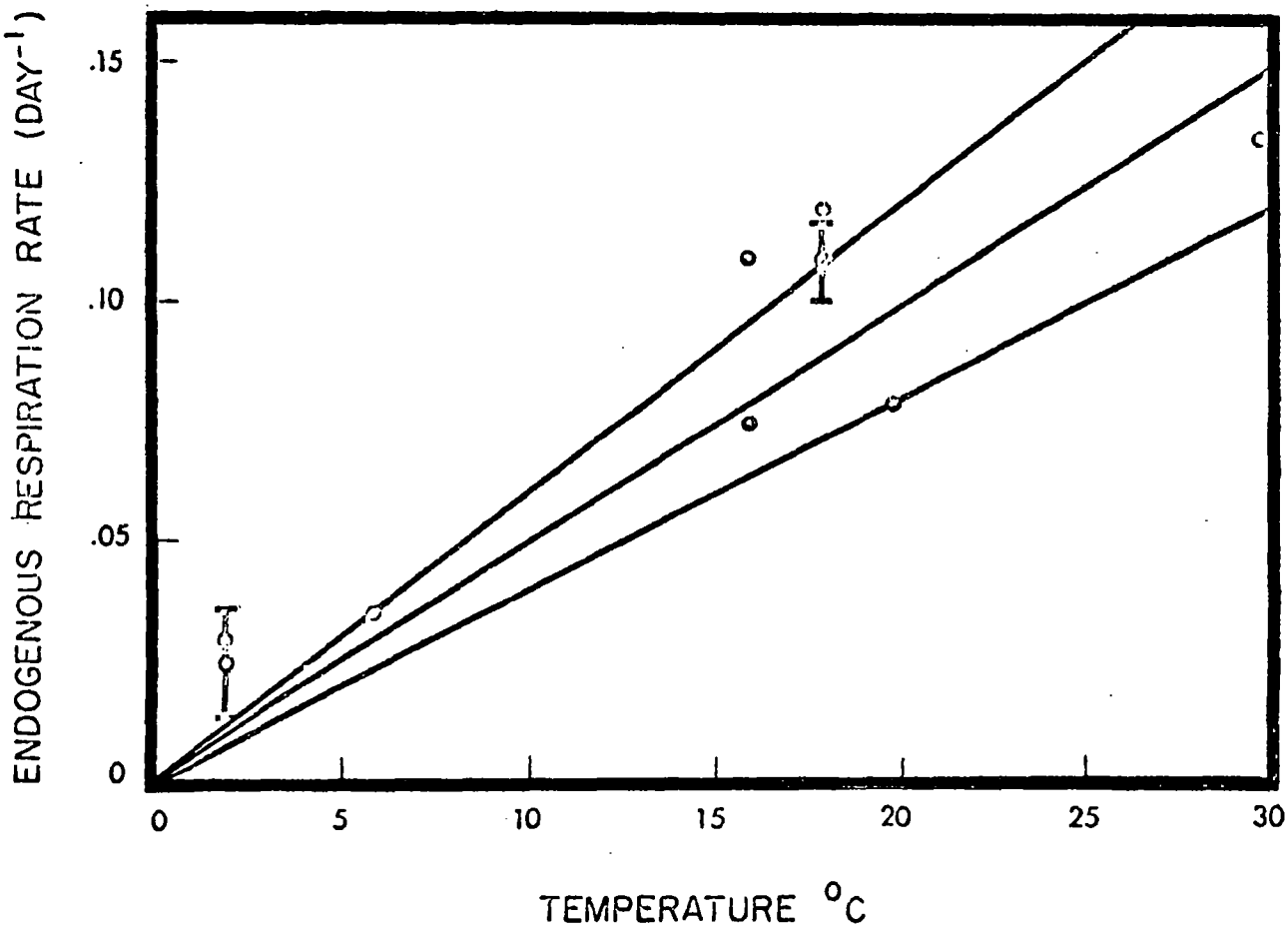

Fig. 23 Endogenous Respiration Rate of Phytoplankton vs. Temperature; after Riley (1949)

and this is why a mass death occurs in the nutrient-depleted epilimnion after the vernal maximum." In terms of the respiration rate, the resting stage corresponds to a lowering of the

Table 8

Endogenous Respiration Rates of Phytoplankton
(Riley, 1949)

Organism	Temperature °C	Endogenous Respiration Rate, Day^{-1} ($Base_e$)
Nitzschia closterium	6	0.035
	35	0.170
Nitzschia closterium	20	0.08
Coscinodiscus excentricus	16	0.075
	16	0.11
Natural Association	2	0.03
	18	0.12
	2.0	0.024±0.012
	17.9	0.110±0.007

respiration rate as the nutrient concentrations decrease. Thus, a Michaelis-Menton expression for the respiration rate nutrient dependence may also be required, and this dependence should be investigated experimentally. This mechanism is quite significant from a water quality point of view since the deaths of algae after a bloom is of primary concern in protecting the quality of natural bodies of water. The resulting mass of dead algal cells becomes a sink of dissolved oxygen which can dangerously lower the available oxygen for fish and other aquatic animals.

The interaction between the phytoplankton population and the

next trophic level, the herbivorous zooplankton, is a complex process for which only a first approximation can be given. A basic mechanism by which zooplankters feed is by filtering the surrounding water and clearing it of whatever phytoplankton and detritus is present. Thus, the presence of zooplankton prey on phytoplankton as a food source. The filtering or grazing rate of some species of zooplankton have been measured and are presented in Table 9. The grazing rate is sometimes reported as a volume of water filtered per unit time per individual. In order to be applicable to a natural zooplankton population consisting of differing species, these grazing rates are converted to a filtering rate per unit biomass of zooplankton and denoted by C_g. A convenient biomass unit for zooplankton concentration is their dry weight. As can be seen from Table 9, the resulting values of C_g vary considerably. This variation is not unexpected since the measurement of grazing rates of zooplankters is a difficult procedure and subject to large variations in the estimates.

Variations of the filtering rate with temperature change have been reported (Anraku, 1963). Examples of this variation are presented in Figure 24 for four species of genus Daphnia, a small crustacean (Burns, 1969); two species of Acartia (Conover, 1956); and two species of Centropages (Anraku, 1963), both copepods. The copepods show a marked grazing rate temperature-dependence while the grazing rates of the Daphnia do not vary as markedly. The filtering rate also varies as a function of the size of the phytoplankton cell being ingested (Mullin, 1963), the concentration of phytoplankton (McMahon, 1965), and the amount of particulate matter present (Burns, 1967). Selective grazing of certain phytoplankton species has also been reported (Burns, 1969). The complexity of this aspect of phytoplankton mortality is such that the use of one grazing coefficient to represent the process must be viewed as a first

Table 9

Grazing Rates of Zooplankton

Reference	Organism	Reported Grazing Rate	Grazing Rate Liter/ mg Dry Wt.-Day
	ROTIFER		
Hutchinson 1967	Brachionus calyciflorus	0.05-0.12[a]	0.6-1.5
	COPEPOD		
Riley 1949b	Calanus sp.	67-208[b]	0.67-2.0
Adams, Steele 1966	Calanus finmarchicus	27[a]	0.05
Mullin, Brooke 1967	Rhincalamus nasutus	98-670[a]	0.3-2.2
Anraku Omori,1963	Centropages hamatus		0.67-1.6
	CLADOCERA		
Wright,1958	Daphnia sp.		1.06
Burns,1969	Daphnia sp		0.2-1.6
Ryther,1954	Daphnia magna	81[a]	0.74
McMahon, 1956	Daphnia magna	57-82[a]	0.2-0.3
	NATURAL ASSOC.		
Riley,1949b	Georges Bank	80-110[b]	0.8-1.10

[a] Ml/animal-day
[b] Ml/mg wet wt-day

approximation. However, since this mathematical expression does represent a physiological mechanism that has been investigated and for which reported values of C_g are available, this approximation is a realistic first step. Also, it is difficult to see, aside from refinements as to temperature and phyto

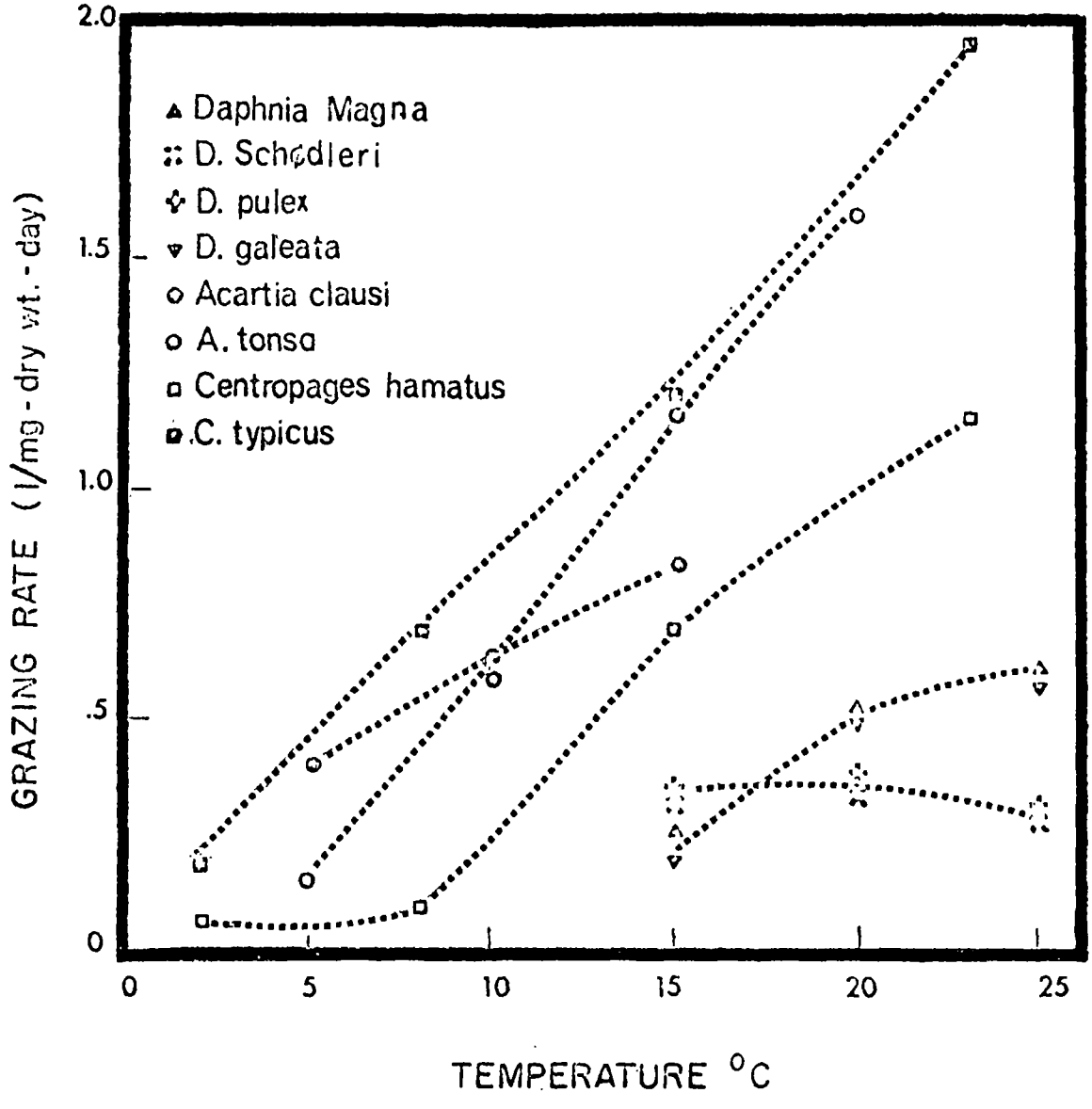

Fig. 24 Grazing Rates of Zooplankton vs. Temperature

plankton concentration dependence, what further improvements could be made in the formulation so long as the phytoplankton and zooplankton population are represented by a biomass measurement which ignores the species present and their individual characteristics. For simplicity in this investigation, the grazing rate is assumed to be a constant. The death rate of phytoplankton resulting from the grazing of zooplankton is given by the expression $C_g Z_j$, where Z_j is the concentration of herbivorous zooplankton biomass in the j^{th} volume element.

For models of the phytoplankton populations in coastal oceanic waters and in lakes, the sinking rate of phytoplankton cells is an important contribution to the mortality of the population. The cells have a net downward velocity, and they eventually sink out of the euphotic zone to the bottom of the water body. This mechanism has been investigated and included in phytoplankton population models (Riley, 1949; Chen, 1970). However, for the application of these equations to a relatively shallow vertically well mixed river or estuary, the degree of vertical turbulence is sufficient to eliminate the effect of sinking on the vertical distribution of phytoplankton.

Therefore, considering only the phytoplankton respiration and the predation of zooplankton, the death rate of phytoplankton is given by the equation

$$D_{pj} = K_2 T + C_g Z_j \tag{74}$$

and for a zooplankton biomass concentration Z_j, the mortality rate can be calculated from this equation.

This completes the specification of the growth and death rates of the phytoplankton population in terms of the physical vari-

ables: light and temperature, the nutrient concentrations, and the zooplankton present. With these variables known as a function of time, it is possible to calculate the phytoplankton population resulting throughout the year. However, the zooplankton population and the nutrient concentrations are not known a priori since they depend on the phytoplankton population which develops. That is, these systems are interdependent and cannot be analyzed separately. It is therefore necessary to characterize both the zooplankton population and the nutrients in mathematical terms in order to predict the phytoplankton population which would develop in a given set of circumstances.

The Zooplankton System

As indicated in the previous section, the zooplankton population exerts a considerable influence on the phytoplankton death rate by its feeding on the phytoplankton. In some instances, it has been suggested that this grazing is the primary factor in the reduction of the concentration of phytoplankton after the spring bloom. In the earlier attempts to model the phytoplankton system, the measured concentration of zooplankton biomass was used to evaluate the phytoplankton death rate resulting from grazing. However, it is clear that the same arguments used to develop the equation for the conservation of phytoplankton biomass can be applied directly to the zooplankton system. In particular, the source of zooplankton biomass S_{zj} within a volume element V_j can be given as the difference between a zooplankton growth rate G_{zj} and a zooplankton death rate D_{zj}. Thus, the equation for the source of zooplankton biomass, which is analogous to Equation (54) is

$$S_{zj} = (G_{zj} - D_{zj}) Z_j \tag{75}$$

where G_{zj} and D_{zj} have units day^{-1} and Z_j is the concentration of zooplankton carbon in the volume element V_j. The magnitude of the growth rate in comparison with the death rate determines whether the net rate of zooplankton biomass production in V_j is positive, indicating net growth rate, or negative, indicating a net death rate.

As in the case of the phytoplankton population, the growth and death rates, and in fact the whole life cycle of individual zooplankters, are complicated affairs with many individual peculiarities. The surveys by Hutchinson (1967) and Raymont (1963) give detailed accounts of their complex biology. It is, however, beyond the scope of this report to summarize all the differences and species-dependent attributes of the many zooplankton species. The point of view adopted is macroscopic, with the population characterized in units of biomass. The resulting growth and death rates can be thought of as averages over the many species present. These simplifications are made in the interest of providing a model which is simple enough to be manageable and yet representative of the over-all behavior of the populations.

The grazing mechanism of the zooplankton provides the basis for the growth rate of the herbivorous zooplankton, G_{zj}. For a filtering rate C_g, the quantity of phytoplankton biomass ingested is $C_g P_j$, where P_j is the phytoplankton biomass concentration in V_j. To convert this rate to a zooplankton growth rate, a parameter which relates the phytoplankton biomass ingested to zooplankton biomass produced, a utilization efficiency, a_{zp}, is required. However, this utilization efficiency or yield coefficient is not a constant. At high phytoplankton concentrations, the zooplankton do not metabolize all the phytoplankton that they graze, but rather they excrete a portion of the phytoplankton in undigested or semidigested form (Riley,

1947). Thus, utilization efficiency is a function of the phytoplankton concentration. A convenient choice for this functional relationship is $a_{zp}K_{mp}/(K_{mp} + P_j)$ so that the growth rate for the zooplankton population is

$$G_{zj} = a_{zp}C_g K_{mp}\left(\frac{P_j}{K_{mp} + P_j}\right) \qquad (76)$$

The resulting growth rate has the same form as that postulated for the nutrient-phytoplankton relationship, namely, a Michaelis-Menton expression with respect to phytoplankton biomass. In fact, the argument which is used to justify its use in Equation (67) can be repeated in this context. The difference is that in this case the substrate or nutrient is phytoplankton biomass, and the microbes are the zooplankton. The Michaelis constant K_{mp} is the phytoplankton biomass concentration at which the growth rate G_{zj} is one-half the maximum possible growth rate $a_{zp}C_g K_{mp}$. The fact that at high phytoplankton concentrations the zooplankton growth rate saturates was incorporated by Riley (1947) in the first model proposed for a zooplankton population.

The assimilation efficiency of the zooplankton at low phytoplankton concentrations, a_{zp}, which is the ratio of phytoplankton organic carbon utilized to zooplankton organic carbon produced has been estimated by Conover (1966) for a mixed zooplankton population. The results of 26 experiments gave an average of 63% and a standard deviation of 20%. Other reported values are within this range. Experimental values for K_{mp}, which in effect set the maximum growth rate of zooplankton, are not available and would probably be highly species-dependent. Perhaps a more effective way of estimating K_{mp} is first to estimate the maximum growth rate at saturating phytoplankton concentrations, $a_{zp}C_g K_{mp}$, and then calculate K_{mp}. Growth rates for copepods through their life cycle

average 0.18 day^{-1} (Mullin, 1967). For the Georges Bank population, Riley used 0.08 day^{-1} (Riley, 1947) for the maximum zooplankton growth rate. For a value of the grazing coefficient C_g of 0.5 liter/mg-dry wt-day and an assimilation coefficient of 65%, the Michaelis constant for zooplankton assimilation, K_{mp}, ranges between 0.25 and 0.55 mg-dry wt/liter of phytoplankton biomass. However, these values should only be taken as an indication of the order of magnitude of K_{mp}. It is probable that its value can vary substantially in different situations.

The fact that the growth rate reaches a maximum or saturates is an important feature of the formulation of the zooplankton growth rate since in some cases the phytoplankton concentration during part of the year exceeds that which the zooplankton can effectively metabolize. If the zooplankton growth rate is not limited in some way and, instead, is assumed simply to be proportional to the phytoplankton concentration, as proposed in simpler models, the resulting zooplankton growth rate during phytoplankton blooms can be very much larger than is physiologically possible for zooplankton, an unrealistic result. The saturating growth rate also has implications in the mathematical properties of the resulting equations. In particular, the behavior differs significantly from the classical Volterra Preditor-Prey equations (Lotka, 1956). This is discussed further in a subsequent section.

The growth of the zooplankton population as a whole, of which the herbivorous zooplankton are a part, is complicated by the fact that some zooplankters are carnivorous or omnivorous. Thus, the nutrient for the total population should include not only phytoplankton but also organic detritus as a food source since this is also available to the grazing zooplankton. However, for cases where the phytoplankton are abundant and

the growth rate saturates for the significant growing periods, the simplification introduced by ignoring the detritus is probably acceptable.

The death rate of herbivorous zooplankton is thought to be caused primarily by the same mechanisms that cause the death of the phytoplankton, namely, endogeneous respiration and predation by higher trophic levels. The endogeneous respiration rate of zooplankton populations has been measured and the results of some of these experiments are presented in Figure 25 and Table 10.

It is clear from these measurements that the respiration rate of zooplankters is temperature-dependent. It is also dependent on the weight of the zooplankter in question and its life cycle stage (Comita, 1968). As a first approximation, a straight line dependence is adequate, and the endogeneous respiration rate is given by the equation: respiration rate = K_3T where $K_3 = 0.1 \pm 0.005 (\text{day } ^\circ C)^{-1}$. The conversion from the reported units to a death rate is made by assuming that 50% of the zooplankton dry weight represents the carbon weight and that carbohydrate (CH_2O) is being oxidized. The data are somewhat variable and serve only to establish a range of values within which the respiration rate of a natural zooplankton association might be expected.

The death rate attributed to predation by the higher trophic levels, specifically the carnivorous zooplankton, has been considered by previous models in a more or less empirical way. The complication resulting from another equation and the uncertainty as to the mechanisms involved are quite severe at this trophic level. In particular, it is probable that an equation for organic detritus is necessary to describe adequately the available food. Hence, it is expedient to break the causal chain at this point and assume that the herbivorous

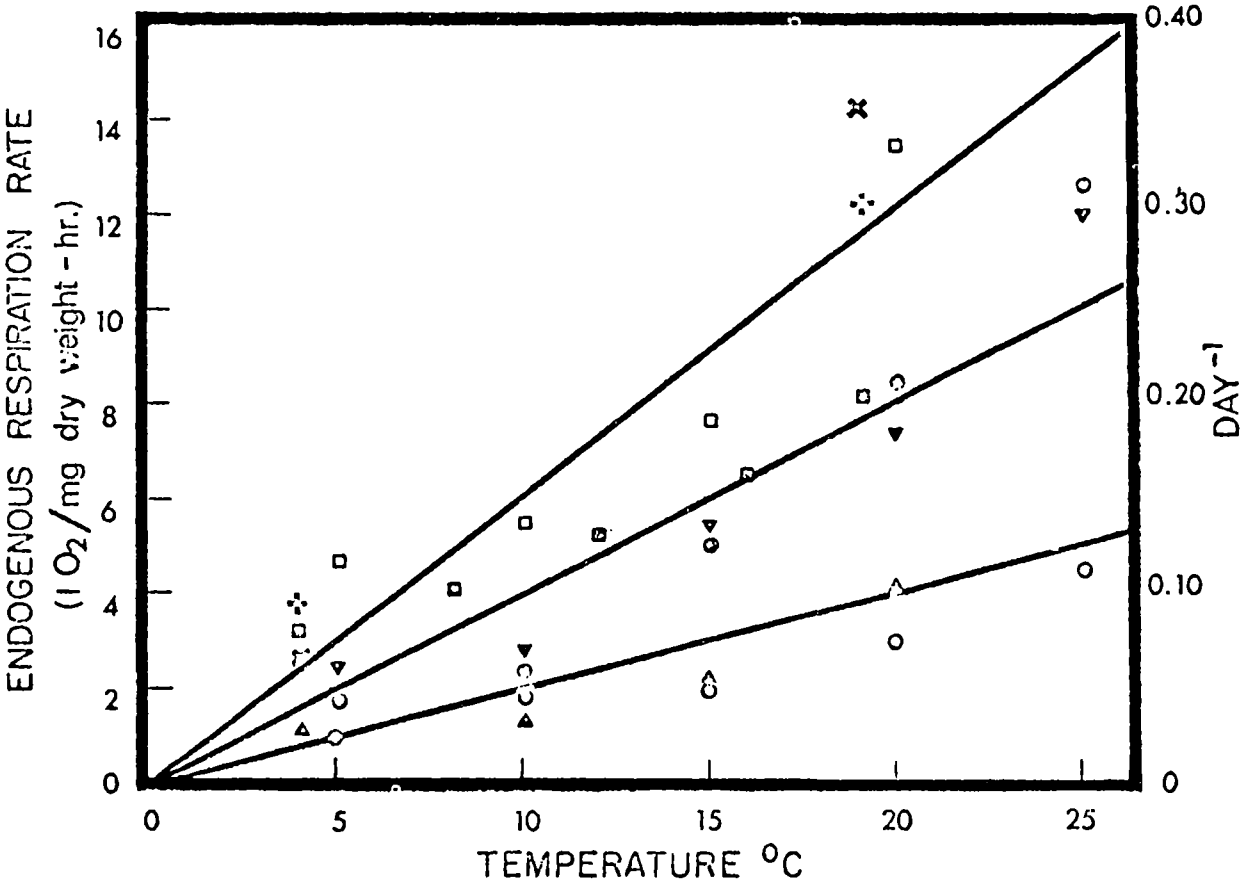

Fig. 25 Endogenous Respiration Rate of Zooplankton vs. Temperature

Table 10

Endogenous Respiration Rate of Zooplankton

Reference	Organism	Plotting Symbol	Temp. °C	Respiration Rate, Ml O_2/Mg Dry Wt-Day
Bishop 1968	Cladocerans	X	18	14.2
			4	2.7
"	Copepods	+	18	12.2
			4	3.8
"	Copepods	■	18	8.2
			16	6.5
			12	5.2
			8	4.1
			4	3.4
Riley 1963	Calanus finmarchicus	▲	20	4.2
			15	2.3
			10	1.4
			4	1.3
Comita 1968	Diaptomus leptopus	▼	25	12.1
			20	7.4
			15	5.3
			10	2.8
			5	2.5
"	D. clavipes	●	25	12.5
			20	8.5
			15	5.1
			10	2.4
			5	1.8
"	D. siciloides	□	25	21
			20	13.5
			15	7.8
			10	5.5
			5	4.8
"	Diaptomus sp.	○	25	4.3
			20	3.0
			15	2.1
			10	1.7
			5	1.1

zooplankton death rate resulting from all other causes is given by a constant, the magnitude of which is to be determined empirically. The severity of this assumption can be tested by examining the sensitivity of the solutions of the phytoplankton and zooplankton equations to the magnitude of this constant. Hence, the resulting zooplankton death rate is given by

$$D_{zj} = K_3T + K_4 \qquad (77)$$

where K_4 is empirically determined.

With the growth and death rates given by Equations (76) and (77), respectively, the source term for herbivorous zooplankton biomass is given by Equation (75). The conservation of mass equation which describes the behavior of Z_j is given by Equation (53), with Z_j as the dependent variables replacing P_j and S_{zj} replacing S_{pj} as the source terms.

This completes the formulation of the equations which describe the zooplankton system. The equations for the nutrient system remain to be formulated.

The Nutrient System

The conservation of mass principle is applied to the nutrients being considered in the same way as it has been previously applied to the phytoplankton and zooplankton biomass within a volume segment. The number of mass conservation equations required is equal to the number of nutrients that are explicitly included in the growth rate formulation for the phytoplankton. For the sake of simplicity, the formulation for only one nutrient is discussed below.

The source term S_{nj} in the conservation of mass equation for the concentration of the nutrient N_j in the j^{th} volume segment V_j is the sum of all sources and sinks of the nutrient within V_j. The primary interaction between the nutrient system and the phytoplankton system is the reduction or sink of nutrient connected with phytoplankton growth. The rate of increase of phytoplankton biomass is $G_{pj}P_j$. To convert this assimilation rate to the rate of utilization of the nutrient, the ratio of biomass production to net nutrient assimilated is required. Over a long time interval, this ratio approximates the nutrient-to-biomass ratio of the phytoplankton population. For example, if the nutrient being considered is total inorganic nitrogen and the phytoplankton biomass is characterized in terms of dry weight, then this ratio is the nitrogen-to-dry-weight ratio of the population. For both nitrogen and phosphorus, these ratios have been studied for a number of phytoplankton species and natural associations. An example of this information is presented in Table 11, condensed from Strickland (1965). If a_{np} is the nutrient-to-phytoplankton biomass ratio of the population, then the sink of the nutrient owing to phytoplankton growth is $a_{np}G_{pj}P_j$.

A secondary interaction between the biological system and the nutrient systems is the excretion of nutrients by the zooplankton and the release of nutrients in an organic form by the death of phytoplankton and zooplankton. The excretion mechanism has been considered by Riley (1965) in a generalization of the equations of Steele. The rate of phosphorus excretion has also been measured experimentally (Martin, 1968). Using the formulation for zooplankton growth rate proposed herein, the rate of nutrient excretion is the rate grazed, $a_{np}C_gP_jZ_j$, minus the rate metabolized, $a_{np}G_{zj}Z_j$; that is,

the excretion rate is

$$a_{np} C_g Z_j P_j \left(1 - \frac{a_{zp} K_{mp}}{K_{mp} + P_j}\right) \qquad (78)$$

At high phytoplankton concentrations, almost all the grazed phytoplankton is excreted since the bracketed term in Equation (78) approaches unity.

Table 11

Dry Weight Percentage[a] of Carbon, Nitrogen, and Phosphorus in Phytoplankton[b]

	% Carbon		% Nitrogen		% Phosphorus	
Phytoplankter	Average	Range	Average	Range	Average	Range
Myxophyceae	36	(28-45)	4.9	(4.5-5.8)	1.1	(0.8-1.4)
Chlorophyceae	43	(35-48)	7.8	(6.6-9.1)	2.9	(2.4-3.3)
Dinophyceae	43	(37-47)	4.4	(3.3-5.0)	1.0	(0.6-1.1)
Chrysophyceae	40	(35-45)	8.4	(7.8-9.0)	2.1	(1.2-3.0)
Bacillariophyceae	33	(19-50)	4.9	(2.7-5.9)	1.1	(0.4-2.0)

[a]The units are (mg of carbon, nitrogen, or phosphorus)/(mg dry weight of phytoplankton) X 100%.

[b]Condensed from Strickland (1965).

There is a difficulty, however, in using this term directly as a source of nutrient. To illustrate this difficulty, assume that the nutrient is inorganic nitrogen. A part of the excreted nitrogen, however, is in organic form, and a bacterial decomposition into the inorganic forms must precede utilization by the phytoplankton. The same is true for the nutrient released by the death of phytoplankton, $a_{np}K_2TP_j$, and that released by the death of zooplankton, $a_{nz}K_3TZ_j$, where a_{nz} is the nutrient-to-zooplankton biomass ratio. Therefore, strictly speaking, a conservation of mass equation for the organic form of the nutrient is required. The organic form is then converted to the inorganic form. For the case of nitrogen, the kinetics of this conversion have been investigated and applied to stream and estuarine situations (Thomann, 1963). If the conversion rate is large by comparison with the other rates in the phytoplankton and zooplankton equations, then the direct inclusion of these sources is approximately correct.

The sources of nutrients arising from man-made inputs, such as wastewater discharges and agricultural runoff, are included explicitly into the source term since these sources are usually the major control variables available to influence the biological systems. An extensive review of the magnitude and relative importance of these sources of nutrients, primarily nitrogen and phosphorus, has recently been made (Vollenweider, 1968). A useful distinction is made between diffuse sources such as agricultural runoff loads and ground water infiltration, which are difficult to measure and control, and point sources such as wastewater discharges from municipal and industrial sources, for which more information is available. The nitrogen and phosphorus loads from agricultural runoff are quite variable and depend on many variables such as soil type, fertilizer application, rainfall, and irrigation practice. The nutrient

sources from point loads can be estimated more directly. For example, the nutrient load from biologically treated municipal wastewater is in the order of 10 g/capita-day total nitrogen and 2 g/capita-day total phosphorus. The ratio of per capita phosphorus to physiologically-required phosphorus is approximately 2 to 3, the excess being primarily the result of detergent use. Industrial loads can also be important, especially effluents from food processing industries. If the required loading rates are available, their loads should be included in the nutrient mass balance equations. In particular, if the investigation of the phytoplankton population is directed at the probable effects of increasing or decreasing the nutrient load, these loads must be explicitly identified and their magnitude assessed.

Let W_{nj} be the rate of addition of the nutrient to the j^{th} volume element. This source is then included as a component in the nutrient source term in the mass balance equation.

An important additional source of inorganic nutrients which may influence the availability of nutrients is the interaction of the overlying water either with the underlying mineral strata if exposed or with whatever sediment is present. These interactions can complicate the source term but they should be included if they add significantly to the available nutrient.

The source term which results from the inclusion of the phytoplankton utilization sink, the zooplankton excretion and the mortality sources, and the man-made additions is

$$S_{nj} = \frac{W_{nj}}{V_j} - a_{np}G_{pj}P_j + a_{np}C_g Z_j P_j \left(1 - \frac{a_{zp}K_{mp}}{K_{mp} + P_j}\right) + a_{np}K_2 TP_j + a_{nz}K_3 TZ_j \tag{79}$$

Any additional sources and sinks that contribute can be added to the source term as needed. With the source term formulated, the conservation of nutrient mass equation is given by Equation (53) with N_j as the dependent variable replacing P_j and S_{nj} replacing S_{pj}.

The Equations of the Model

In the previous sections, the equations for phytoplankton and zooplankton biomass and nutrient concentration within one volume element have been formulated. The resulting equations are an attempt to describe the kinetics of the growth and death of the phytoplankton and zooplankton populations and their interaction with the nutrients available. The form of the equations for the volume V_j are as follows:

$$\dot{P}_j = [G_{pj}(P_j,N_j,t) - D_{pj}(Z_j,t)]\ P_j + S_{pj}(P_j,Z_j,N_j,t) \quad (80)$$

$$\dot{Z}_j = [G_{zj}(P_j,t) - D_{zj}(t)]\ Z_j + S_{zj}(P_j,Z_j,t) \quad (81)$$

$$\dot{N}_j = S_{nj}(P_j,Z_j,t) \quad (82)$$

where G_{pj} and D_{pj} are given by Equations (67) and (74), G_{zj} and D_{zj} are given by Equations (76) and (77), and S_{nj} by Equation (79). The dependence of the growth and death rates on the concentration of the three dependent variables and time is made explicit in this notation.

These equations describe only the kinetics of the populations in a single volume element V_j. However, in a natural water body there exists significant mass transport as well. The mass transport mechanisms can be conveniently represented by the matrix A with elements a_{ij}. If for particular segments

i and j the matrix element a_{ij} is nonzero, then the volume segments V_i and V_j interact, and mass is transported between the two segments. Letting P, Z, and N be the vectors of elements P_j, Z_j, and N_j and letting S_p, S_n, S_z be the vectors of elements S_{pj}, S_{zj}, and S_{nj}, the conservation of mass equations for the three systems including the mass transport and kinetic interactions are

$$\overset{\circ}{VP} = AP + VS_p \tag{83}$$

$$\overset{\circ}{VZ} = AZ + VS_z \tag{84}$$

$$\overset{\circ}{VN} = AN + VS_n \tag{85}$$

where V is the diagonal matrix of the volumes of the segments. These are the equations which form the basis for the phytoplankton population model. The detailed formulation and evaluation of the mass transport matrix has been discussed elsewhere (Thomann, 1963; O'Connor & Thomann, 1966; O'Connor et al, 1971).

The form of Equations (83)-(85) makes explicit the linear and nonlinear portions of the equations. In the equation for P, the phytoplankton biomass, the concentration P_j, in the volume element V_j, is linearly coupled to the other P_k's through the matrix multiplication by A. However, there is no nonlinear interaction between P_j and any other P_k, $k \neq j$. The reason is that the transport processes are described by linear equations. It is usually the case, however, that the A matrix is a function of time, since at least the advective terms usually vary in time. The nonlinear terms in the vector S_p involve P_j itself and the corresponding Z_j and N_j. Hence, the P equation is coupled to the Z and N equations through this term. Note, however, that P_j is not coupled to the Z_k, $k \neq j$, in any other segment, so that the coupling takes place only within each volume segment.

Therefore, the nonlinearities provide the coupling between the phytoplankton, zooplankton, and nutrient systems. This coupling is accomplished within each volume and does not extend beyond the volume boundary. The coupling among the volumes is accomplished by the linear transport interaction represented by the matrix A. This matrix may be time-varying but its elements are not functions of the phytoplankton, zooplankton, or nutrient concentrations. Hence, in many ways these equations behave linearly. In particular, their spatial behavior is unaffected by the nonlinear source terms. However, the temporal behavior and the relationships between each P_j, Z_j, and N_j are distinctly nonlinear.

Comparison with Lotka-Volterra Equations

The classical theory of predator-prey interaction as formulated by Volterra involves two equations which express the growth rate of the prey and the predator (Lotka, 1956). Within the context of phytoplankton and zooplankton population, the prey is the phytoplankton and the predator zooplankton. In the notation of the previous sections, for a one-volume system, the Lotka-Volterra equations are:

$$\frac{dP}{dt} = (G_p - D_p') P - C_g PZ \tag{86}$$

$$\frac{dZ}{dt} = - D_z Z + a_{zp} C_g PZ \tag{87}$$

where all the coefficients, G_p, D'_p, C_g, D_z, and a_{zp} are assumed to be constants and $G_p > D'_p$. This is a highly simplified situation since, as indicated previously, the growth and death rates are functions of time and, in the case of the phytoplank-

ton growth rate, of the phytoplankton and nutrient concentrations as well. However, for a situation with adequate nutrients and low initial phytoplankton concentration, the nonlinear interaction is small initially, and the time variation of G_p can be small during the summer months. In any case, the analysis of this simplified situation is quite instructive.

Although no analytical solution is available for these simplified equations, their properties are well understood (Davis, 1962). In particular, the equations have two sets of singular points corresponding to the solution of the righthand side of Equations (86) and (87) equated to zero: the trivial solutions $P^* = 0$, $Z^* = 0$, and

$$P^* = \frac{D_z}{a_{zp} C_g}, \quad Z^* = \frac{G_p - D'_p}{C_g} \tag{88}$$

A perturbation analysis of Equations (86) and (87) about this singular point shows that the solutions whose initial conditions are close to P^*, Z^*, oscillate sinusoidally about this singular point. Hence, no constant solution is possible. The prey and predator populations continually oscillate and are out of phase with each other. When the predator predominates, the prey is reduced, which in turn causes the predator to die for lack of food, which allows the prey to proliferate for lack of predator, which then causes the predator to grow because of the prey available as a food supply, and so on. The interesting feature is that these oscillations continue indefinitely.

The classical Lotka-Volterra equations assume an isolated population with no mass transport into or out of the volume being considered. To simulate the effect of mass transport into the volume, assume that an additional source term of

phytoplankton biomass exists and has constant magnitude P_o. For this situation, the equations become

$$\frac{dP}{dt} = (G_p - D'_p)\, P - C_g PZ + P_o \tag{89}$$

$$\frac{dZ}{dt} = D_z Z + a_{zp}\, C_g PZ \tag{90}$$

The nontrival singular point for these equations is

$$P^* = \frac{D_z}{a_{zp} C_g}, \quad Z^* = \frac{a_{zp} P_o}{D_z} + \frac{(G_p - D'_p)}{C_g} \tag{91}$$

The perturbation analysis about this singular point yields a second order linear ordinary differential equation whose characteristic equation has the roots λ_1 and λ_2 where

$$\lambda_{1,2} = -\frac{a_{zp} P_o C_g}{2 D_z} \pm \sqrt{\left[\frac{a_{zp} P_o C_g}{2 D_z}\right]^2 - a_{zp} C_g P_o - (G_p - D'_p) D_z} \tag{92}$$

Since for $P_o > 0$, these roots have negative real parts, this singular point is a stable focus, and the steady state values given by Equation (91) are approached either by a damped sinusoid or an exponential (Davis, 1962). Note that for $P_o = 0$, the classical case, the roots are purely imaginary, and the oscillation persists indefinitely.

This analysis suggests that the effect of transport into the system stabilizes the behavior of the equations and in particular allows the solutions to achieve a constant solution. This is in marked contrast to the behavior of the classical Lotka-Volterra equations.

Another modification, which has been introduced into the zooplankton equations, changes the behavior of the proposed

equations in contrast to the Lotka-Volterra equations. It has been argued that the zooplankton growth rate resulting from grazing must approach its maximum value when the phytoplankton population becomes large since the zooplankters cannot metabolize the continually increasing food that is available. Thus, the growth rate $a_{zp}C_gPZ$ is replaced by $a_{zp}C_gZP\ K_{mp}/(P + K_{mp})$ where K_{mp} is a Michaelis constant for the reaction. The equations then become

$$\frac{dP}{dt} = (G_p - D'_p)P - C_gPZ + P_o \tag{93}$$

$$\frac{dZ}{dt} = - D_zZ + \frac{a_{zp}C_gZPK_{mp}}{P + K_{mp}} \tag{94}$$

The nonzero singular points are

$$P^* = \frac{D_zK_{mp}}{a_{zp}C_gK_{mp} - D_z} \tag{95}$$

$$Z^* = \frac{P_o}{C_gP^*} + \frac{(G_p - D'_p)}{C_g} \tag{96}$$

This solution reduces to the previous situation, Equation (91), for large K_{mp}. This is expected since for K_{mp} large with respect to P, the expression $K_{mp}/(P + K_{mp})$ approaches one. However, an interesting modification from classical predator-prey behavior occurs if the following condition is met

$$a_{zp}C_gK_{mp} = D_z + \varepsilon \tag{97}$$

where ε is a small positive number. For this condition, P* is large and positive. What happens in this case is that the zooplankton population, although it continues to grow expo-

nentially, cannot grow quickly enough to terminate the phytoplankton growth by grazing, and the phytoplankton continue to grow exponentially until P* is reached. Of course, in the actual situation, for which G_p is not a constant, other phenomena such as nutrient depletion and self-shading exert their effect, and the growth may be stopped sooner. However, if the growth rate of zooplankton at a phytoplankton concentration equal to the Michaelis constant K_{mp} is only slightly larger than their death rate D_z, then the zooplankton alone do not rapidly terminate the bloom.

This condition is an important dividing line for the possible behavior of the phytoplankton-zooplankton equations set forth in the previous sections. In particular, it indicates what must be true for a system wherein the zooplankton are a significant feature in the resulting phytoplankton solution. However, if Equation (97) is satisfied, then the zooplankton are not the dominant control of the phytoplankton population.

Application - San Joaquin River

As an example of the application of the equations proposed herein, consider the phytoplankton and zooplankton population observed at Mossdale Bridge on the San Joaquin River in California during the two years 1966-1967. Mossdale is located approximately 40 miles from the confluence of the San Joaquin and the Sacramento Rivers. The data presented below have been supplied to the investigators by the Dept of Water Resources, State of Calif (Anon,1966), as part of an ongoing project to assess the effects of proposed nutrient loads and flow diversions on the water quality of the San Francisco Bay Delta (O'Connor et al, 1972).

In order to simplify the spatial segmentation and the calculations, a one-volume segment is chosen for the region of the San Joaquin for which Mossdale is representative. The volume of this segment is, of course, somewhat arbitrary, and a more representative spatial segmentation would remove this uncertainty. However, it is instructive to consider the behavior of the solution of this simplified model.

The nutrient data available indicate that phosphate, biocarbonate, silicate, calcium, and magnesium are available at concentrations well above the levels for which it has been suggested that these nutrients limit growth. Only the ammonia and nitrate concentrations are low, and they both decrease markedly during the 1966 spring bloom. Hence, these nutrients must be considered explicitly. To simplify the computations, the ammonia and nitrate nitrogen are combined, and the nutrient considered is total inorganic nitrogen.

There is some uncertainty concerning the magnitude and the temporal variation of the inorganic nitrogen load being discharged to the system during the time interval of interest. For lack of a better assumption, the inorganic nitrogen load W_n being discharged into the volume is assumed to be a constant, the magnitude of which is determined by comparison with the observed inorganic nitrogen concentration data at Mossdale.

The variation of the environmental variables being considered - namely, temperature, solar radiation, and advective flow in the San Joaquin during the two-year period of interest - and the straight line approximations that are used directly in the numerical computation are shown in Figure 26. The influent advective flow, which is assumed to have constant concentrations of phytoplankton and zooplankton biomass and inorganic nitrogen,

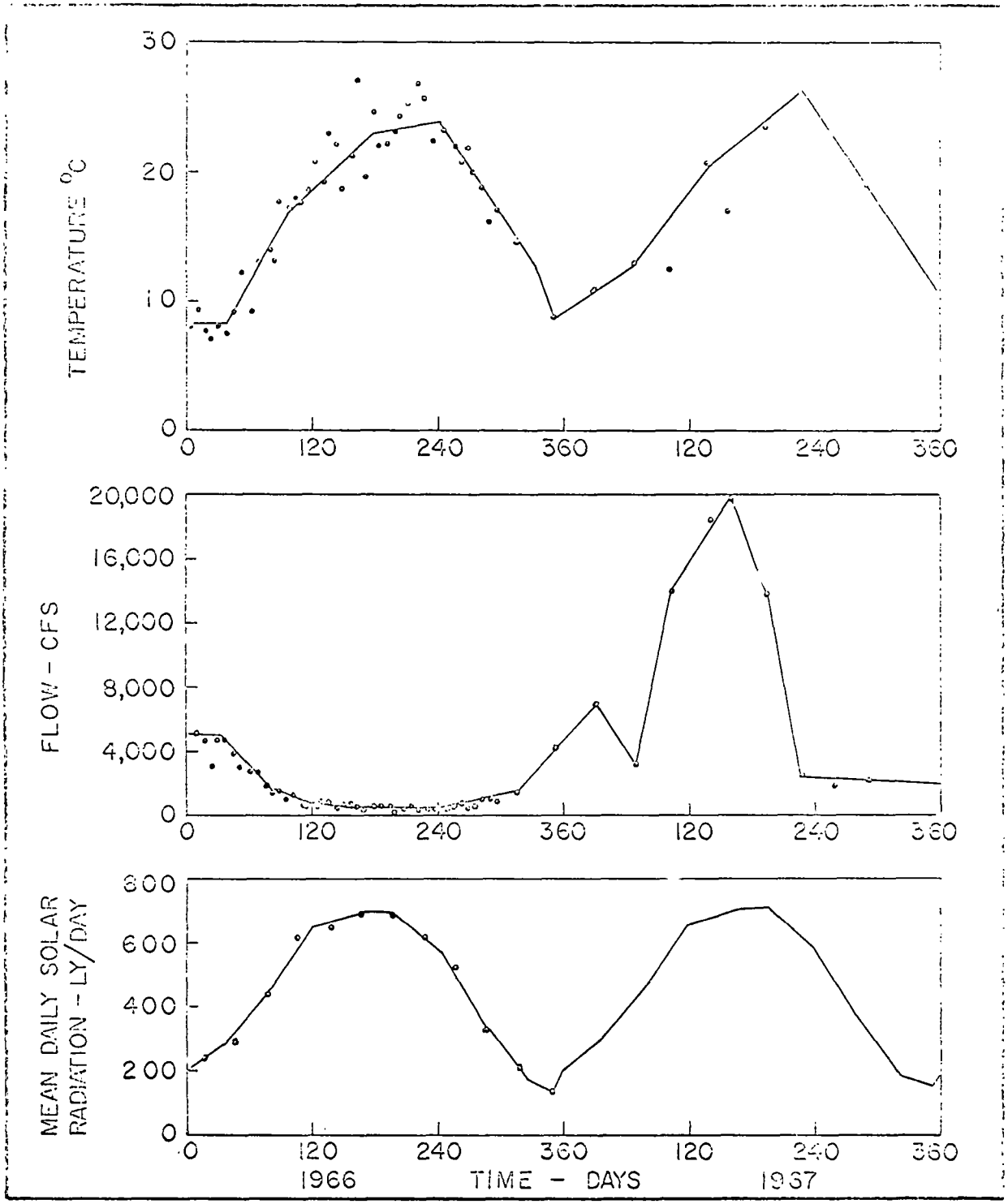

Fig. 26 Temperature, Flow, and Mean Daily Solar Radiation; San Joaquin River, Mossdale, 1966-1967

is routed through the volume. Since Mossdale is located above the saline portion of the San Joaquin, no significant dispersive mass transfer is assumed to exist by comparison with the advective mass transfer.

The equations which represent this one-segment model are

$$\dot{P} = (G_p - D_p)P + \frac{Q}{V}(P_o - P) \tag{98}$$

$$\dot{Z} = (G_z - D_z)Z + \frac{Q}{V}(Z_o - Z) \tag{99}$$

$$\dot{N} = - a_{np}G_pP + \frac{W_n}{V} + \frac{Q}{V}(N_o - N) \tag{100}$$

where $Q = Q(t)$ is the advective flow entering and leaving the volume; V is the volume of the segment; P_o, Z_o, and N_o are the phytoplankton, zooplankton, and inorganic nitrogen concentration of the flow entering the volume. The remaining terms have been defined previously by Equations (67), (74), (76), and (77). In the nutrient equation, only the direct source of inorganic nitrogen, W_n, has been included; the organic feedback terms representing excreted nitrogen, etc., Equation (79), have been dropped. Since the magnitude of W_n is uncertain and is assigned by comparison with observed data and computed model output, these feedback terms can be thought of as being incorporated in the value obtained for W_n.

The solution of Equations (98), (99), and (100) requires numerical techniques. For such nonlinear equations, it is usually wise to employ a simple numerical integration scheme which is easily understood and pay the price of increased computational time for execution rather than using a complex, efficient, numerical integration scheme where unstable behavior is a distinct possibility. A variety of simple methods

are available for integrating a set of ordinary first order differential equations. In particular, the method of Huen, described by Stiefel (1966), is effective and stable. It is self-starting and consists of a predictor and a corrector step. Let $y = f(t,y)$ be the vector differential equation and let h be the step size. The predictor is that of Euler: with y_o the initial condition vector at t_o, the predictor value of y at $t_o + h = t_1$ is

$$y_1^* = y_o + hf(t_o, y_o) \tag{101}$$

the corrector value is simply

$$y_1 = y_o + \frac{h}{2} [f(t_o,y_o) + f(t_1,y_1^*)] \tag{102}$$

That is, the corrector uses the predictor value at t_1 to estimate the slope at t_1 which is averaged with the slope at t_o to provide the slope of the straight line approximation. A variation of this method is discussed at some length by Hamming (1962).

Another simple two-step method is that of Runge, described by Levy (1950). The Euler predictor is used with a half-step integration.

$$y^* = y_o + \frac{h}{2} f(t_o, y_o) \tag{103}$$

This value of y is used to estimate the slope at the midpoint of the interval, which is then used as the slope of the straight line approximation

$$y_1 = y_o + hf(t_o + \frac{h}{2}, y^*) \tag{104}$$

Both of these methods are second order methods, being accurate to terms of order Δt^2 in a comparison of Taylor series expansions of the exact and approximate values, and both methods require two derivative evaluations per step. The method of Runge has been used in the calculations presented below.

The equations themselves are programmed for solution using a continuous simulation language and a digital computer. The language, in this case CSMP/1130, is based on a block diagram, analog computer, representation of the differential equations. The flexibility of these languages which allow changes in the equation structure to be made easily is an asset in modeling complex systems.

The biomass variables used in the calculations are total cell counts for the phytoplankton and rotifer counts for the zooplankton. The rotifer population represented the large majority of the zooplankton present on a weight basis as well. In order to relate these variables to comparable units, a series of conversion factors have been used. The phytoplankton count -chlorophyll concentration ratio was measured. However, the carbon-chlorophyll or dry weight-chloroplyll conversions are unknown. Hence, the conversion to an organic carbon basis is made rather arbitrarily. However, the carbon-to-chlorophyll ratio which results (see Table 12) is within the range reported in the literature. The same problem exists with the rotifer counts to rotifer carbon conversion: the value used is given in Table 12.

The comparison of the model output and the observed data for the two-year period for which data are available is shown in Figure 27. The parameter values used in the equations are listed in Table 12.

Table 12

Parameter Values for the Mossdale Model

Notation	Description	Parameter Value
K_1	Saturated growth rate of phytoplankton	0.1 day^{-1} °C
I_s	Light saturation intensity for phytoplankton	300 ly/day
k'_e	Extinction coefficient	4.0 m^{-1}
H	Depth	1.2 m
K_m	Michaelis constant for total inorganic nitrogen	0.025 mg N/liter
f	Photoperiod	0.5+0.11 sin[0.0172(t-165)]day
K_2	Endogenous respiration rate of phytoplankton	0.005 day^{-1} $°C^{-1}$
C_g	Zooplankton grazing rate	0.13 liter/mg - C - day
P_o	Influent phytoplankton chlorophyll concentration	5.0 µg Chl/liter
a_{zp}	Zooplankton conversion efficiency	0.6 mg C/mg - C
K_{mp}	Phytoplankton Michaelis constant	60 µg Chl/liter
D_z	Zooplankton death rate	0.075 day^{-1}
Z_o	Influent zooplankton carbon concentration	0.05 mg C/liter
a_{np}	Phytoplankton nitrogen-carbon ratio	0.17 mg N/mg - C
C/Chl	Phytoplankton carbon to total chlorophyll ratio	50 mg C/mg-Chl
N_o	Influent total inorganic nitrogen concentration	0.1 mg N/liter
W_n	Direct discharge rate of nitrogen	12500 lbs/day
V	Segment volume	9.7 x 10^8 ft^3
	Phytoplankton total cell count/phytoplankton	100 cells/ml = 1.75 µg Chl/liter
	Zooplankton count/zooplankton carbon ratio	10^4 No./liter = 1.30 mg C liter

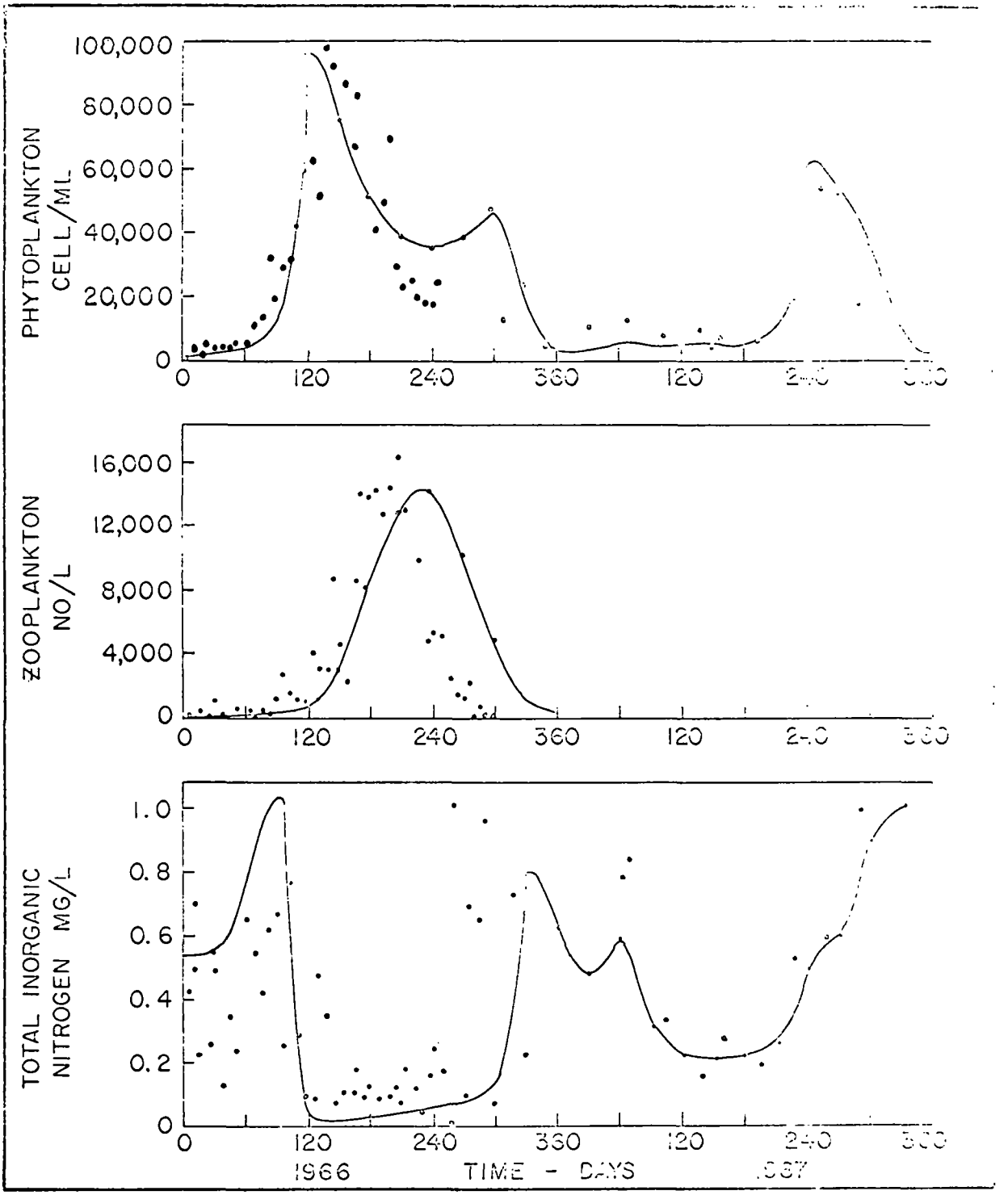

Fig. 27 Phytoplankton, Zooplankton, and Total Inorganic Nitrogen; Comparison of Theoretical Calculations and Observed Data; San Joaquin River, Mossdale, 19666-1967

It is clear from both the data and the model results that a classical predator-prey situation is observed in 1966: the spring bloom of phytoplankton resulting from favorable temperature and light intensity provides the food for zooplankton, which then reduce the population during the summer. The decrease of the zooplankton and the subsequent slight secondary bloom of phytoplankton complete the cycle for the year. It is not clear, however, from a casual inspection of the data, whether the zooplankton population terminated the phytoplankton growth, as in classical predator-prey situations, whether the nutrient concentration dropped to a limiting value that reduced the growth rate, or a combination of the two. This point is elaborated in the next section.

The situation in 1967 is quite different. No significant phytoplankton growth is observed until late in the year. The controlling variable in this case is the large advective flow during the spring and summer of 1967 (see Figure 26) which effectively washes out the population in the region. Only when the flow has sufficiently decreased so that a population can develop do the phytoplankton show a slight increase. However, the dropping temperature and light intensity level terminate the growth for the year.

Growth Rate - Death Rate Interactions

The behavior of the equations which represent the phytoplankton, zooplankton, and nutrient systems in one volume can be interpreted in terms of the growth and death rates of the phytoplankton and zooplankton. The equations are as before

$$\frac{dP}{dt} = (G_p - D_p)P + \frac{Q}{V}(P_o - P) \qquad (105)$$

$$\frac{dZ}{dt} = (G_z - D_z)Z + \frac{Q}{V}(Z_o - Z) \qquad (106)$$

where P_o and Z_o are the concentrations of phytoplankton and zooplankton carbon in the influent flow, Q. A more useful form for these equations is

$$\frac{dP}{dt} = [G_p - (D_p + \frac{Q}{V})]\ P + \frac{Q}{V} P_o \qquad (107)$$

$$\frac{dZ}{dt} = [G_z - (D_z + \frac{Q}{V})]\ Z + \frac{Q}{V} Z_o \qquad (108)$$

A complete analysis of the properties of these equations is quite difficult since the coefficients of P and Z are time variables and also functions of P and Z. However, the behavior of the solution becomes more accessible if the variation of these coefficients is studied as a function of time. The expressions $G_p - (D_p + Q/V)$ and $G_z - (D_z + Q/V)$ can be considered the net growth rates for phytoplankton and zooplankton. The advective or flushing rate, Q/V, is included in these expressions since it acts as a death rate in one segment system.

The sign and magnitude of the net growth rate controls the behavior of the solution. For a linear equation, for which the net growth rate is not a function of the dependent variable (i.e., P or Z), the type of solution obtained depends on the sign and magnitude of the net growth rate. That is, for the equation

$$\frac{dP}{dt} = \alpha P + \frac{Q}{V} P_o \qquad (109)$$

where α, Q, and V are constant, the solution is

$$P(t) = P(o)\ e^{\alpha t} + P_o \frac{Q}{\alpha V} (e^{\alpha t} - 1) \qquad (110)$$

For α negative, that is, for a negative net growth rate, the solution tends to the steady state value $P_o\ Q/|\alpha|V$. However, for α positive, the solution grows exponentially without limit. Thus, for α negative but $|\alpha|$ small, or for α positive, the solution becomes large; whereas for α negative but $|\alpha|$ large, the solution stays small. Hence, the behavior of the solution can be inferred from the plots of the net growth rates. Figure 28a is a plot of the following terms from the 1966 Mossdale calculation: G_p without the Michaelis-Menton multiplicative factor included - i.e., the growth rate at nutrient saturation denoted by G_p (I,T); G_p itself denoted by G_p (N,I,T) - i.e., the growth rate considering the nutrient effects. The net growth rate $G_p - (D_p + Q/V)$ is also plotted. Similarly, in Figure 28b the growth rate of zooplankton G_z, the mortality rate D_z, the flushing rate $Q(t)/V$, and the net growth rate $G_z - (D_z + Q/V)$ are plotted.

The analysis of the 1966 model calculations can now be made by inspecting these figures. The net growth rate for the phytoplankton $G_p - (D_p + Q/V)$ becomes positive at t = 85 days owing to an increase in G_p, the result of rising temperature and light intensity, and a decrease in Q/V as the advective flow decreases. The positive net growth rate of the population causes their numbers to increase exponentially fast until the nutrient begins to be in short supply. This is evidenced by the departure of the G_p curve from the G_p at nutrient saturation curve. At the same time, the D_p curve is showing a marked increase because of the increased zooplankton population and their grazing. The result is that the net growth rate becomes zero and then negative as the zooplankton reduce the phytoplankton population by grazing. The growth of the zooplankton can be analyzed in a similar fashion using Figure 28b. The net

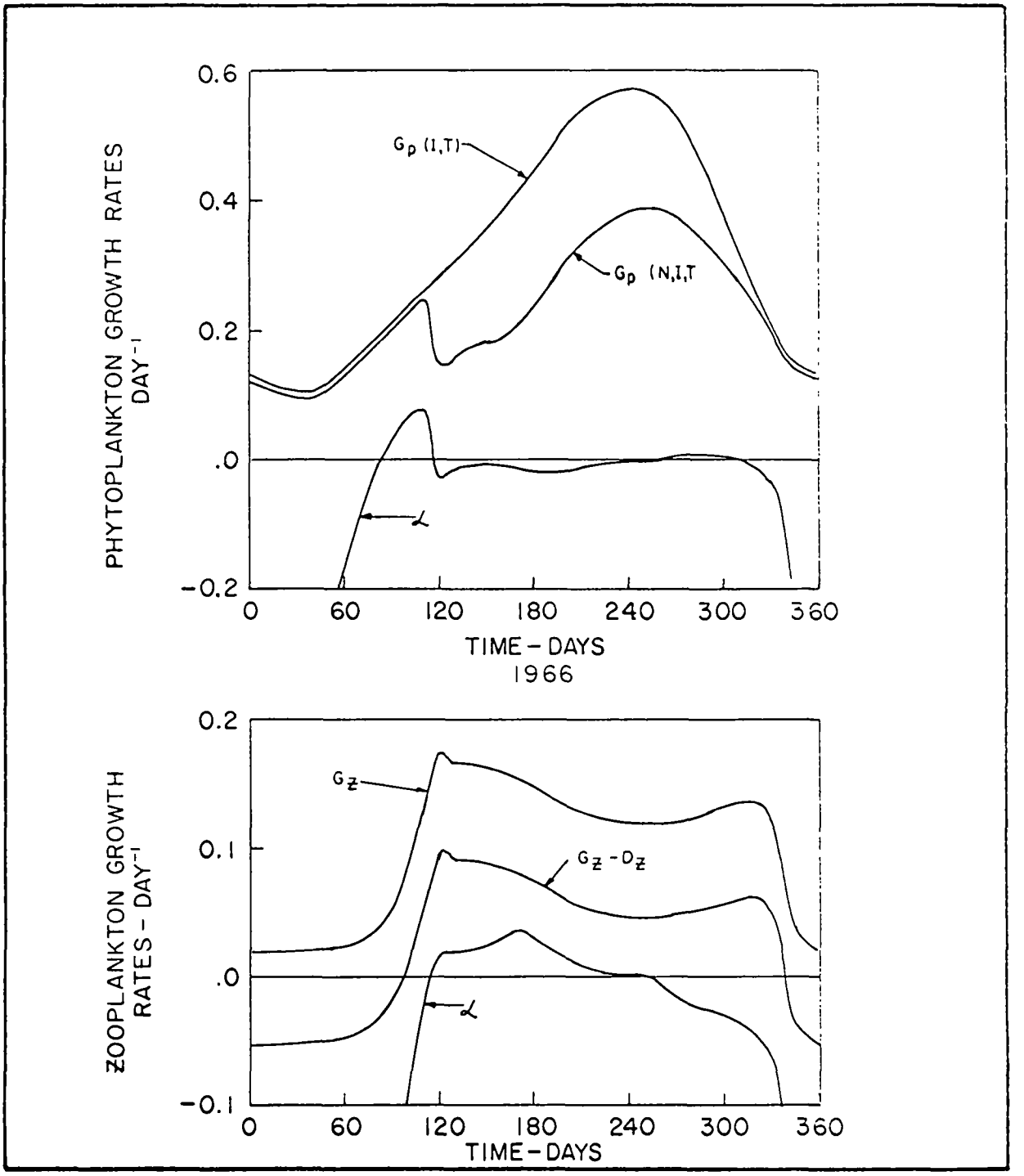

Fig. 28 Theoretical Growth Rates for Phytoplankton and Zooplankton Populations

growth rate becomes positive when the phytoplankton population is large enough to sustain the zooplankters. Then the zooplankton grow until they have reduced the phytoplankton population to a level where they are no longer numerous enough to sustain the zooplankton. The net zooplankton growth rate then becomes negative and the population diminishes in size. This small zooplankton population no longer exerts a significant effect on the death rate of the phytoplankton, D_p, and its value decreases, causing the net phytoplankton growth rate to become positive again, and the smaller autumn bloom results. The decreasing temperature and light intensity and the increasing advective flow then effectively terminate the bloom as the year ends.

SECTION VI

A PRELIMINARY MODEL OF PHYTOPLANKTON DYNAMICS IN THE UPPER POTOMAC ESTUARY

The Potomac Estuary has been the subject of investigation and analysis over many decades and most intensively within the past several years. This work has been motivated in large measure by the location of Washington D.C. along its shores and by a long history of poor water quality. Also, if water quality is to be improved nationally, the river flowing through the Nation's capital must serve as a model situation. Several Enforcement Conferences have been held on the water quality of the Potomac River with the aim of establishing required effluent controls to achieve specified water quality objectives. Important recommendations which evolved from these efforts included waste load allocations which restrict the mass discharge of oxygen demanding material, and nitrogen and phosphorus residuals. These recommendations relied to some degree on the application of detailed mathematical modeling of key water quality constituents such as dissolved oxygen and various nitrogen and phosphorous forms.

The purpose of this section is to present a preliminary model of the dynamic behavior of phytoplankton in the Upper Potomac Estuary. This research extends the previous modeling efforts on the Potomac to incorporate explicitly the space-time variability of chlorophyll a as a water quality parameter indicative of a eutrophied environment. The research also extends previous work in this report (see Section V to an estuarine situation dominated presently by municipal waste discharges. This preliminary phytoplankton model is intended therefore to shed further light on the water quality changes that can be expected when a

waste reduction program is completed for the Potomac Estuary. Primary emphasis here is on the efficacy of nutrient removal programs especially in the Washington D. C. area and downstream.

The area of interest of the model is centered in the upper forty-mile reach of the Potomac Estuary although as indicated below,the model geographically extends over the entire 114-mile length of the estuary from Little Falls to Chesapeake Bay. The upper reach of 30 - 40 miles is generally unaffected by the incursion of saltsfrom Chesapeake Bay. The Potomac is tidal in the vicinity of Washington D.C. and is several hundred feet wide with a shipping channel of minimum depth of 24 feet maintained to Washington. The tidal portion averages about 18 feet and is characterized by numerous coves and embayments along its length with average depths significantly less than the main estuary. Presently, the major waste source in the upper reach of the Potomac is the effluent from the Washington D.C. secondary treatment plant.

Water quality problems include low values of dissolved oxygen in the vicinity of the District of Columbia and high concentrations of phytoplankton especially of Anacystis, a blue green form. Detailed reviews are given bv Jaworski et al (March 1969), Jaworski (Nov 1969), Aalto et al (1970) and Jaworski et al (1971).

Model Geometry and Kinetics

The basic model builds on previous efforts of phytoplankton dynamics (Di Toro et al, 1971) and nitrification effects in estuaries (Thomann et al, 1970).

Spatially, the estuary is divided into twenty-three longi-

tudinal segments using data on depth,cross-sectional areas and segment volume given by earlier modeling work in the Potomac and summarized in Jaworski and Clark (undated). Figure 29 shows the location of these main estuary segments. As discussed more fully below, it was found necessary to include the effects of the tidal bays on main channel quality. The tidal flat areas have been cited as an important phenomenon in the Potomac River as far back as 1916 (Phelps). Accordingly, an additional fifteen spatial segments were incorporated in the model to reflect lateral effects of the shallow water areas. These tidal bay segments are also shown in Figure 29. A total of thirty-eight spatial segments were therefore used to represent the Potomac with primary emphasis on segments #1 - #15, the Upper Estuary. Each segment is assumed completely mixed and therefore represents a finite difference approximation to a continuous medium. In order to simplify the analysis, waste loads were inputted into segments #5, 6 and 7 which accounts for the major portion of direct discharge load. No attempt was made in this preliminary model to input urban or suburban runoff or overflows from combined sewers.

The model incorporates interactions between nine variables which are space and time dependent. The variables in the model are

1) Phytoplankton chlorophyll "a" - P
2) Zooplankton carbon - Z
3) Organic nitrogen - N_1
4) Ammonia nitrogen - N_2
5) Nitrate nitrogen - N_3
6) Organic phosphorous - N_{p1}
7) Inorganic phosphorous - N_{p2}
8) Carbonaceous biochemical oxygen demand - L
9) Dissolved oxygen - C

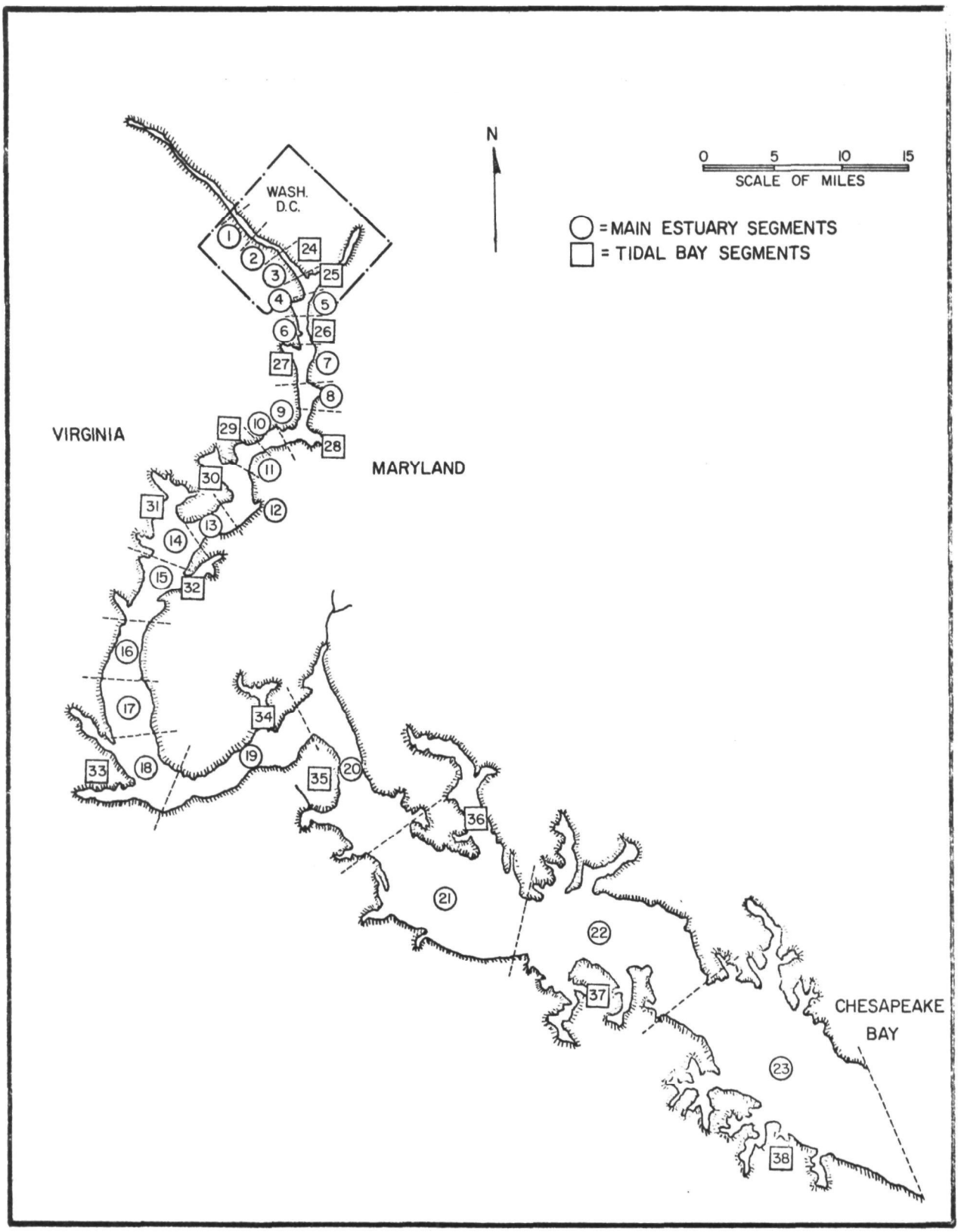

Fig. 29 Map of Potomac Estuary Showing Longitudinal and Lateral Segments

Other variables, constructed from these primary variables are also tracked through the estuary. These secondary variables include total nitrogen and total phosphorous as the most important.

Figure 30 shows the general interaction scheme of the nine primary system variables. The major interactions and phenomena are a) predator-prey relationships between phytoplankton and zooplankton systems 1 and 2 (which is apparently not an important phenomenon at present in the upper Potomac); b) nitrification of oxidizable nitrogen, given by systems #3, 4, and 5; c) conversion of organic phosphorous to inorganic phosphorous and d) dissolved oxygen depletions due to carbonaceous waste loads and effects of nitrification. Nutrient interactions are shown with phytoplankton chlorophyll. The basic kinetic equations are discussed below for each system.

The general matrix equation for the phytoplankton chlorophyll system (Di Toro et al, 1971) under a finite difference approximation is

$$[V]\frac{d(P)}{dt} = [A](P) + [V](S_p) \qquad (111)$$

where (P) is an n x 1 phytoplankton chlorophyll "a" vector, [A] is an n x n matrix of transport and dispersion effects, [V] is an n x n diagonal matrix of segment volumes and (S_p) is an n x 1 vector of source terms. Specifically for segment j

$$S_{pj} = (G_{pj} - D_{pj})\, P_j$$

where G_{pj} is the growth rate and D_{pj} is the death rate. Turning first to the growth rate, the light and temperature effects are as given in Eq. (67). The interaction with nitrogen and phosphorous is given by a product of Michaelis

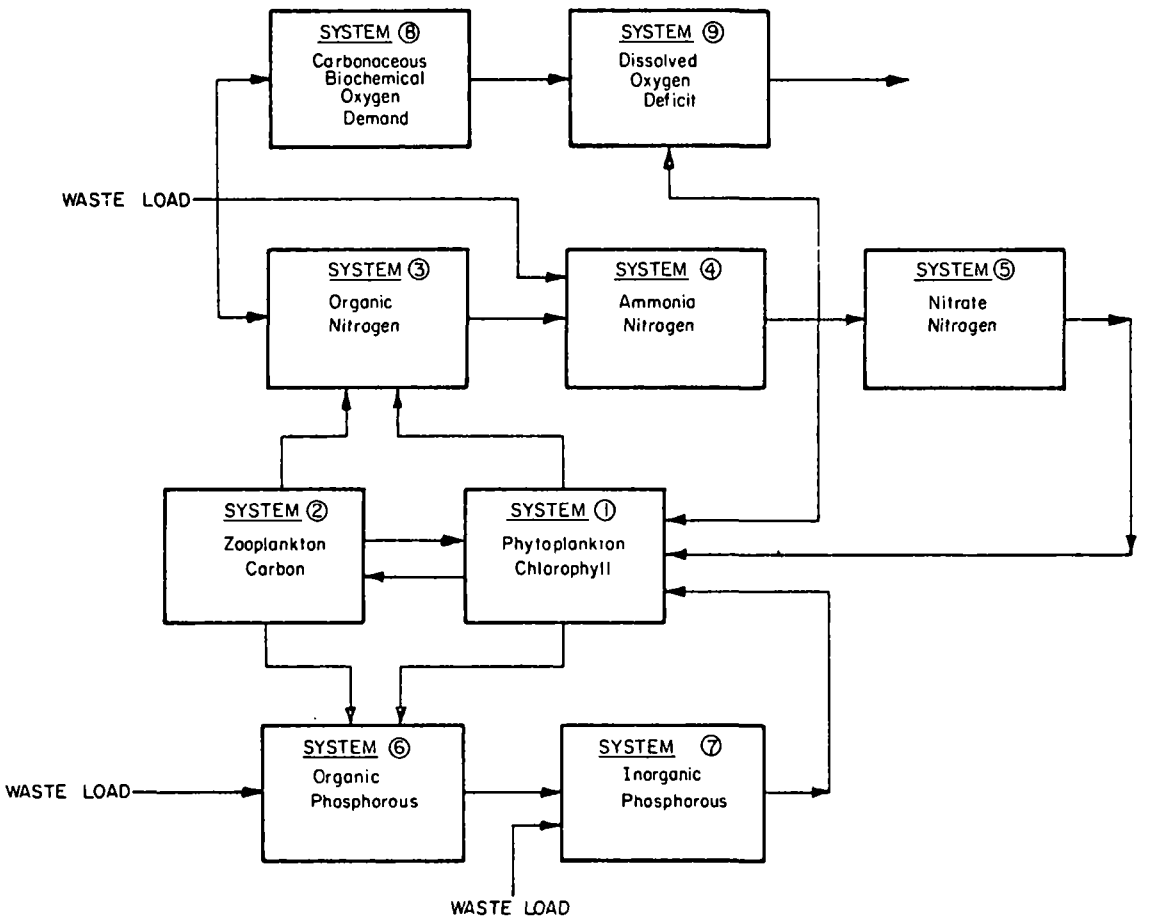

Fig. 30 Interactions of Nine Systems Used in Preliminary Phytoplankton Model

effects. Therefore,

$$G_{pj} = G_{It}(I,T,f,H,K) \quad \frac{N_{In}}{K_{mn}+N_{In}} \quad \frac{N_p}{K_{Mp}+N_p} \tag{112}$$

where N_{In} is the total inorganic nitrogen with K_{mn} as Michaelis constant, N_p is orthophosphate concentration with K_{mp} as the Michaelis constant. G_{It} represents the functional relationships of the growth rate and the solar radiation, I; photoperiod, f; water temperature, T; depth, H and light extinction coefficient, K. The latter coefficient is incorporated as a non-linear relationship with chlorophyll as

$$K = KE + .0088\ P + .054\ P^{.67} \tag{113}$$

where KE is the extinction coefficient (1/meter) estimated at zero phytoplankton concentration. The death rate, D_{pj} is as given in Eq. (74) and incorporates phytoplankton respiration as a function of temperature and grazing by phytoplankton.

The governing equation for the zooplankton carbon system is

$$[V]\frac{d(Z)}{dt} = [A](Z) + [V][G_z - D_z](Z) \tag{114}$$

where Z is a n x 1 column vector of zooplankton carbon concentration. The expressions for G_{zj} and D_{zj} are identical to those used in the earlier work. Actually, this system did not play a role in the verifications discussed below. Some sensitivity runs were made however to show the effect of different levels of zooplankton grazing.

The organic nitrogen system includes non-living forms of organic nitrogen generated by the model and includes sources due to death of zooplankton and phytoplankton and grazed but unassimilated phytoplankton nitrogen. The mass balance

equation for organic nitrogen, N_1, is

$$[V]\frac{d(N_1)}{dt} = [A](N_1) + [V](S_{n1}) + N_{n1} \qquad (115)$$

where (N_{n1}) is a vector of input sources of N_1.

The generalized source - sink term is given by

$$S_{n1} = \frac{a_1}{a_c} D_z Z + f(Z,P,G_z) + a_1 G(P) N_1 - K_{33} + K_{34}(T) N_1 \qquad (116)$$

where a_1 is the ratio of nitrogen to chlorophyll, a_c is the ratio of carbon to chlorophyll, K_{33} is the settling rate of organic nitrogen K_{34} is the hydrolysis rate of organic nitrogen - a function of water temperature and $f(Z,P,G_z)$ is the excretion of organic nitrogen (see Eq. 78).
Ammonia nitrogen (System #4) is produced by the feed forward hydrolysis reaction of the organic nitrogen and any direct sources of ammonia due to waste inputs or river runoff. The oxidation of the ammonia to nitrate forms an important subsystem of the overall model. This nitrification effect is used as a sink of dissolved oxygen. The mass balance equation for ammonia nitrogen N_2, is

$$[V]\frac{d(N_2)}{dt} = [A](N_2) + [V](S_{N_2}) + (W_{N_2}) \qquad (117)$$

where (W_{N_2}) is a vector of input sources of ammonia. The source-sink term for the ammonia is

$$S_{N_2} = K_{45}N_1 - K_{45}(T)N_2 + a_1 G_p P\alpha \qquad (118)$$

where K_{45} is the rate of oxidation of ammonia due to nitrifying bacteria (a function of temperature) and α represents an

assumed ammonia preference by phytoplankton and is given by

$$\alpha = N_2/(N_2 + K_{mn}) \tag{119}$$

The first term in Eq. (118) therefore represents the production of ammonia due to hydrolysis of organic nitrogen. The second term represents the utilization of ammonia by phytoplankton and the oxidation of ammonia by nitrifying bacteria. Note that at concentrations of ammonia greater than about 0.5 mg/l Eq. (119) indicates a preference for ammonia of about 95% at a K_{mn} = 0.025 mg/l.

The primary source of nitrate nitrogen (System #5) is the oxidation of ammonia by nitrifying bacteria. The primary sink of nitrate is the utilization of nitrate by phytoplankton. The governing equation used is

$$[V]\frac{d(N_3)}{dt} = [A](N_3) + [V](S_{N_3}) + (W_{N_3}) \tag{120}$$

where N_3 is the nitrate nitrogen concentration. The nitrate source-sink is

$$S_{N_3} = K_{45} N_2 - a_1 G_p P(1-\alpha) \tag{121}$$

The first term in Eq. (121) represents the production of nitrate by nitrification while the second term represents the utilization by phytoplankton.

The organic phosphorous system is assumed to be generated from the death of phytoplankton and zooplankton plus any additions of organic phosphorous due to the discharge of wastes. The organic phosphorous of this system therefore represents the "hon-living" phosphorous. The sinks for System #6 are the

conversion of organic phosphorous to inorganic dissolved phosphorous forms and an assumed sink of organic phosphorous out of the estuary itself due to sorption of turbidity particles and subsequent settling.

The equation for System #6 is then

$$[V]\frac{d(N_{pl})}{dt} = [A](N_{pl}) + [V](S_{N_{pl}}) + W_{N_{pi}} \qquad (122)$$

where N_{pl} is the organic phosphorous and the source sink term is given by

$$(S_{N_{pl}}) = \frac{a_p}{a_c} D_z Z + f(Z,P,G_z) + a_p D_p P - K_{66} N_{pl} \qquad (123)$$

where a_p is the ratio of phosphorous to chlorophyll and K_{66} is the overall decay of organic phosphorous.

The inorganic dissolved phosphorous system receives the output from the conversion of organic nitrogen and any direct sources of waste as input. The primary sinks of the dissolved phosphorous are the uptake by the phytoplankton and sorption on suspended material. The System #7 equation is

$$[V]\frac{d(N_{p2})}{dt} = [A](N_{p2}) + [V](S_{N_{p2}}) + [V](S_{N_{p2}}) + W_{N_{p2}} \qquad (124)$$

where N_{p2} is the dissolved inorganic phosphorous and

$$S_{N_{p2}} = K_{67} N_{pl} - a_2 G_p P - K_{77} N_{p2} \qquad (125)$$

where K_{67} is the rate of production of dissolved inorganic

phosphorous from the organic form and K_{77} is the overall loss coefficient of inorganic phosphorous from the water column. Total organic phosphorous and total phosphorous are computed from Systems #1, #2, #6 and #7 with appropriate conversion factors.

In the carbonaceous BOD system only the direct sources of biochemical oxygen demand (carbonaceous) are included. A traditional first-order decay is assumed. The equation is

$$[V] \frac{d(L)}{dt} = [A](L) + [V](S_L) + (W_L) \tag{126}$$

where L is the carbonaceous BOD and S_L is simply

$$S_L = - K_{88} (T) L$$

The DO deficit System #9 is classical in concept except that the effect of nitrification is computed internally using the output from System #4. The governing equation is

$$[V] \frac{d(D)}{dt} = [A](D) + [V](S_D) \tag{127}$$

where D = DO deficit. The source-sink term for the deficit is given by

$$S_D = 4.57 (K_{45} N_2) + K_{89} L - K_a D + f_1(P) \tag{128}$$

where K_{89} is the deoxygenation coefficient due to carbonaceous BOD, K_a is the reaeration coefficient. The first term in Eq. (128) represents the utilization of oxygen due to nitrification while the last term represents the effect of phytoplankton on the dissolved oxygen.

The nine system equations for each of 38 spatial segments results in a total of 342 simultaneous non-linear ordinary differential equations. The entire set was programmed for solution by a CDC 6600 computer. For a one-year simulation at integration time steps of about 0.1/day, normal central processing times were about 6 minutes.

Verification and Sensitivity Analysis

1968 Data

Two data periods were available for testing the validity and degree of applicability of the preliminary model. The procedure followed in the verification was to "tune" the model to the first data set collected in 1968. A forecasting situation was then set up for 1969. The validated model for 1968 was used to independently estimate the 1969 data. The only new input data used for 1969 was the river inflow with associated water quality, water temperature and waste loads. All coefficients determined from the 1968 validation were used without modification for the 1969 verification. This latter verification then provides the basis for determining the degree to which the model will simulate future conditions under different waste removal policies.

Figure 31 shows the data periods and the flow and temperature regimes used for the 1968 and 1969 runs. During the 1968 data period, Figure 31 indicates a significant flow transient in June 1968 with a lesser transient in September. The piecewise linear approximations to the time variable flow were determined from the available data and do not account for the day to day variability in inflow. The emphasis was rather on describing the seasonal variation rather than on shorter term fluctuations.

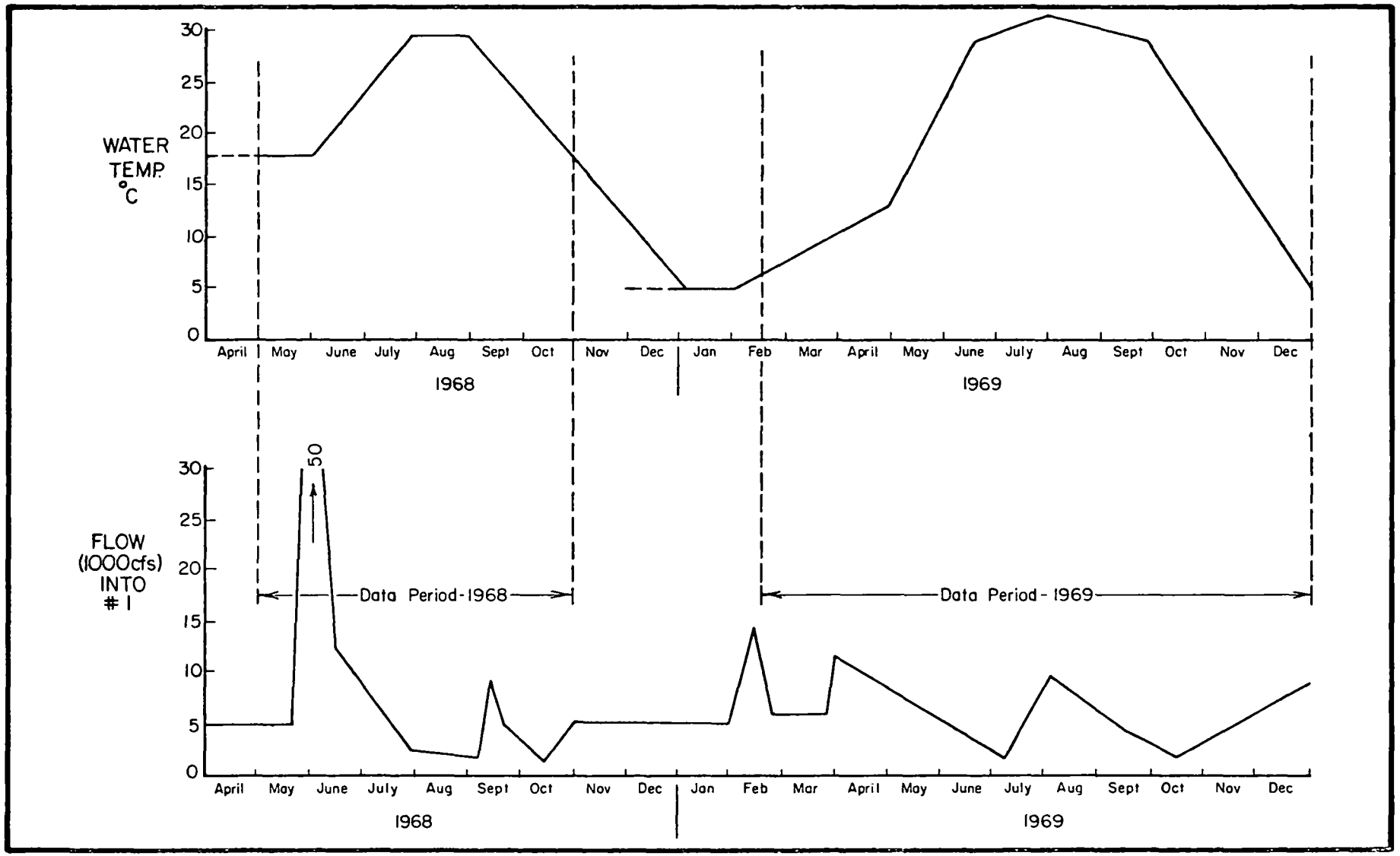

Fig. 31 Temperature and Flow Regimes Used for 1968 and 1969 Verification Runs

Only summary plots of observed data were available for verification of the 1968 data. These plots are given in Jaworski et al (1969). Figures 32 and 33 show a variety of results from the validation analyses of the May to November 1968 data. As indicated previously, the system equations are all time variable; the results in Figures 32 and 33 show the average spatial profile during August 1968, a period of low flow just prior to the late summer flow transient that year.

The three curves of model output in Figures 32 and 33 represent three conditions on the nutrients; nutrients are totally conserved in the model and nutrients are decayed out of the system at rates of .05/day and 0.1/day. As shown, the agreement is good when the organic nitrogen and total phosphorous are allowed to decay at rates of .05/day or 0.1/day but there is poor agreement when the nutrients are totally conserved in the system. This illustrates one of the steps in the "tuning" of the model using the 1968 data. It was obvious from the early runs of the model where the nutrients were allowed to recycle entirely within the model that the results were not desirable below about Mile Point 15. The observed data on all variables shown in Figures 32 and 33 decreased more rapidly than the computations. Accordingly, the hypothesis was adopted that incoming sediment load permitted sorption of phosphorous and nitrogen with subsequent settling to the bottom of the estuary and out of the domain of the modeling framework. This hypothesis is consistent with that given by Jaworski et al (1971) in determining phosphorous balances in the estuary.

In addition, the determination of model parameters using the 1968 data indicated that zooplankton grazing of the phytoplankton was probably not a significant factor in the Potomac. This is supported by the fact that the phytoplankton of concern

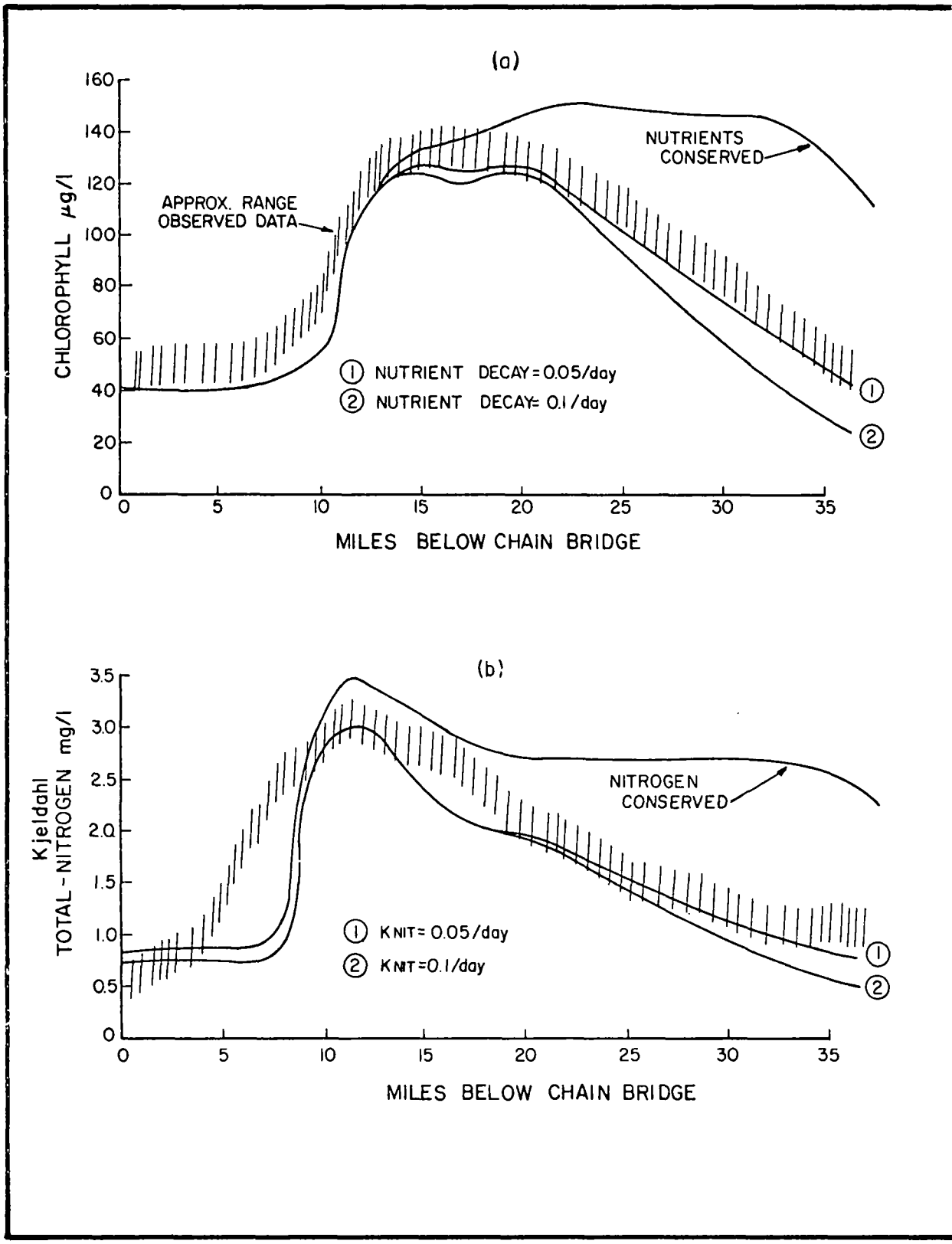

Fig. 32 Comparison of Range of Observed Data and Model Output August 1968 a) Chlorophyll a (µg/l)
b) Total Kjheldahl Nitrogen (mg/l)

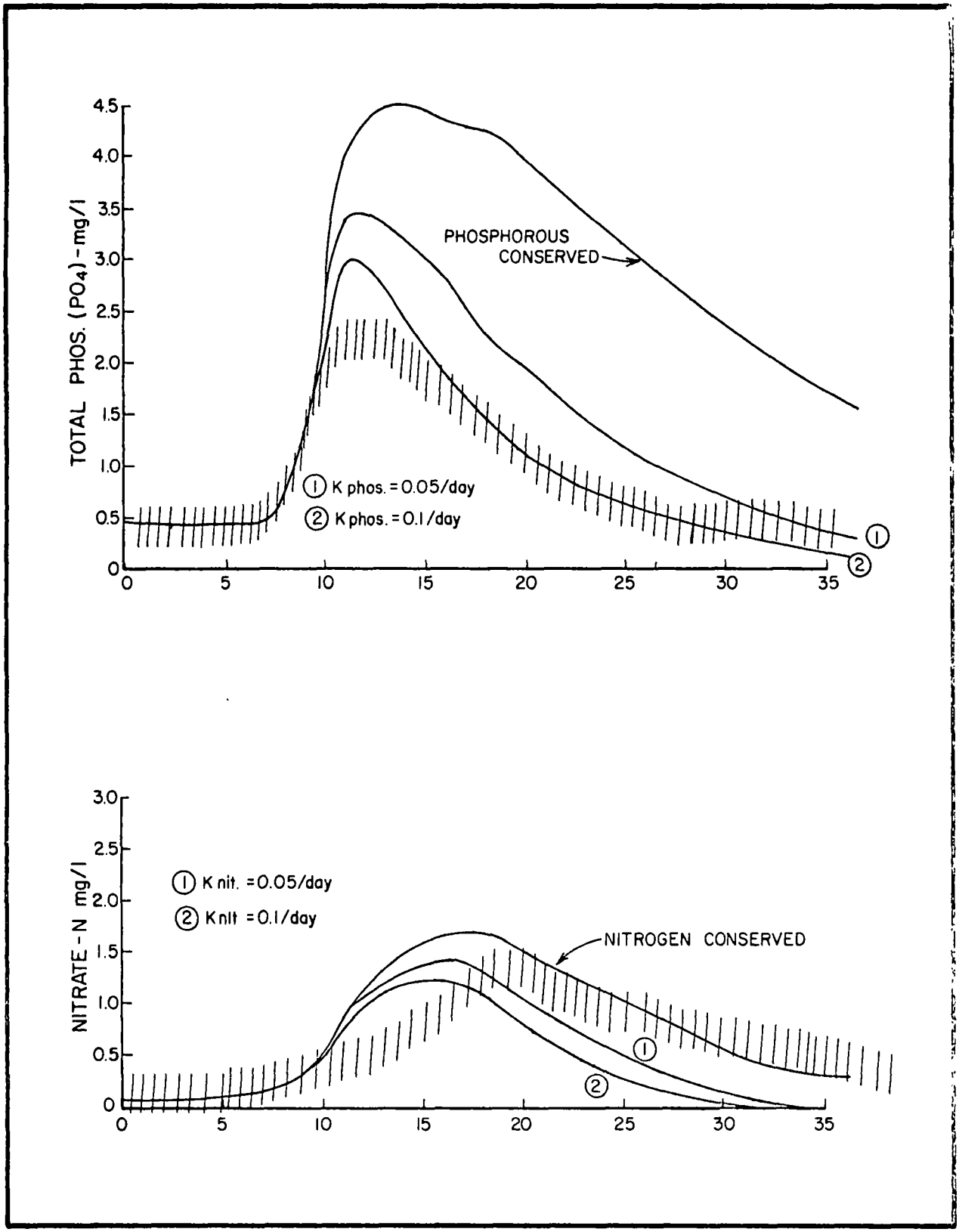

Fig. 33 a) Total Phosphorous - PO_4 (mg/l) Comparison
b) Nitrate Nitrogen Comparison, August 1968

in the Washington D. C. area down to about segment 15 are Anacystis, a blue green form that is toxic to zooplankton. Several runs were made of the model to show the sensitivity of the various systems to perturbations on the zooplankton system.

Figure 34(b) shows the effect of zooplankton grazing on the phytoplankton chlorophyll "a" concentration in segment #9. The time period extends from March to December 1968 with an additional 60 days to show the general trend after December 1968. As indicated in Figure 34(b) with extensive zooplankton grazing, phytoplankton populations are almost completely depleted in September and maximum concentrations of only 60 μg/l are computed as compared to observed values of about 130 μg/l. It is interesting to note that the sharp drop in zooplankton at day 90 is the effect of flow transient at that time and as a consequence phytoplankton populations remain high since the predators are flushed past the segment.

Figure 34(a) with no zooplankton grazing is considerably closer to the observed data range as shown. The transient drop around September 1968 is due to a flow increase as shown in Figure 31.

The effect of zooplankton predation on the nutrient forms is interesting and is shown in Figure 35. As shown, the ammonia nitrogen is quite insensitive to the zooplankton effect under the conditions run. The drop in ammonia concentration at day 90 and day 180 is due to flow transients during that time (see Figure 31). With the cycling of organic nitrogen to ammonia nitrogen there is a sufficient feed forward to the ammonia system even when the phytoplankton population is high.

The effect on the nitrate concentration is marked however as shown in the top of Figure 35. Under extensive zooplankton

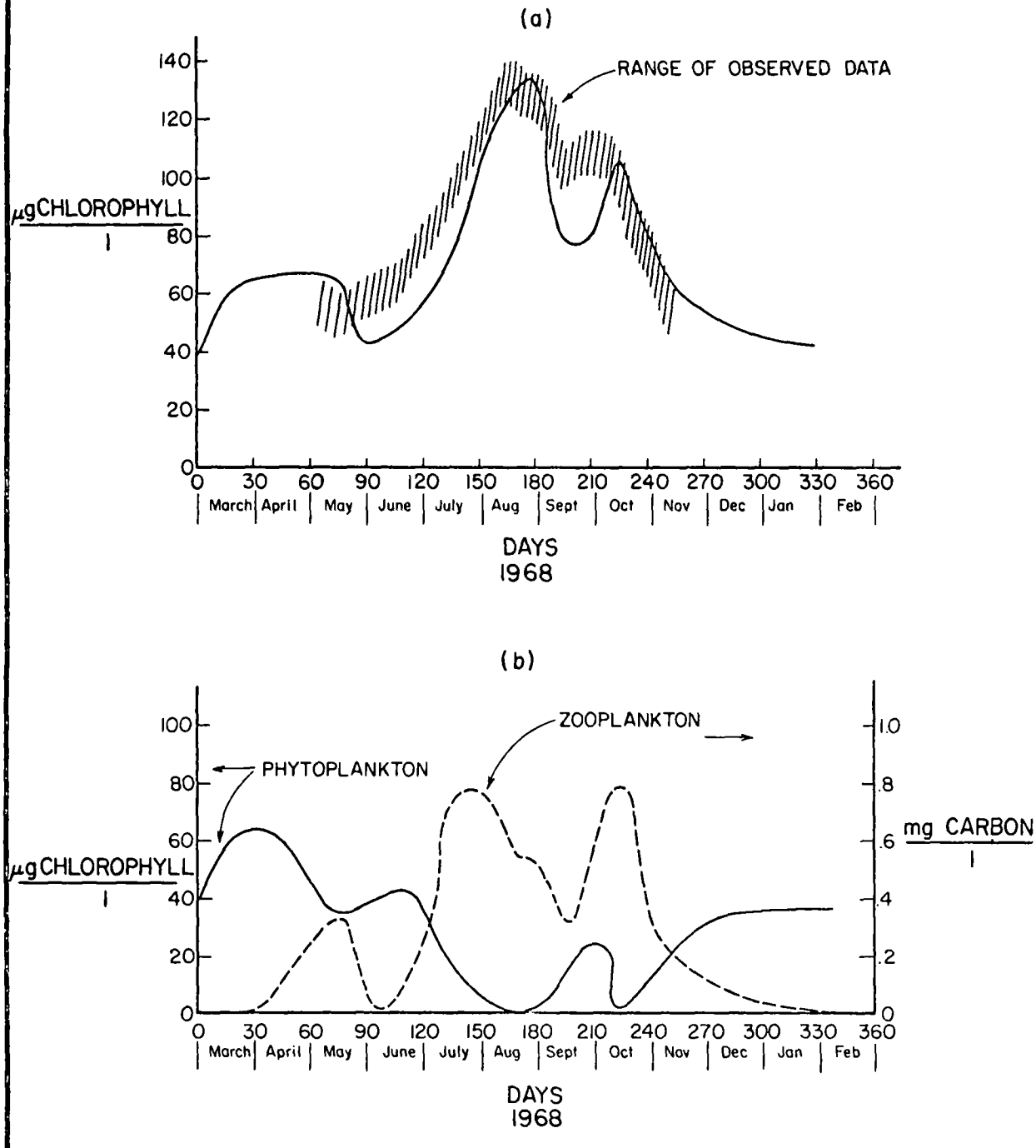

Fig. 34 Effect of Zooplankton Grazing on Phytoplankton in Segment #9 a) No Zooplankton Grazing b) Zooplankton Grazing at 0.42 1/mg Carb-Day. 1968 Flow Regime

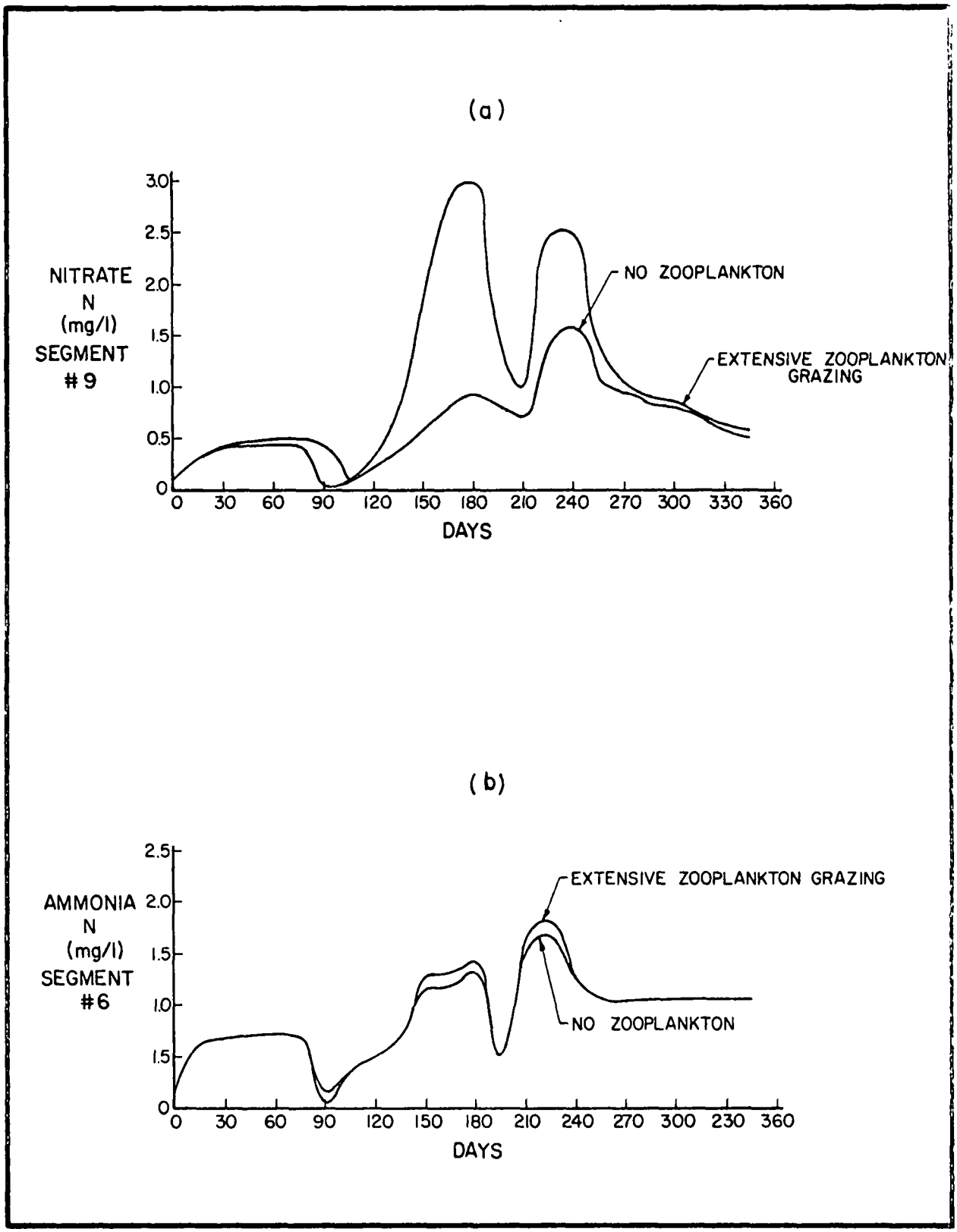

Fig 35 Effect of Zooplankton Grazing on Nitrate Nitrogen (top) in Segment #9 and Ammonia Nitrogen (bottom) in Segment #6, 1968 Flow Regime

grazing, the utilization of nitrate is decreased and nitrate approximately behaves as a conservative variable responding only to changes in the flow regime while being fed by the nitrification system. As a consequence, NO_3 values build up to 3 mg/l under extensive zooplankton grazing - considerably greater than observed (see Figure 33b). With no zooplankton grazing, phytoplankton populations increase and therefore utilize nitrate nitrogen and reduce the values to the 1 - 1.5 mg/l level. This is the range observed during 1968. All of these runs indicate that even with minimal grazing rates of the zooplankton on the phytoplankton, the phytoplankton population is never computed to grow to the levels observed in 1968. It was concluded therefore that the predatory effect of zooplankton on the phytoplankton was minimal at least for the upper end of the estuary below Washington D.C.

A sensitivity run was also made to indicate the effects of including the tidal bay segments. The results are shown in Figure 36. Observed chlorophyll concentration in the main channel appear to be significantly influenced by the growth of phytoplankton in the shallower side-channel areas. With average depths of about 5 feet in some of the tidal bay segments, significant populations are computed to grow in these areas. These populations are then tidally exchanged with the main channel flow and contribute to the population at that location. It is hypothesized then that the growth of phytoplankton in the shallow areas is significant (even without direct discharges to embayments) and can account for as much as 40 µg/l chlorophyll in the observed main channel data.

Verification Analysis - 1969 Data

The parameters determined from the 1968 verification analysis are listed in Table 13. This set of parameters was then used

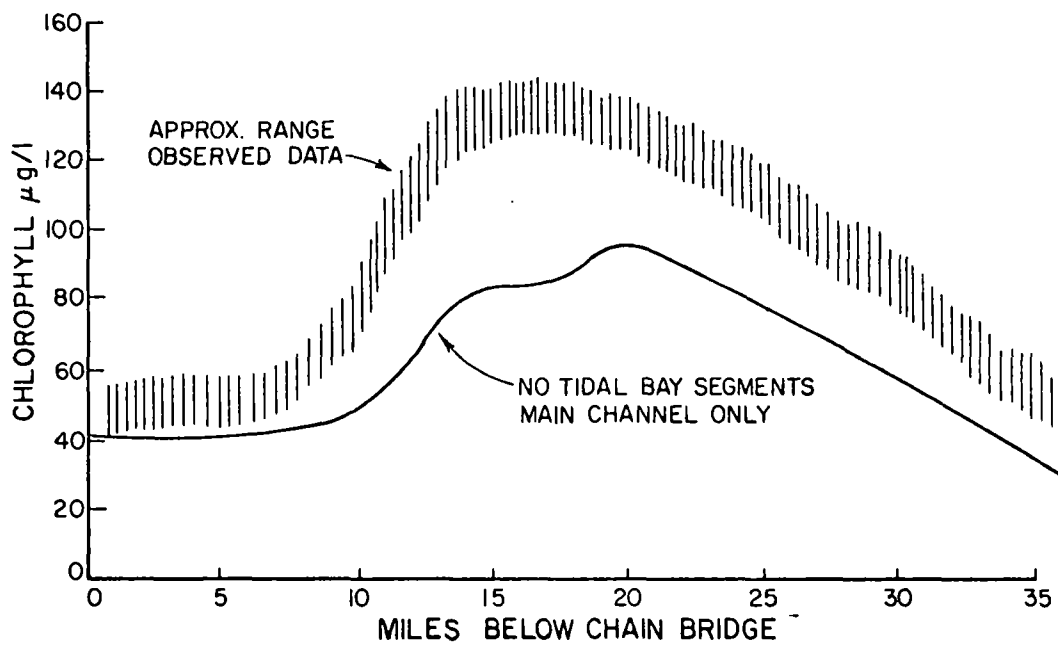

Fig. 36 Sensitivity Run - No Tidal Bay Segments. Aug. 1968 Profile and 1968 Conditions

Table 13

Parameters Used in Verifications
of 1968 and 1969 Potomac River Data
Preliminary Phytoplankton Model

Program Name	Description	Unit	Value
KIT	Saturated Growth Rate-Phyto.	1/day- °C	0.1
IS	Saturating Light Intensity	ly/day	300.0
KMN	Michaelis' Constant-Nitrogen	mg-N/l	.025
KMP	Michaelis' " Phosphorous	mg-P/l	.005
KMPL	Michaelis' " Phyto.Chlor	µg-Chlor/l	60.0
K2T	Phyto. Endogeneous Respiration Rate	Rate 1/day-°C	.005
CCHL	Carbon-Chlorophyll Ratio	mg Carb/µg Chlor	.05
NCHL	Nitrogen-Chlor. Ratio	mg Nit/µg Chlor	.01
PCHL	Phos.-Chlor. Ratio	mg P/µg Chlor	.001
K34T	Org.N-NH_3 Hydrolysis Rate	1/day-°C	.007
K33	Decay of Organic Nit.	1/day	0.10
K45T	NH_3-NO_3 Nitrification	1/day-°C	.01
K67T	Org P-Inorg.P Conversion Rate	1/day-°C	.007
K77	Decay of Org. P.	1/day	0.10
K66	Decay of Inorg. P.	1/day	0.10
K11T	BOD Decay Coef.	1/day-°C	0.01

to verify independently the 1969 data under the flow and temperature regime showed in Figure 31. As shown in Figure 31, fresh water inflow conditions were generally unsteady throughout 1969. There was a gradual decrease in the flow from April to mid-July at which point the flow increased markedly.

Figures 37 and 38 show the comparison between the computed output and some observed data for the period at the end of the gradual decline in river inflow, from June 30, 1969 to July 15, 1969. Three data surveys were conducted during this period. It should be recalled that the computed output for 1969 was generated directly using the parameters from the 1968 runs; the parameters were not adjusted for the 1969 runs. Only flow, temperature and incoming concentrations into segment #1 based on observed 1969 data were used in the 1969 computations. It should be noted, however, that boundary conditions at segment #1 do influence results for about the first 15 miles of the estuary. Incoming chlorophyll concentrations were not measured during 1969; the first station for which data were available was at Key Bridge, Mile 3.3. Boundary chlorophyll values were inputted to approximately duplicate the order of magnitude of observed data at that station. The values ranged from 4 µg/l in the winter to a high of 55 µg/l in September 1969.

Figure 37 shows the comparison between chlorophyll values as observed and the computed values for the beginning and end of the survey period. The June 30 values varied markedly especially in the vicinity of Mile 15 where a low value of 30 µg/l was observed, an apparently abnormal value for this location at that particular time of year. The general shape of the spatial profile as computed is good and approximately reproduces the spatial behavior of the observed data.

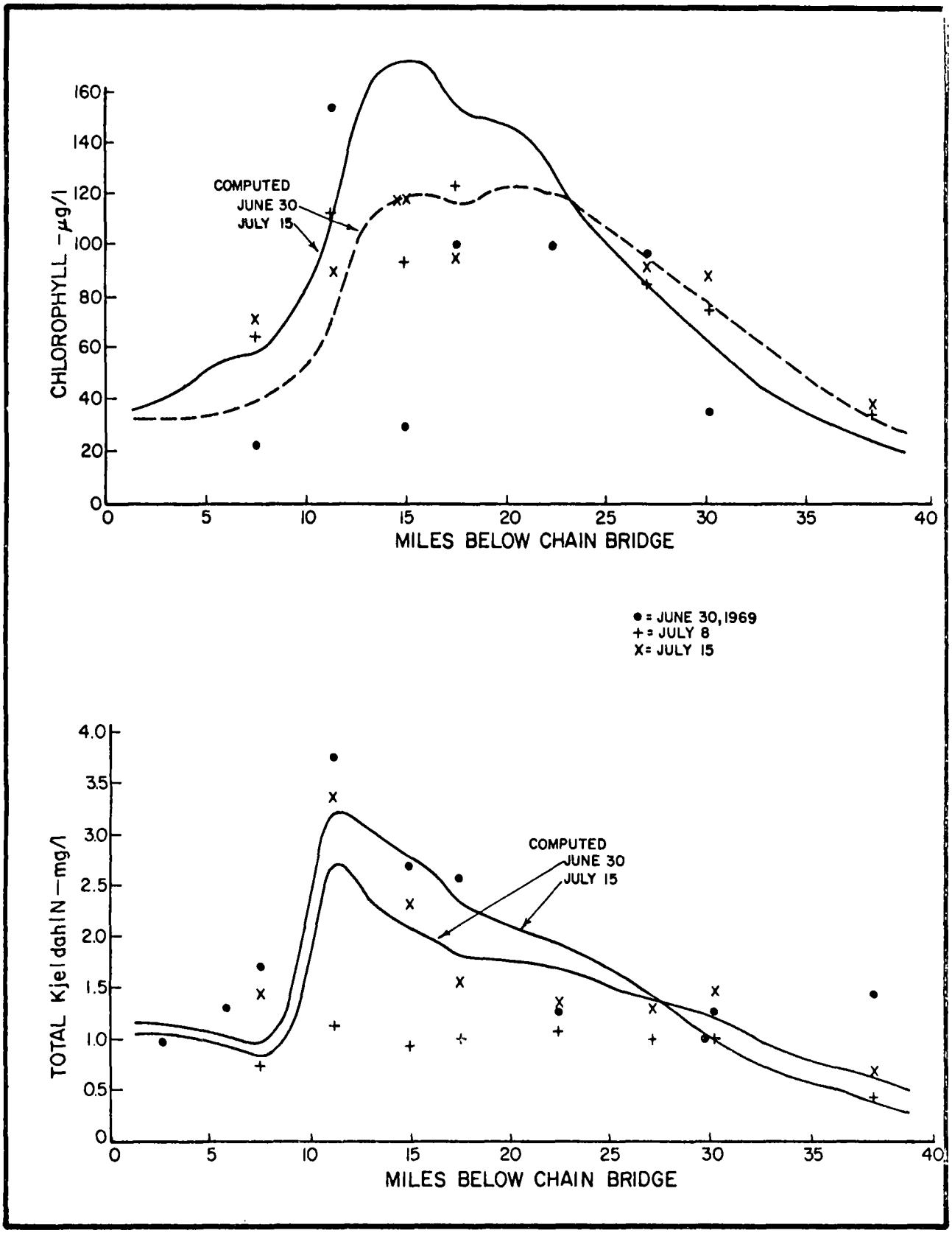

Fig. 37 Spatial Profile Comparison of Observed 1969 Data and Computed Values for Chlorophyll a (top) and Total Kjeldahl Nitrogen (bottom)

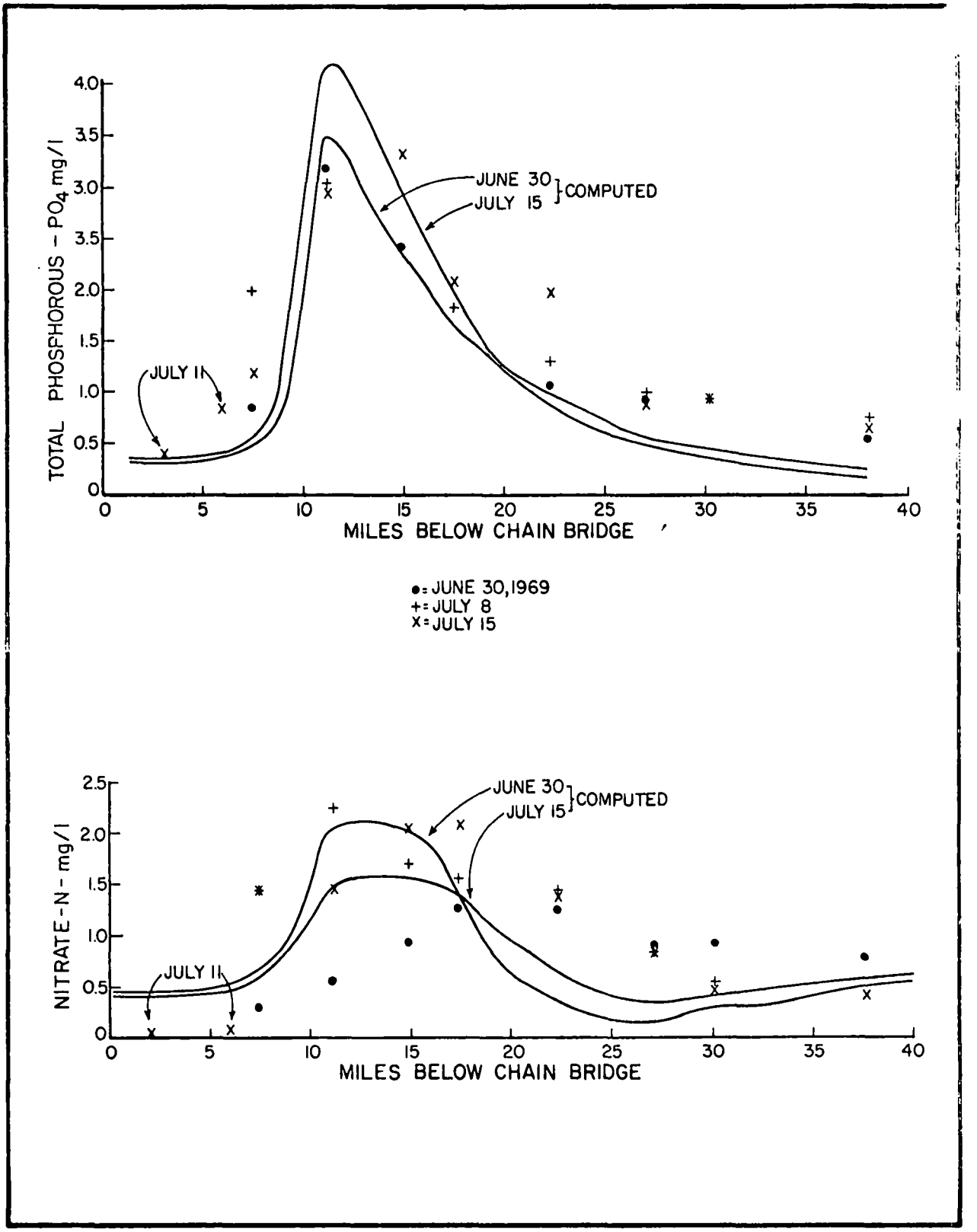

Fig. 38 Spatial Profile Comparison of Observed 1969 Data and Computed Values for Total Phosphorous (top) and Nitrate Nitrogen (bottom)

Peak values as computed during the period tend to be higher than observed although the average of the two computed lines of June 30 and July 15 is reasonably close to the average of the observed data and differs in the peak region by about 20 µg/l and by 5 - 10 µg/l downstream of the peak region.

The total Kjeldahl nitrogen verification is also shown in Figure 37 and agreement is very good with the exception of the July 8 survey where there was no observed increase in nitrogen in the vicinity of the major discharges. There is no readily apparent explanation for this discrepency.

Figure 38 shows the comparison between the spatial profile of total phosphorous (as PO_4) as observed during the surveys of June 30, July 8 and July 15, 1969 and the computed profiles for the time period bracketing those surveys. As shown the agreement is quite good although in the downstream direction, computed values decline more rapidly than observed values. This is probably a consequence of the simple first order adsorption kinetics that were used. A second order assumption as used by Jaworski et al, 1971, would give better results. Computed values in general are within 0.5 - 1.0 mg/l of observed values of PO_4.

The nitrate profiles are also shown in Figure 38. The agreement is good for the July 8 and July 15 surveys. Agreement was not obtained for the June 30 survey. During that survey the observed data showed a considerable downstream shift in the observed nitrate data which was not duplicated by the computed values. This could possibly be due to low dissolved oxygen values which would delay the onset of nitrification but DO data were not available to confirm this hypothesis. There is a more rapid decline in computed values of nitrate nitrogen in the vicinity of Mile 20 than was observed. This

discrepency may be due to the simple preference structure used in the model. A more detailed analysis of phytoplankton preference for differing forms of nitrogen appears to be warranted to provide better agreement.

In summary, the spatial agreement between observed and computed data for 1969 conditions is good. The general shapes of the spatial profiles are obtained and approximate quantitative agreement is obtained. Several areas remain to be explored, notably the model structure of the different nitrogen forms where anomalous results were occasionally obtained.

Figures 39 and 40 show comparisons between the temporal variation in chlorophyll a at four stations. As shown in Figure 39, the observed data are scattered but with a general peak in July 1969. The order and timing of this peak for both Mile 12.1 and Mile 18.3 is properly duplicated by the model. The rapid drop in chlorophyll concentration at the end of July is attributed to an increase in fresh water inflow (see Figure 31) at that time. The decrease is also successfully duplicated by the model. The model approximates the subsequent fall bloom of phytoplankton at Mile 18.3 but at Mile 12.1 the model calculations are somewhat higher than the observed data.

Figure 40 shows the comparison at two stations further downstream. At both stations a winter bloom of phytoplankton occurred which was not modeled in this work. At Hallowing Point, Mile 26.9, the spring growth pattern and subsequent decrease is adequately modeled. In the fall of 1969 at Hallowing Point, however, data indicated a significant increase in phytoplankton (maximum levels of 445 µg/l chlorophyll). This fall bloom was not duplicated by the phytoplankton model as constructed. It is not clear from the

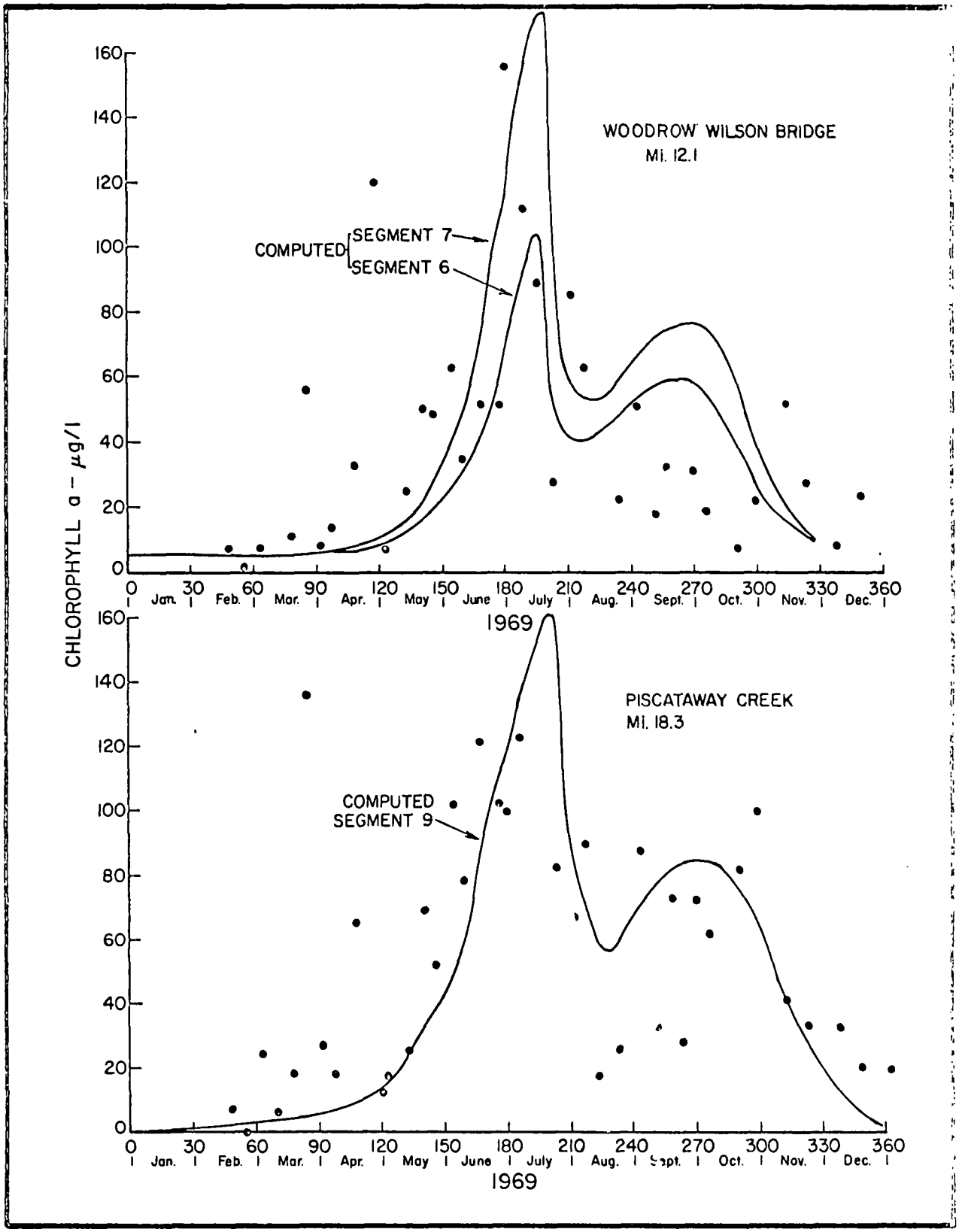

Fig. 39 Temporal Comparison of Observed 1969 Data and Computed Values for Stations at Miles 12.1 and 18.3

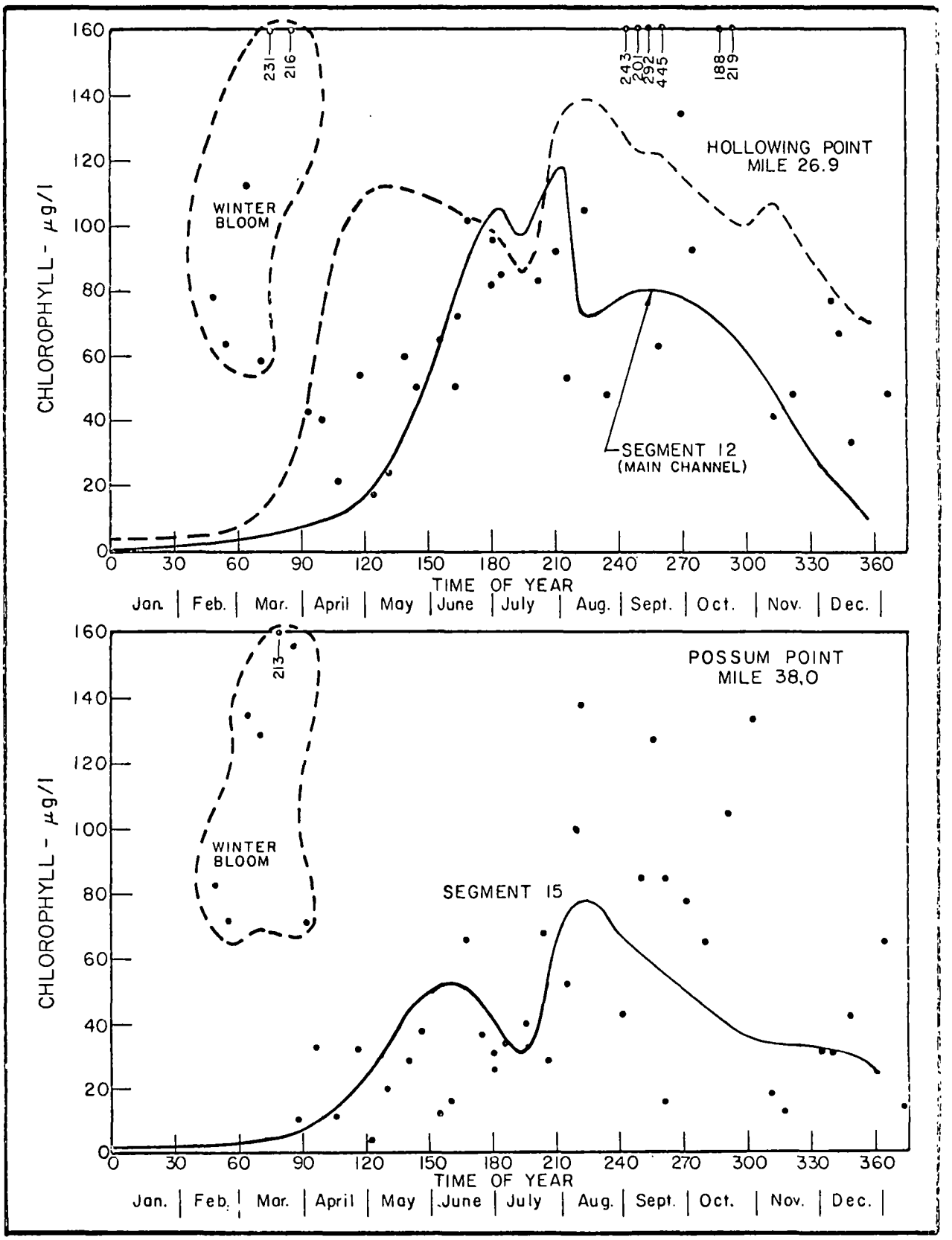

Fig. 40 Temporal Comparison of Observed 1969 Data and Computed Values for Stations at Miles 26.9 and 38.0

data as presented whether the high values in the fall of 1969 at Mile 26.9 are a surface phenomenon and therefore beyond the scope of the model formulation or whether the high values extended throughout the water column.

For Mile Point 38, Possum Point, similar comments can be made. The apparent winter bloom of phytoplankton is not captured by the model since the growth parameters for the phytoplankton biomass reflect a warm water population. The model does reasonably well until about August 1969 after which a wide scatter of chlorophyll values was observed. Peak values during August to October are not obtained by the model although the model does approximate conditions again during November and December.

In general, the phytoplankton model as formulated herein, provided a reasonable approximation to 1969 conditions using a 1968 "tuning" of the model. As an independent check, recognizing that no changes were made to the model from the results of the 1968 analysis, the verification for 1969 provides an added measure of credibility to the overall model structure. Overall spatial profiles during July 1969 verified well to about 40 miles downstream from Chain Bridge. Dynamic variability in phytoplankton was verified well throughout the first 20 miles and then only approximately for the remaining 20 miles. Transient blooms in the late winter and early fall of 1969 were not duplicated by the model.

Model Application

In order to illustrate the application of the preliminary model, two simulations were prepared. It should be stressed that this model is largely explanatory in nature and the

simulations discussed below are not to be considered as quantitative projections. At best, the simulations indicate general qualitative trends. Both simulations used a 90% removal policy of present raw waste loads. For the first simulation the 1969 flow regime was used; untreated nitrogen, phosphorous and carbonaceous waste loads were reduced by 90%; and incoming boundary values into segment #1 were the same as those used in the 1969 verification analysis. For the second simulation, median flow conditions were used with reduced waste inputs as in the first simulation. In addition several boundary conditions on chlorophyll were explored in the median flow simulation. For both simulations it was assumed that all organic and ammonia nitrogen was converted to nitrate nitrogen at the treatment plants and all phosphorous residual load is inorganic phosphorous. The summary of the waste loads is given in Table 14.

Table 14

Direct Discharge Waste Loads

	Waste Input for Verification lbs/day	Waste Input for Simulation lbs/day
Total Nitrogen (N)	46,500	7,070
Total Phosphorous (P)	20,300	2,620
Carbonaceous BOD	151,200	10,000

As shown, the 90% removal of the untreated waste loads results in about a 15% residual discharge of the 1968-1969 discharged loads. Although the residual loads used in the simulations are in excess of the allocations established for the Potomac (Jaworski et al, 1971) the level is considered a practical achievable level on a continued sustained basis.

Figure 41 shows the spatial chlorophyll profile for June 30 - July 15, 1969 and the 1969 simulation with 90% reduction of nutrient waste discharge. As indicated, even after waste reduction, maximum concentration of phytoplankton chlorophyll exceed 100 μg/l or four times the objective of 25 μg/l. The effect of the removal program is significant however from about Mile 25 to Mile 40. It should be recalled that no distributed sources of nutrient were included which would increase the nutrients available for growth.

Figures 42 - 49 show space-time computer generated contour plots from the 1969 simulations. As indicated in Figure 42 for almost two months, chlorophyll concentrations are greater than 25 μg/l due in part to the incoming concentration as given at segment #1. Figure 43, a plot of the computed Michaelis expression $N_p/(K_{mp} + N_p)$ as in Eq. (112) indicates that phosphorous limits the growth and essentially results in the decrease of the population from its peak value during July. The flow transients create the "waves" in the contour plot. As shown in Figure 43, the estuary from about segment #12 on, is increasingly limited by phosphorous almost uniformly throughout the year. Figure 44 shows the accompanying inorganic phosphorous levels and indicates the large area of the estuary at which phosphorous is at the Michaelis constant concentration (see Table 13). Note in Figure 44 the lack of significant temporal dependence of the phosphorous. Also, concentrations of inorganic phosphorous in the vicinity of Washington D.C. range from .05 to .1 mg/l P significantly above the Michaelis constant indicating that in that immediate area, phosphorous is not limiting. This is also indicated in Figure 43. It should also be recalled that other sources of nutrients from urban and suburban runoff were not included.

Figure 45 is a contour plot of the saturated growth rate of

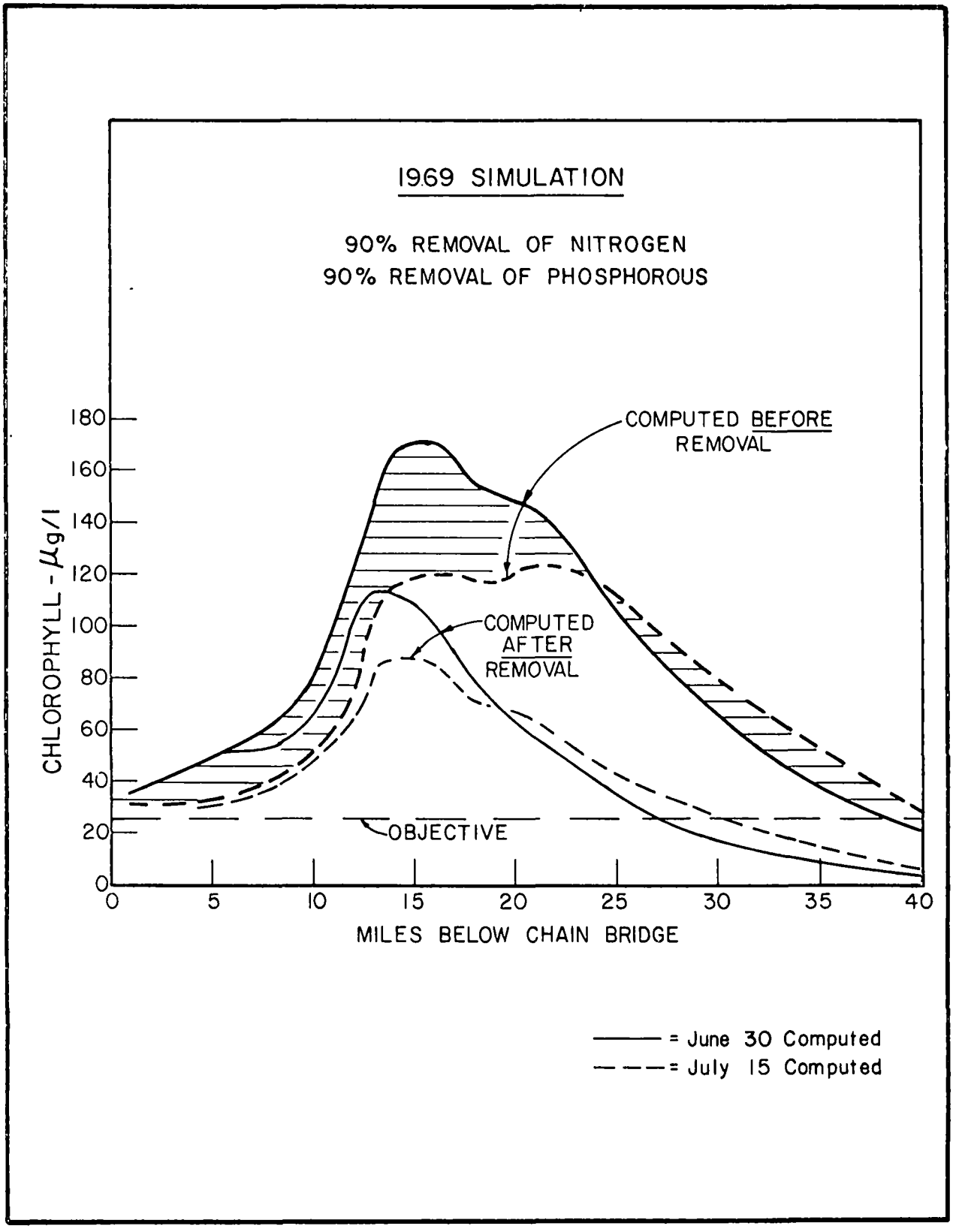

Fig. 41 1969 Simulation of Chlorophyll. Dashed Line, June 30: Solid Line, July 15 Profile. Compare to Fig. 37

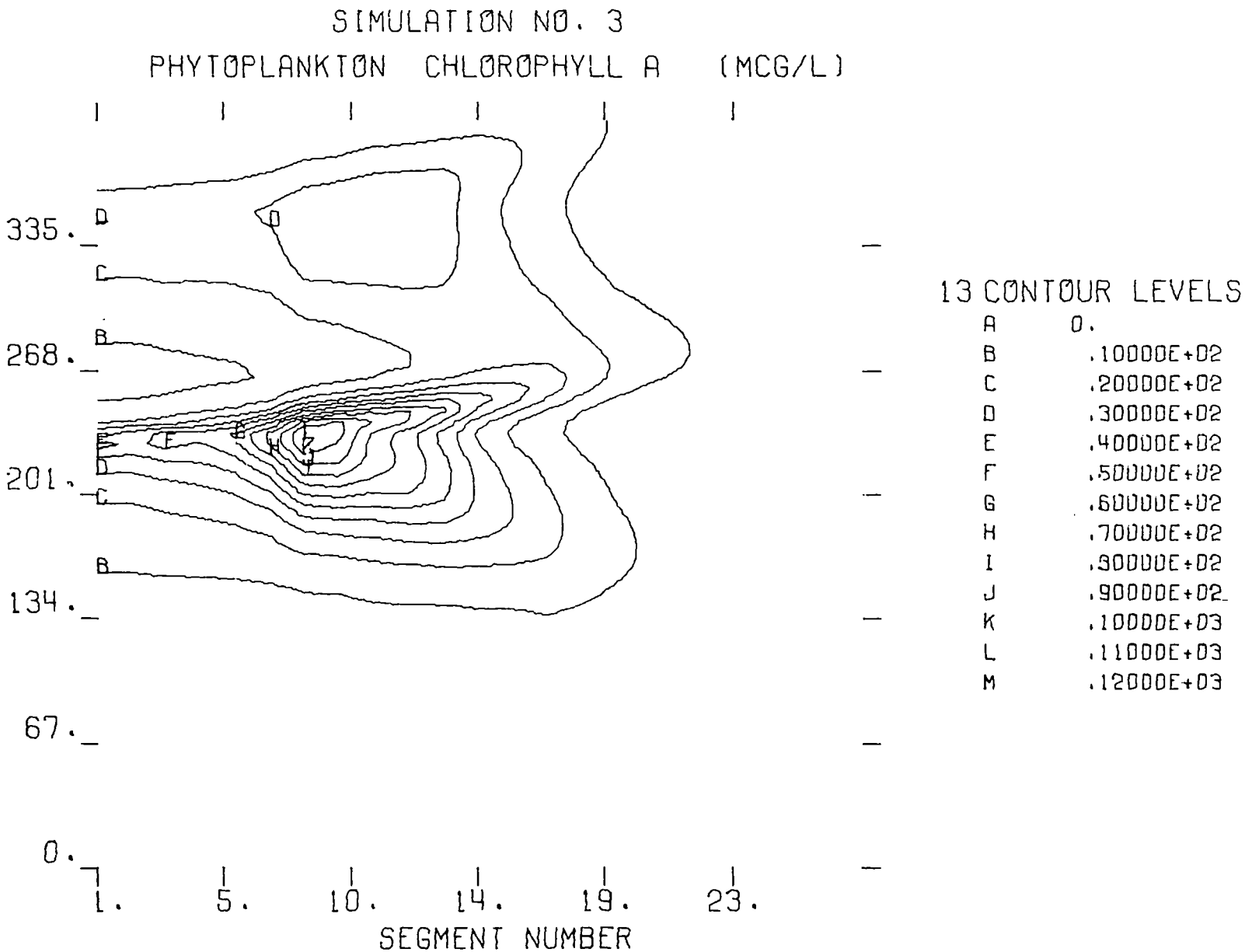

Fig. 42 1969 Simulation Contour Plot

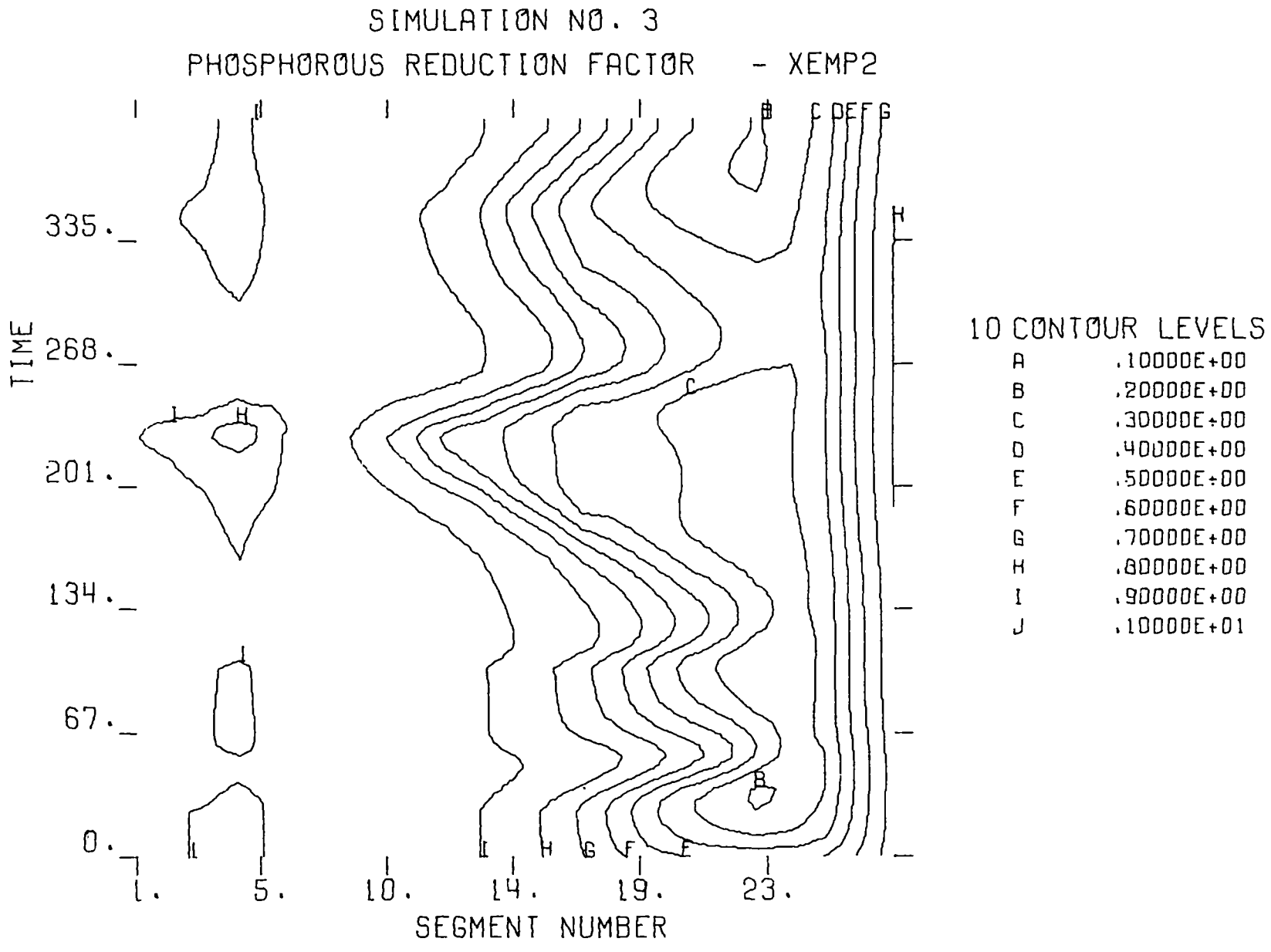

Fig. 43 1969 Simulation Contour Plot

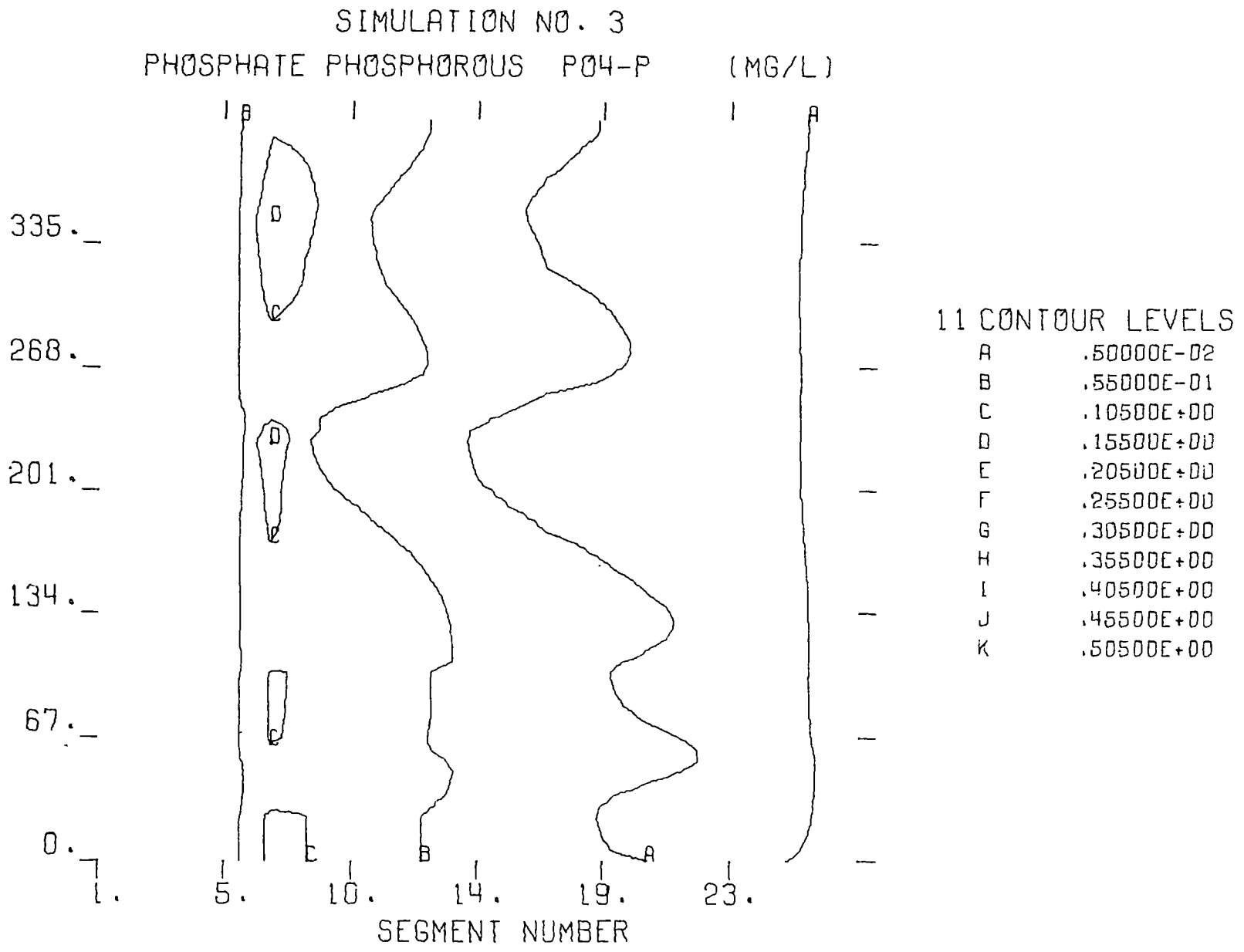

Fig. 44 1969 Simulation Contour Plot

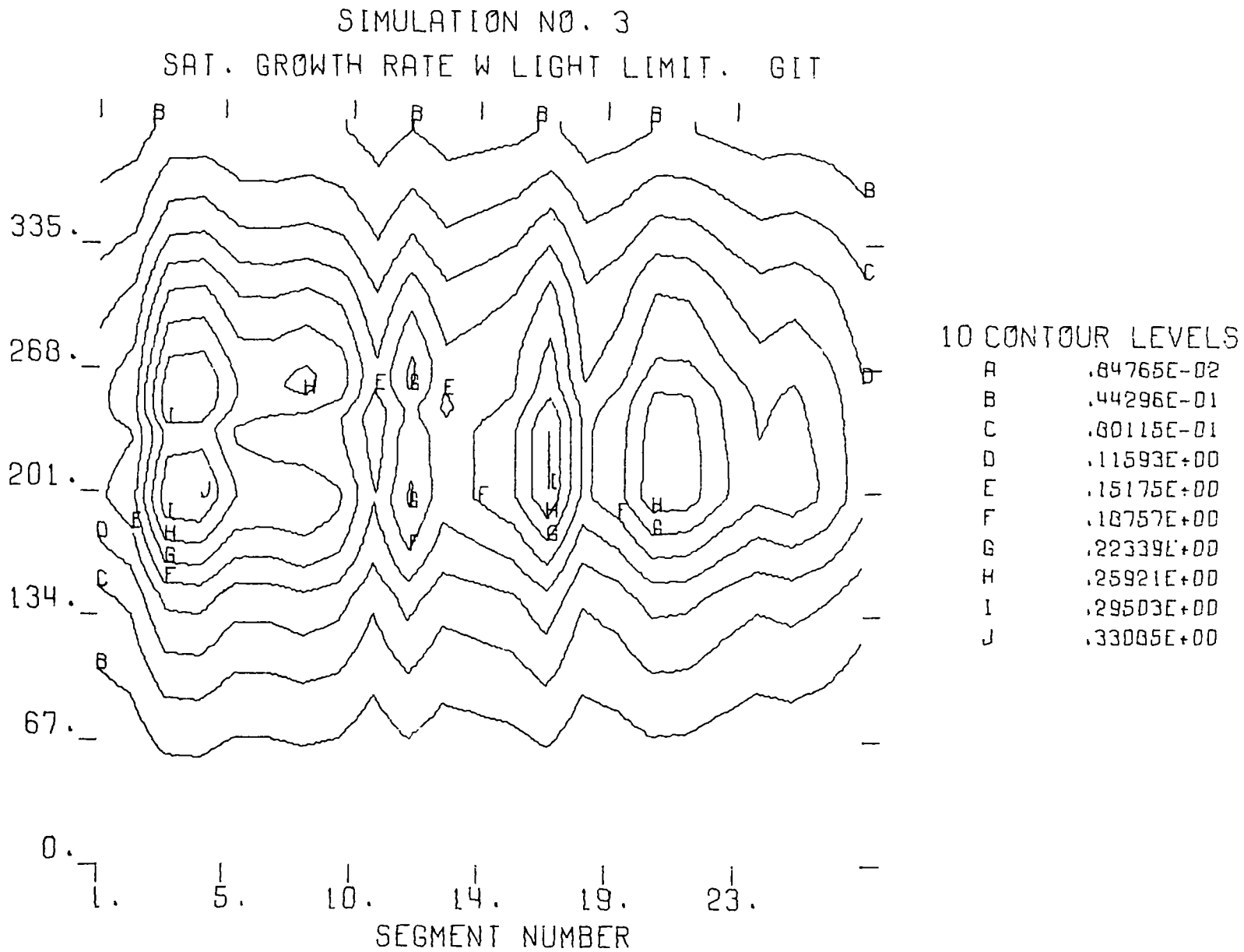

Fig. 45 1969 Simulation Contour Plot

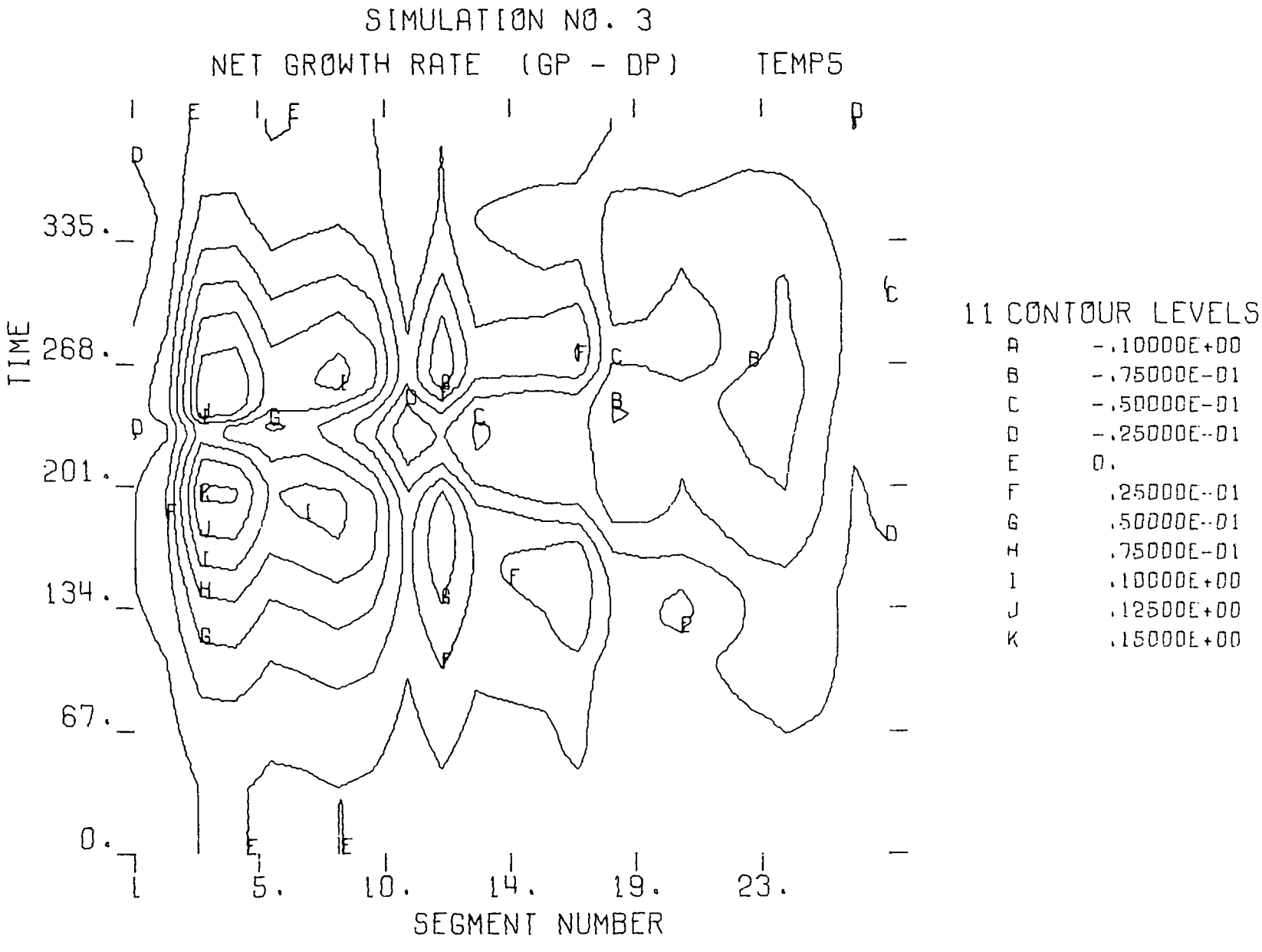

Fig. 46 1969 Simulation Contour Plot

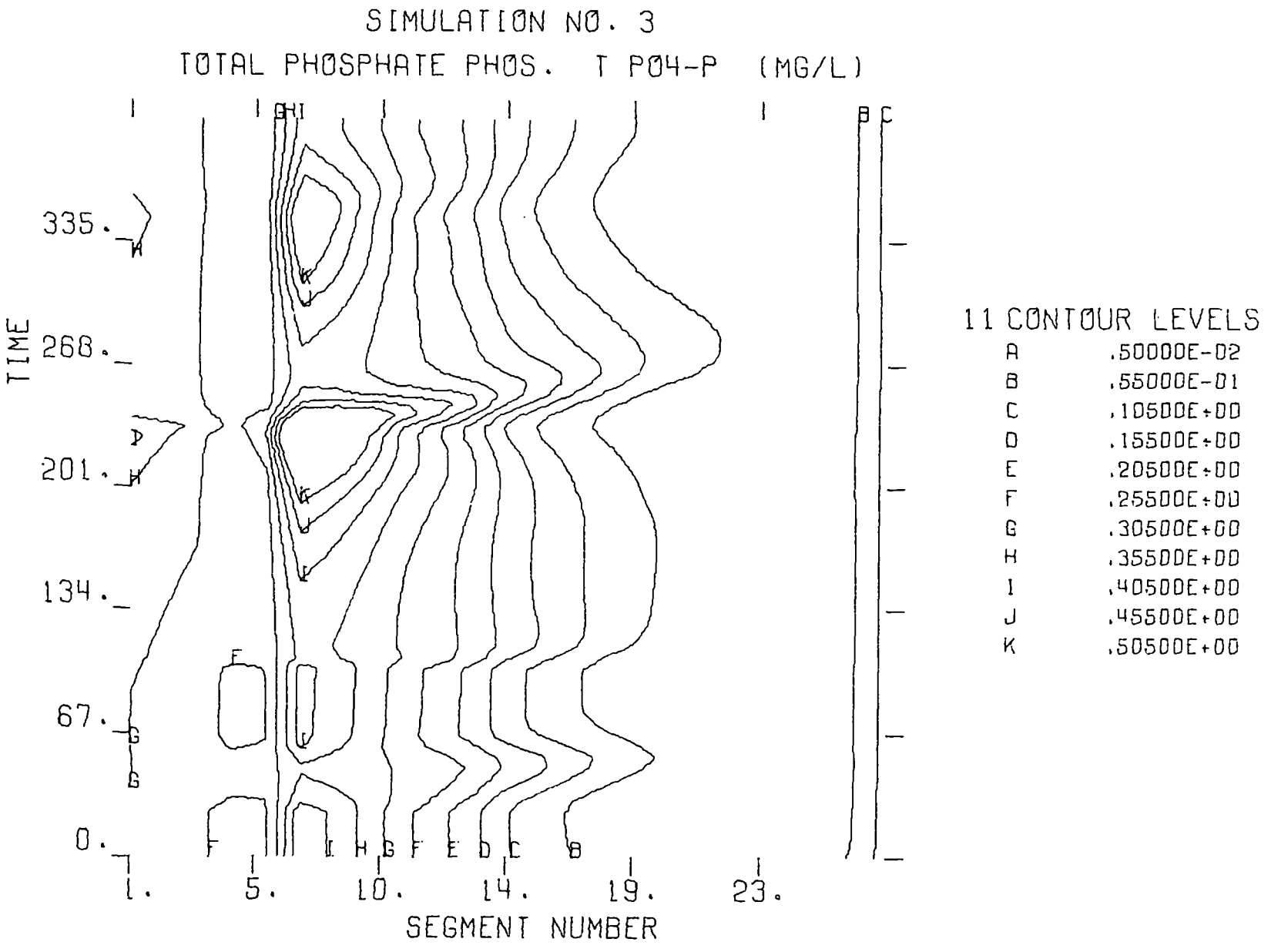

Fig. 47 1969 Simulation Contour Plot

Fig. 48 1969 Simulation Contour Plot

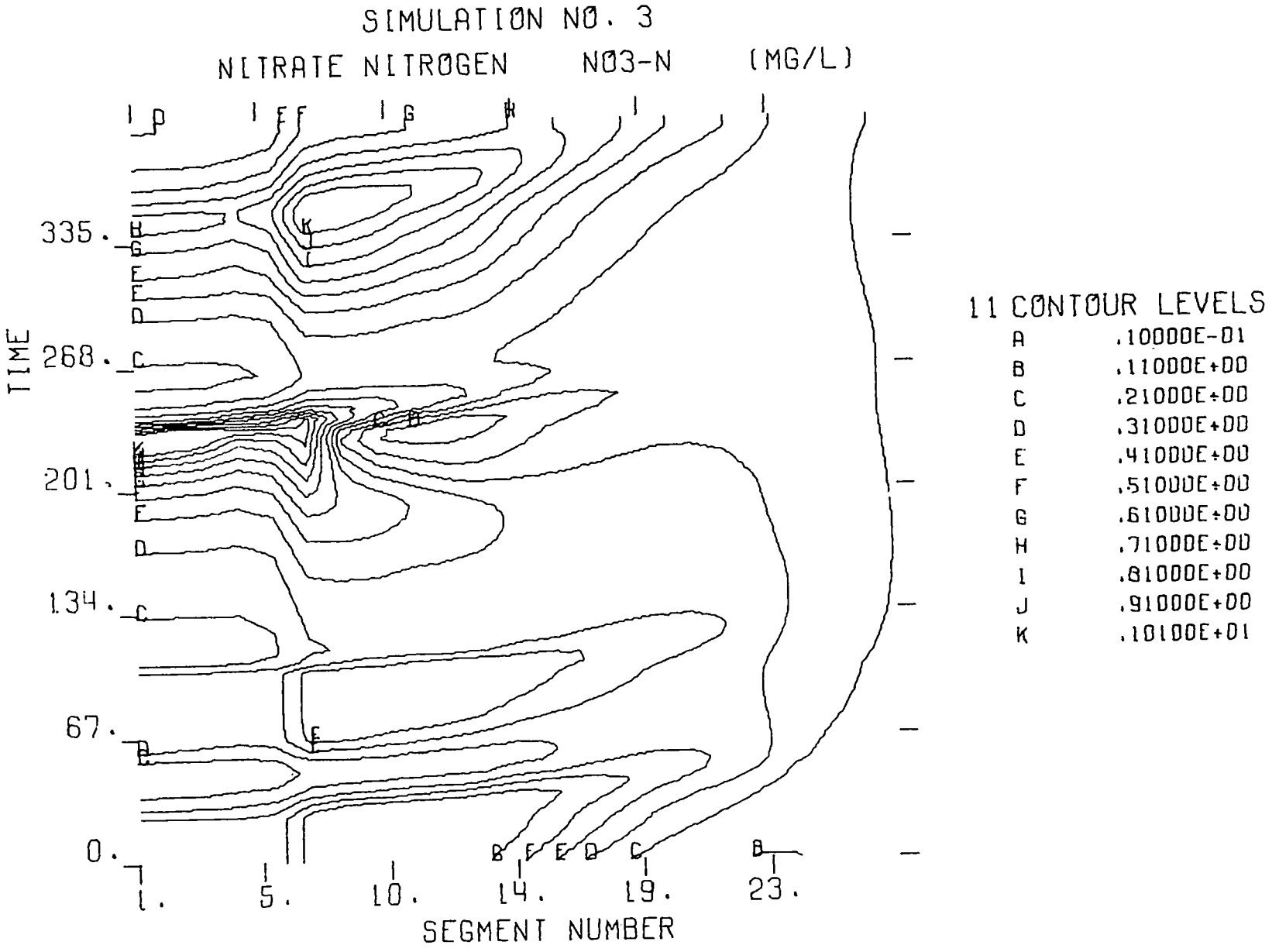

Fig. 49 1969 Simulation Contour Plot

the phytoplankton with the light limitation. At the beginning and end of the year, growth rates are less than about .01/day throughout the length of the estuary. During the peak growing season, growth rates reached maximum levels of .2 - .3/day. The interaction of phytoplankton population and light penetration is evident in the vicinity of segments #7 - #10 during the peak growth season. Figure 46 shows the net growth rate - growth versus death and predation. As indicated, there is a large region in space and time where the net growth rate is positive but it should be recalled that the transport structure will substantially modify the net growth rate due to "wash out" effects.

Figure 47 displays the total phosphorous surface. As shown, total phosphorous downstream of segment #10 is temporally constant and uniformly decreases spatially. In the vicinity of Washington D.C. total phosphorous concentrations range from .3 - 0.5 mg/l PO_4-P even with 90% removal at the plant.

Ammonia nitrogen and nitrate nitrogen are shown in Figures 48 and 49. The shape of these surfaces can be compared to the phosphorous surfaces of Figures 44 and 47. The comparison indicates the more complex interactions and structure of the ammonia and nitrate nitrogen. Significant temporal and spatial variations occur reflecting the recycling of the different nitrogen forms. Nitrogen in all regions is above limiting concentrations.

Flows for the median flow simulation ranged from 13,000 cfs during the winter to a high of 20,500 cfs in the spring, decreasing to 4,200 cfs in the later summer and then increasing again to 9,500 cfs in December. Incoming boundary concentrations as noted previously have an important relative impact on the estuary especially after waste loads are reduced by

treatment. For the nutrients, median concentrations as given in Jaworski et al, 1971, were used. Kjehldahl nitrogen of 0.95 mg/l and nitrate nitrogen levels ranging from 0.1 to 0.9 mg/l were inputted as boundary values. Organic phosphorous of 0.05 mg/l and an inorganic phosphorous concentration of 0.05 mg/l were also inputted as constant values throughout the year into segment #1. The effect of incoming phytoplankton chlorophyll was examined under median flows for two cases: a) chlorophyll a concentrations of 1 µg/l entering the estuary from up-river and b) chlorophyll a boundary concentration of 25 µg/l, the promulgated EPA criterion.

Figure 50 shows the temporal variation in chlorophyll for the main channel segment #9 and its associated tidal embayment, segment #28, Piscataway embayment, using median flows. For the case of 1 µg/l chlorophyll entering the estuary (Figure 50a), it is seen that the effect of the reduced waste discharge on the main channel is minor and results in a late summer increase to about 14 µg/l chlorophyll. In the embayment section, however, chlorophyll concentrations rise to about 55 µg/l (twice the objective) for a period of about 120 days. It should be noted however that the level of 50 µg/l is considerably less than the concentrations of 150 - 200 µg/l before any nutrient reduction. The incoming concentration of 1 µg/l chlorophyll is unrealistic however and one would normally expect higher incoming concentrations.

Figure 50b shows the effect of constraining the boundary chlorophyll concentration at a level equal to the objective of 25 µg/l. As indicated, main channel chlorophyll levels rise to over 50 µg/l in August and in the embayment, concentrations rise to over 70 µg/l again for a period of about 4 months.

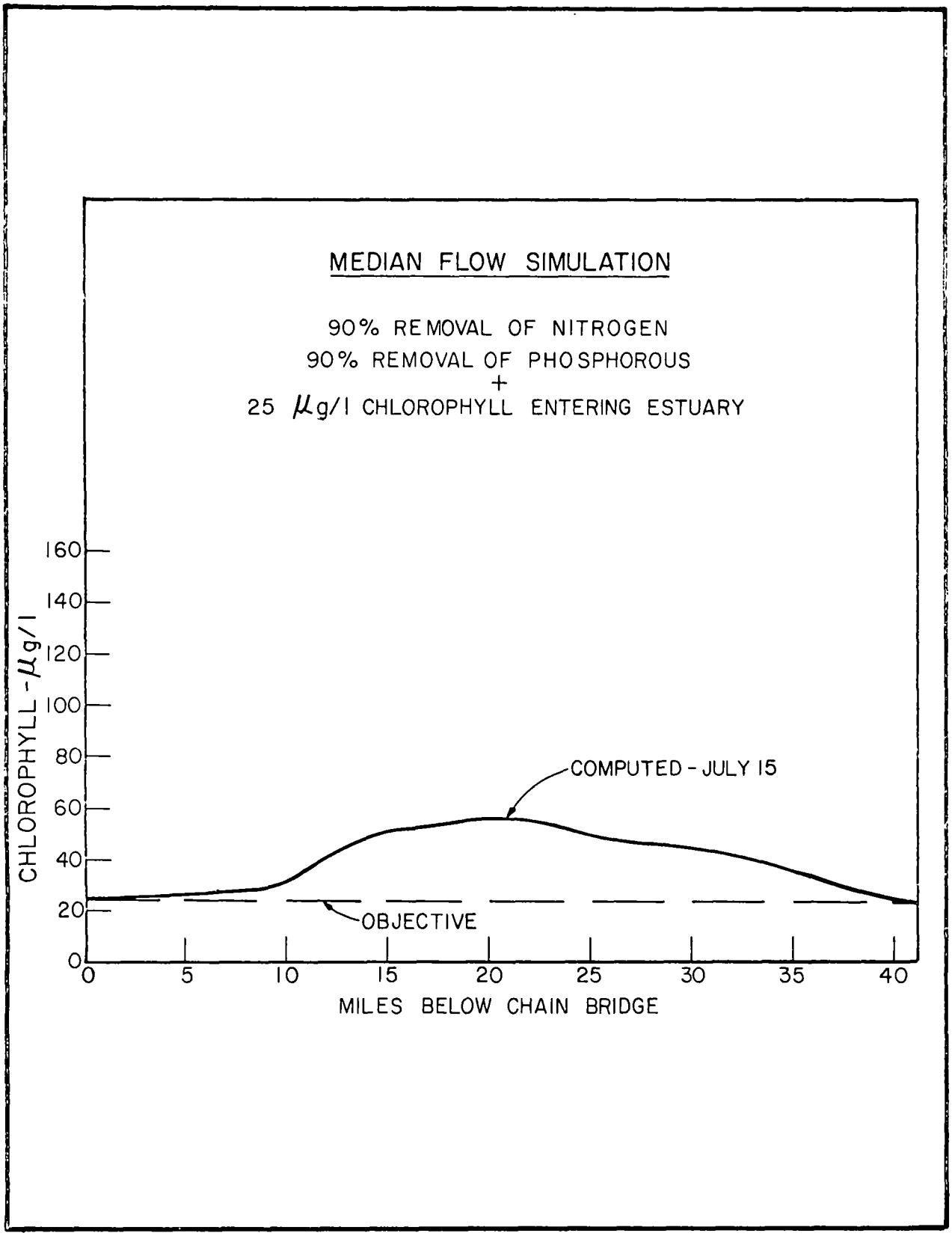

Fig. 50 Temporal Variation in Chlorophyll a at Segments #9 and #28, Median Flow Simulation. a) 1µg/l Chlorophyll Boundary b) 25µg/l Chlorophyll Boundary

Figure 51 is a longitudinal profile for July 15 for the median flow simulation and a 25 µg/l chlorophyll boundary condition. For about a 25 mile region of the estuary, the concentration of phytoplankton chlorophyll exceeds the objective and rises to a maximum value of almost 60 µg/l. Although this is above the objective, it is nevertheless a reduction of about 60% from maximum chlorophyll concentrations before any nutrient removals.

These simulations permit the following general observations. Achievement of the objective of 25 µg/l chlorophyll in the estuary may not be possible, primarily because of the effect of discharges from the Upper Potomac into the estuary. Even under a median flow regime (4,000 cfs during the growing season), maximum concentrations of 50 µg/l chlorophyll are calculated for the main channel and 75 µg/l in some embayments. It should also be noted that additional sources of nutrients such as local drainage and urban runoff have not been included in the model. Therefore, even if reductions greater than the 90% used in these applications could be achieved, such reductions would be probably offset by other distributed nutrient sources. On the basis of the preliminary model, then, state-of-the-art nutrient reduction (90% or better) in the Potomac may provide reductions in average chlorophyll levels by about 60% under median flow conditions. Again, the simulations should be considered as indicative of general trends only and not as a predictive certainty.

Summary

A non-linear dynamic model of phytoplankton chlorophyll in the Upper Potomac estuary verifies the observed 1968 and 1969 phytoplankton and nutrient temporal and spatial trends and approximately verifies the associated concentration levels.

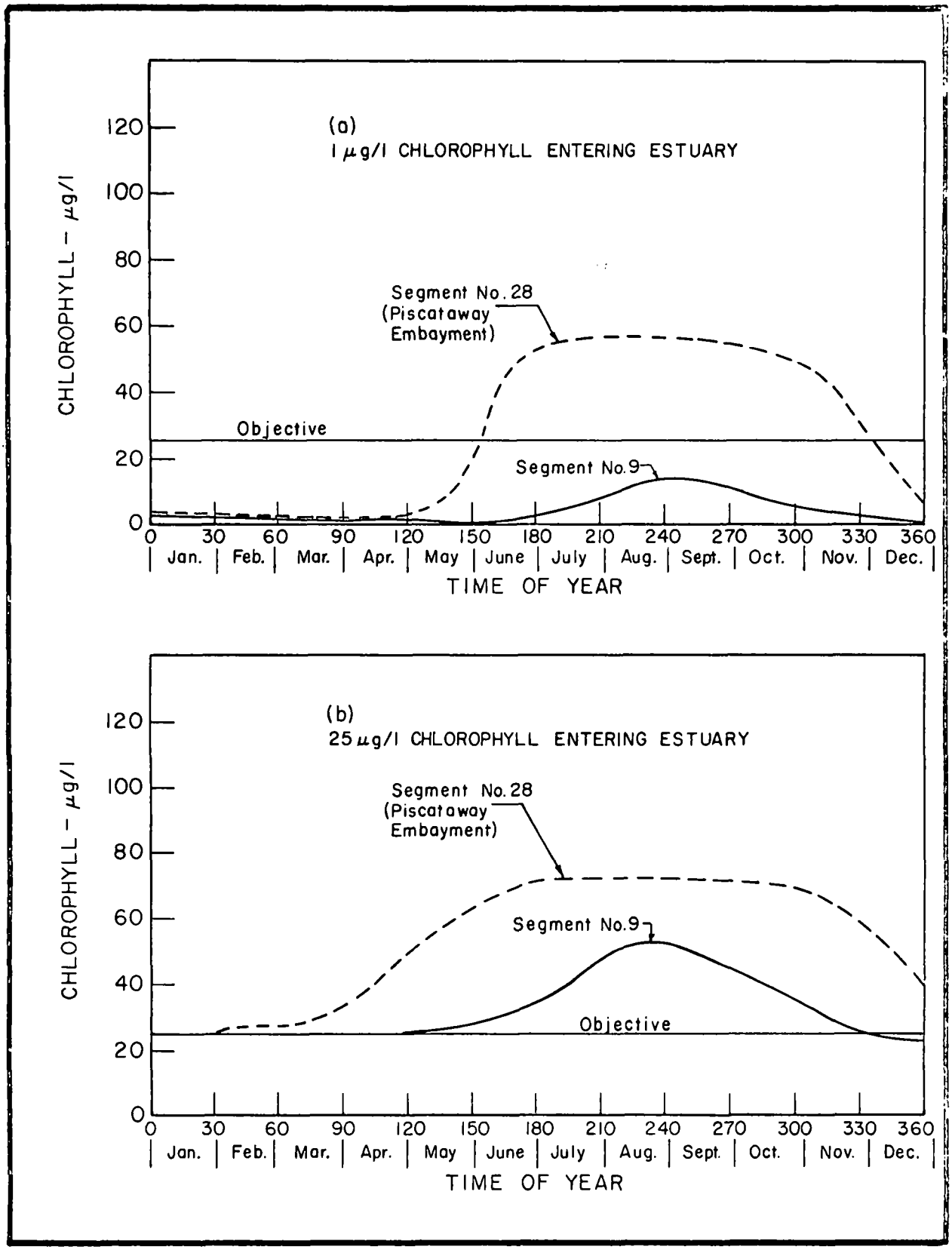

Fig. 51 Median Flow Simulation Profile of Chlorophyll
July 15

The data for 1968 were used to tune the model and the 1969 data were then used for independent verifications using coefficients from 1968 data and changing only flow, temperature and incoming boundary conditions for the 1969 verification. Late fall blooms of phytoplankton were not completely verified and a late winter bloom was not verified. Phytoplankton species discrimination is not incorporated in the model.

The transport through the estuary assumes an important role in the phytoplankton dynamics of the Upper Potomac Estuary. The nutrients and phytoplankton associated with the incoming river flow are particularly important. Unlike other problem contexts such as dissolved oxygen, critical conditions for phytoplankton growth may occur during non-drought flow conditions. This is due primarily to the addition of nutrients during high flows. The verification analyses indicate that, at present, phosphorous and nitrogen are probably sorbed from the estuary and enter the estuarine sediments. The preliminary model does not incorporate any recycle of nutrients from the sediments although the model does indicate that phosphorous and nitrogen are not conserved in the water column and losses to the sediment can be considerable. These losses could alter the effect of incoming river concentrations.

Simulations with the preliminary model indicate that under non-drought flows and a 90% reduction of untreated raw nutrient loads, chlorophyll concentrations in the main channel may rise to about 50 µg/l with embayment values over 70 µg/l. These concentrations are considerably above the objective of 25 µg/l but are about 60% less than present levels. The simulations are intended only to show possible trends under future loading conditions and are not to be interpreted in any detailed quantitative fashion. Models of the type presented herein require additional evaluation and testing on a continuing basis.

Further refinement of the model is therefore necessary before any definitive statements can be made of the effects of nutrient reduction on phytoplankton chlorophyll in the Upper Potomac Estuary.

SECTION VII

ACKNOWLEDGMENTS

The authors are pleased to acknowledge the guidance and support of Walter Sanders of the Southeast Water Laboratory, Environmental Protection Agency , in this research.

The Participation of John L. Mancini, Hydroscience, Inc., is also gratefully acknowledged.

The application of the nitrification model to the Delaware Estuary was accomplished through a contractual arrangement between the Delaware River Basin Commission and Hydroscience Inc.

The assistance of Gerald Cox and Jack Hodges of the Department of Water Resources and Harold Chadwick of the Department of Fish and Game, State of California is also gratefully acknowledges.

Richard Winfield, Research Engineer, Manhattan College, assisted significantly in the verification and application of the eutrophication model of the Potomac Estuary and his input is specifically acknowledged.

Finally the authors are pleased to acknowledge the effect and forebearance of Mrs. Berenice Maguire in the preparation of this report.

SECTION VIII

REFERENCES

1. Aalto, J.A., Jaworski, N.A. and Lear, D.W. "Current Water Quality Conditions and Investigations in the Upper Potomac River Tidal System" Tech. Report No. 41, Ches. Tech. Support Lab., FWQA, Annapolis, Md., May 1970, V. Chapters.

2. Adams, J.A., Steele, J.H. "Some Contemporary Studies in Marine Science" Shipboard Experiments on the Feeding of Calanus Finmarchicus p. 19-35, H. Barnes, Ed., G. Allen and Unwin Ltd., London, 1966.

3. Allison, F.E. "The Enigma of Soil Nitrogen Balance Sheets" Advances in Agronomy p. 213-250, A.G. Norman, Ed., Academic Press Inc., N.Y. 1955.

4. Anon, "Effects of Polluting Discharges on the Thames Estuary" Water Pollution Res. Tech. Paper No. 11, Dept. of Scien. & Ind. Res., Her Majesty's Stationary Office, 609 pp + xxvlll, 1964.

5. Anon, Department of Water Resources, State of California private communication, 1966.

6. Anon, "Nitrification in the Delaware Estuary" Prepared by Hydroscience Inc., Westwood, N.J. for Delaware River Basin Comm., Trenton, N.J., June 1969, 43 pp + Append.

7. Anon, "Eutrophication of Surface Waters - Lake Tahoe" Lake Tahoe Area Council, South Lake Tahoe, Calif. 95705, Report for FWPCA, Dept. of Interior, WPD 48-02, May 1969b.

8. Anraku, M., Omori, M., "Preliminary Survey of the Relationship between the Feeding Habits and the Structure of the Mouth Parts of Marine Copepods" Limnol. Oceanog. 1963, 8(1), 116-26.

9. Azad, H.S., Borchardt, J.A. "A Method for Predicting the Effects of Light Intensity on Algal Growth and Phosphorus Assimilation" J. Water Pollution Control Federation, 1969, 41 (11), part 2.

10. Bishop, J.W. "Respiration Rates of Migrating Zooplankton in the Natural Habitat" Limnol. Oceanog., 1968, 13 (1) 58-62.

11. Bormann, F.H. et al "Nutrient Loss Accelerated by Clear-Cutting of a Forest Ecosystem" Science, Vol. 159, Feb. 23, 1968, pp. 882-884

12. Burns, C.W., Rigler, F.H., "Comparison of Filtering Rates of Daphnia in Lake Water and in Suspensions of Yeast" Limnol. Oceanog., 1967, 12 (3) 492-502.

13. Burns, C.W. "Relation between Filtering Rate Temperature and Body Size in Four Species of Daphnia" Limnol. Oceanog. 1969, 14(5), 693-700.

14. Buswell et al, "Study of the Nitrification Phase of the BOD Test" Sewage & Ind. Wastes, 22, 4, 508, 1959.

15. Chen, C.W. "Concepts and Utilities of Ecologic Model" J. Sanit. Engr. Div., Amer. Soc. Civil Eng., Oct. 1970, 96, 1085-97.

16. Cole, C.R. "A Look at Simulation through a Study on Plankton Population Dynamics" Report BNWL-485, p. 1-19, Battelle Northwest Lab, Richland, Wa., 1967.

17. Comita, G.W. "Oxygen Comsumption in Diaptomus" Limnol. Oceanog., 1968, 13(1) 51-7.

18. Conover, R.J. "Oceanography of Long Island Sound, 1952-1954 VI Biology of Acartia Clausi and A. tonsa" Bull. Bingham Oceanog. Coll, 1956, 15 156-233.

19. Conover, R.J. "Assimilation of Organic Matter by Zooplankton" Limnol. Oceanog., 1966, 11, 338-45.

20. Davidson, R.S., Clymer, A.B. "The Desirability and Applicability of Simulating Ecosystems" Ann. N.Y. Acad.Sci, 1966, 128 (3) 790-4

21. Davis, H.T. "Introduction to Nonlinear Differential and Integral Equations" pp 99-109, Dover, N.Y. 1962.

22. Delwiche, C.C. "Biological Transformations of Nitrogen Compounds" Ind. & Eng. Chem., Vol. 48, No. 9, Sept. 1956, pp 1421-1427.

23. Di Toro, O'Connor, D.J. and Thomann, R.V. "A Dynamic Model of the Phytoplankton Population in the Sacramento-San Joaquin Delta" Adv. in Chemistry Series, No. 106, Amer.Chem. Soc., 1971, pp 131-180.

24. Droop, M.R., "Physiology and Biochemistry of Algae" Organic Micronutrients, p. 141-60, R.A. Lewin, Ed., Academic Press, New York, 1962.

25. Dugdale, R.C. "Nutrient Limitation in the Sea: Dynamics, Identification and Significance" Limnol. Oceanog, 1967, 12(4) 685-95.

26. Eppley, R.W., Rogers, J.N., McCarthy, J.J. "Half Saturation Constants for Uptake of Nitrate and Ammonium by Marine Phytoplankton" Limnol. Oceanog., 1969, 14(6), 912-20.

27. Feth, J.H. "Nitrogen Compounds in Natural Water - A Review" Water Res. Research, Vol. 2, No. 1, 1966, pp 41-58.

28. Fogg, G.E. "Algal Cultures and Phytoplankton Ecology" p. 20, University of Wisconsin Press, Madison, Wis. 1965.

29. Gerloff, Skoog, "Nitrogen as a Limiting Factor for the Growth of Microcystis Aerugmosa in Southern Wisconsin Lakes" Ecology, 1957, 38, 556-61.

30. Hamming, R.W. "Numerical Methods for Scientists and Engineers" p. 194-210, McGraw Hill, N.Y. 1962.

31. Hetling, L.J. and O'Connell, R.L. "An O_2 Balance for the Potomac Estuary" Unpublished Manuscript, Chesapeake Field Sta., Ches. Bay-Sus. River Basin Project, FWPCA, Feb. 1968.

32. Hutchinson, G.E. "A Treatise on Limnology, Vol. I" J. Wiley & Sons, Inc., New York, N.Y. 1957, 1015 pp + xiv.

33. Hutchinson, G.E. "A Treatise on Limnology Vol. II. Introduction to Lake Biology and the Limnoplankton" p. 306-54, Wiley, New York, 1967.

34. Hutchinson, G.E. and Viets, F.G. "Nitrogen Enrichment of Surface Water by Absorption of Ammonia Volatilized from Cattle Feedlots" Science, Vol. 166, Oct. 24, 1969, pp. 514-515.

35. Jaworski, N.A., Lear, D.W. and Aalto, J.A. "A Technical Assessment of Current Water Quality Conditions and Factors Affecting Water Quality in the Upper Potomac Estuary" Tech. Report No. 5 Ches. Tech. Sup. Lab, FWQA, Annapolis, March, 1969.

36. Jaworski, N.A. et al "Nutrients in the Potomac River Basin" Tech. Rept. No. 9, Ches. Tech. Sup. Lab., FWPCA, Dept. of Int., May 1969, 40 pp.

37. Jaworski, N.A. "Water Quality and Wastewater Loadings, Upper Potomac Estuary During 1969" Tech. Rept. No. 27, Ches. Tech. Sup. Lab., FWQA, Annapolis, Md., Nov. 1969, VII Chapters.

38. Jaworski, N.A., Clark, L.S. and Feigner, K.D. "A Water Resource Water Supply Study of the Potomac Estuary" Tech. Rept. No. 35, Ches. Tech. Sup. Lab, EPA, Annapolis, Md., April 1971, XII Chapters.

39. Jaworski, N.A. and Clark, L.J. "Physical Data, Potomac River Tidal System Including Mathematical Model Segmentation" Tech. Rept. No. 43, Ches. Tech. Sup. Lab., FWQA, Annapolis, Md. undated, unpaginated.

40. Ketchum, B.H. "The Absorption of Phosphate and Nitrate by Illuminated Cultures of Nitzschia Closterium" Am. J. Botany, June 1939, 26.

41. Knowles, G., Downing, A.L. and Barrett, M.J. "Determination of Kinetic Constants for Nitrifying Bacteria in Mixed Culture, with the Aid of an Electronic Computer" J. Gen. Microbiol., Great Britain, 1965, 38, 263-278.

42. Kuentzel, L.E. "Bacteria, Carbon Dioxide and Algal Blooms" J. Water Pol. Control Fed., Oct. 1969, 41 (10).

43. Lawrence, A.W. and McCarty, P.L. "Unified Basis for Biological Treatment Design and Operation" J. SED, ASCE, Vol. 96, No. SA3, June 1970, pp. 757-778.

44. Levy, H., Baggott, E.A. "Numerical Solutions of Differential Equations" p. 91-110, Dover, N.Y. 1950.

45. Lotka, A.J. "Elements of Mathematical Biology" pp. 88-94, Dover, N.Y. 1956.

46. Lund, J.W.G. "The Ecology of the Freshwater Phytoplankton" Biol. Rev, 1965, 40, 231-93.

47. MacIsaac, J.J., Dugsdale, R.C. "The Kinetics of Nitrate and Ammonia Uptake by Natural Populations of Marine Phytoplankton" Deep Sea Res., 1969, 16, 415-22.

48. Martin, J.H. "Phytoplankton Zooplankton Relationships in Narragansett Bay III" Limnol. Oceanog, 1968, 13 (1).

49. McMahon, J.W., Rigler, F.H. "Feeding Rate of Daphnia Magna Straus in Different Foods Labeled with Radioactive Phosphorus" Limnol. Oceanog., 1965, 10 (1) 105-13.

50. Monod, J. "Recherches sur la Croissance des Cultures Bacteriennes" Hermann, Paris, 1942.

51. Mullin, M.M. "Some Factors Affecting the Feeding of Marine Copepods of the Genus Calanus" Limnol. Oceanog., 1963, 8 (2), 239-50.

52. Myers, J. "Algal Culture from Laboratory to Pilot Plant" Growth Characteristics of Algae in Relation to the Problem of Moss Culture, p. 37-54, J.S. Burlew, Ed., Carnegie Inst. of Wash. D.C, Publ. 600, 1964.

53. O'Connor, D.J., Thomann, R.V., "Stream Modeling for Pollution Control" Proc. IBM Sci. Computing Symp. Environ. Sci., Nov. 14-16, 1966, p. 269.

54. O'Connor, D.J. "Water Quality Analysis of the Mohawk River-Barge Canal" Prepared in coop. with Hydroscience, Inc, for N.Y. State Dept. of Health, July 1968.

55. O'Connor, D.J., St. John, J.P. and Di Toro, D.M. "Water Quality Analysis of the Delaware River Estuary, J.SED, ASCE, No. SA6, Dec. 1969, pp 1225-1252.

56. O'Connor, D.J., Di Toro, D.M., Thomann, R.V., Mancini, J.L, "Phytoplankton Population Model of the Sacramento - San Joaquin Delta Bay" Tech. Rept. to Dept. of Water Resources, State of Calif. by Hydroscience Inc., Westwood, N.J. 1971.

57. Oswald, W.J., Gotaas, H.B., Ludwig, H.F., Lynch, V. "Photosynthetic Oxygenation" Sewage Ind. Wastes, 1953, 25 (6), 692.

58. Parker R.A. "Simulation of an Aquatic Ecosystem" Biometrics 1968, 24(4) 803-22.

59. Pearson, E.A. "Kinetics of Biological Treatment" Advances in Water Quality Improvement, pp. 381-394, E. Gloyna and W.W. Eckenfelder, Ed., Univ. of Texas Press, Austin, 1968.

60. Phelps, E.B., Stream Sanitation, pp. 148-49, J. Wiley & Sons, New York, N.Y. 1944.

61. Raymont, J.E.G. "Plankton and Productivity in the Oceans" pp 93-466, Pergamon, N.Y. 1963.

62. Riley, G.A. "Factors Controlling Phytoplankton Populations on Georges Bank" J. Marine Res., 1946, 6(1) 54-73.

63. Riley, G.A. "A Theoretical Analysis of the Zooplankton Population of Georges Bank" J. Marine Res., 1947, 6(2), 104-25.

64. Riley, G.A., Von Arx, R. "Theoretical Analysis of Seasonal Changes in the Phytoplankton of Husan Harbor, Korea, J. Marine Res., 1949, 8 (1) 60-72.

65. Riley, G.A., Stommel, H., Bumpus, D.F. "Quantitative Ecology of the Plankton of the Western North Atlantic" Bull. Bingham Oceanog. Coll, 1949, 12(3) 1-169.

66. Riley, G.A. "Oceanography of Long Island Sound 1952-1954 II. Physical Oceanography" Bull. Bingham Oceanog. Coll. 1956, 15 15-46.

67. Riley, G.A. "The Sea" Theory of Food-Chain Relations in the Ocean, p. 438-63, M. N. Hill, Ed., Interscience, N.Y. 1963.

68. Riley, G.A. "Mathematical Model of Regional Variations in Plankton" Limnol. Oceanog, 1965, 10 (Suppl) R202-R215.

69. Ryther, J.H. "Inhibitory Effects of Phytoplankton upon the Feeding of Daphnia Magna with Reference to Growth, Reproduction and Survival" Ecology, 1954, 35, 522-33.

70. Ryther, J.H. "Phytosynthesis in the Ocean as a Function of Light Intensity" Limnol. Oceanog, 1956, 1, 61-70.

71. Sawyer, C.N. "Chemistry for Sanitary Engineers" McGraw-Hill Bk. Co., New York, 1960, 367 pp + Viii.

72. Shelef, G., Oswald, W.J., McGauhey, P.H. "Algal Reactor for Life Support Systems" J. SED, ASCE, No. SA1, Feb.1970.

73. Small, L.F., Curl, H. Jr. "The Relative Contribution of Particulate Chlorophyll to the Extinction of Light off the Coast of Oregon" Limnol. Oceanog., 1968, 13(1), 84.

74. Sorokin, C., Krauss, R.W. "The Effects of Light Intensity on the Growth Rates of Green Algae" Plant Physiol. 1958, 33, 109-13.

75. Sorokin, C., Krauss,R.W. "Effects of Temperatures and Illuminance on Chlorella Growth Uncoupled from Cell Division" Plant Physiol, 1962, 37, 37-42.

76. Spencer, C.P. "Studies on the Culture of a Marine Diatom" J. Marine Biol. Assoc. U.K., 1954; quoted by Harvey, H.W. "The Chemistry and Fertility of Sea Waters" p. 94, Cambridge Univ. Press, 1966.

77. Steele, J.H. "Plant Production on Fladen Ground" J. Marine Biol. Assoc. U.K., 1956, 35, 1-33.

78. Steele, J.H. "A Study of Production in the Gulf of Mexico" J. Marine Res., 1964, 22, 211-22.

79. Steele, J.H. "Primary Production in Aquatic Environments" Notes on Some Theoretical Problems in Production Ecology, C.R. Goldman, Ed. Mem. Inst. Idrobiol. p. 383-98, 18 Suppl., Univ. of Calif. Press, Berkeley, 1965.

80. Stiefel, E.L. "An Introduction to Numerical Mathematics" p. 163, Academic, New York, 1966.

81. Stratton, F.E. and McCarty, P.L. "Prediction of Nitrification Effects on the Dissolved Oxygen Balance of Streams" Env. Sci. and Tech. Vol. 1, No. 5, May 1967, pp 405-410.

82. Strickland, J.D.H., "Chemical Oceanography" Production of Organic Matter in the Primary Stages of the Marine Food Chain, Vol. 1, p. 503, J.P.Riley and G. Skivow, Eds., Academic, New York, 1965.

83. Tamiya, H., Hase, E., Shibata, K, et al "Algal Culture from Laboratory to Pilot Plant" Kinetics of Growth of Chlorella with Special Reference to Its Dependence on Quantity of Available Light and on Temperature, pp 204-234, J.S. Burlew, Ed., Publ. 600, Carnegie Inst. of Washington D.C. 1964.

84. Thomann, R.V. "Mathematical Model for Dissolved Oxygen" J. Sanit. Eng. Div., Proc. ASCE, Oct. 1963, 83, SA5, 1-30.

85. Thomann, R.V. "Systems Analysis and Water Quality Management", ESSC Pub. Co., Stamford, Conn., 1972.

86. Thomas, W.H., Dodson, A.N. "Effects of Phosphate Concentration on Cell Division Rates and Yield of a Tropical Oceanic Diatom" Biol. Bull., 1968, 134 (1) 199-208.

87. Vollenweider, R.A. "Primary Production in Aquatic Environments" Calculation Models of Photosynthesis - Depth Curves and Some Implications Regarding Day Rate Estimates in Primary Production Measurements, pp 425-57, C.R. Goldman, Ed., Mem. Inst. Idrobiol, 18 Suppl, Univ. of Calif. Press, Berkeley, 1965.

88. Vollenweider, R.A. "Scientific Fundamentals of the Eutrophication of Lakes and Flowing Waters, with Particular Reference to Nitrogen and Phosphorus as Factors in Eutrophication" p. 117, Organization for Economic Cooperation and Development Directorate for Scientific Affairs, Paris, France, 1968.

89. Vollenweider, R.A. Ed., "Manual on Methods for Measuring Primary Production in Aquatic Environments" Ch. 2, p.4-24, Blackwell Scientific Publications, Oxford, England, 1969.

90. Wright, J.C. "The Limnology of Canyon Ferry Reservoir, I. Phytoplankton-Zooplankton Relationships" Limnol. Oceanog. , 1958, 3(2) 150-9.

91. Yentsch, C.S., Lew, R.W. "A Study of Photosynthetic Light Reactions" J. Marine Res, 1966, 24(3).

SECTION IX

PUBLICATIONS

1. "The Management of Time Variable Stream and Estuarine Systems" Robert V. Thomann, Donald J. O'Connor and Dominic M. Di Toro, Chemical Engineering Progress Symposium Series, Vol. 64, Nov. 1968.

2. "Photosynthesis and Oxygen Balance in Streams" Donald J. O'Connor and Dominic M. Di Toro, Journal of the Sanitary Engineering Division, ASCE, Vol. 96, No. SA2, Proc. Paper 7240, April 1970, pp 547-571.

3. "Modeling of the Nitrogen and Algae Cycles in Estuaries" Robert V. Thomann, Donald J. O'Connor and Dominic M. Di Toro, Proc. of Fifth International Water Pollution Conf., San Francisco, Cal., 1970.

4. "A Water Quality Model of Chlorides in Great Lakes", Donald J. O'Connor and John A. Mueller, Journal of the Sanitary Engineering Division, ASCE, Nol. 96, No. SA4, Proc. Paper 7470, Aug. 1970, pp. 955-975.

5. "Recurrence Relations for First Order Sequential Reactions in Natural Waters" Dominic M. Di Toro, Water Resources Research, Vol. 8, No. 1, Feb. 1972.

6. "A Linear Ecologic Model - Nitrification in Estuaries" Donald J. O'Connor, Robert V. Thomann, Dominic M. Di Toro, Systems Approach to Water Management, American Elsevier Co., New York, March 1972.

7. "Effect of Longitudinal Dispersion on Dynamic Water Quality Response of Streams and Rivers" Robert V. Thomann, Water Resources Research, April 1973.

SELECTED WATER RESOURCES ABSTRACTS
INPUT TRANSACTION FORM

1. Report No. | 2 | W

DYNAMIC WATER QUALITY FORECASTING AND MANAGEMENT

5. Report Date
6.
8. Performing Organization Report No. R800369

O'Connor, Donald J., Thomann, Robert V., and Di Toro, Dominic M.

Manhattan College, Bronx, New York, Civil Engineering Dept.

10. Project No. R800369

11. Type Report and Period Covered: Final Report

12. Sponsoring Organization: U. S. Environmental Protection Agency

Environmental Protection Agency report number, EPA-660/3-73-009, August 1973.

This report describes the formulation and initial verification of two modeling frameworks. The first is directed toward an analysis of the impact of the carbonaceous and nitrogenous components and wastewater on the dissolved oxygen resources of a natural water system. The second modeling framework concentrates on the interactions between the discharge of nutrient, both nitrogen and phosphorus, and the biomass of the phytoplankton and zooplankton populations which result, as well as incorporating the overall impact on dissolved oxygen. The models are formulated in terms of coupled differential equations which incorporate both the effect of transport due to tidal motion and turbulence, and the kinetics which describe the biological and chemical transformations that can occur. The modeling frameworks are applied to the Delaware and Potomac estuaries in order to estimate the ability of such models to describe the water quality effects of carbon, nitrogen, and phosphorous discharges. The agreement achieved between observation and calculation indicate that the major features of the impact of wastewater components on eutrophication phenomena can be successfully analyzed within the context of the models presented herein. (O'Connor-Manhattan College)

17a. Descriptors: *Water quality, *Mathematical Models, *Computer Models, Water pollution, Cycling nutrients, Eutrophication, Dispersion, Mass Transfer, Nutrients, Oxygen Demand, Photosynthesis, Simulation Analysis

17b. Identifiers:

17c. COSATI Field & Group: 05C, 05G, 06G

18. Availability	19. Security Class. (Report)	21. No. of Pages	Send To:
	20. Security Class. (Page)	22. Price	WATER RESOURCES SCIENTIFIC INFORMATION CENTER U.S. DEPARTMENT OF THE INTERIOR WASHINGTON, D. C. 20240

Abstractor: Donald J. O'Connor | Institution: Manhattan College, Bronx, New York

*U.S. GOVERNMENT PRINTING OFFICE: 1973 546-311/98 1-3